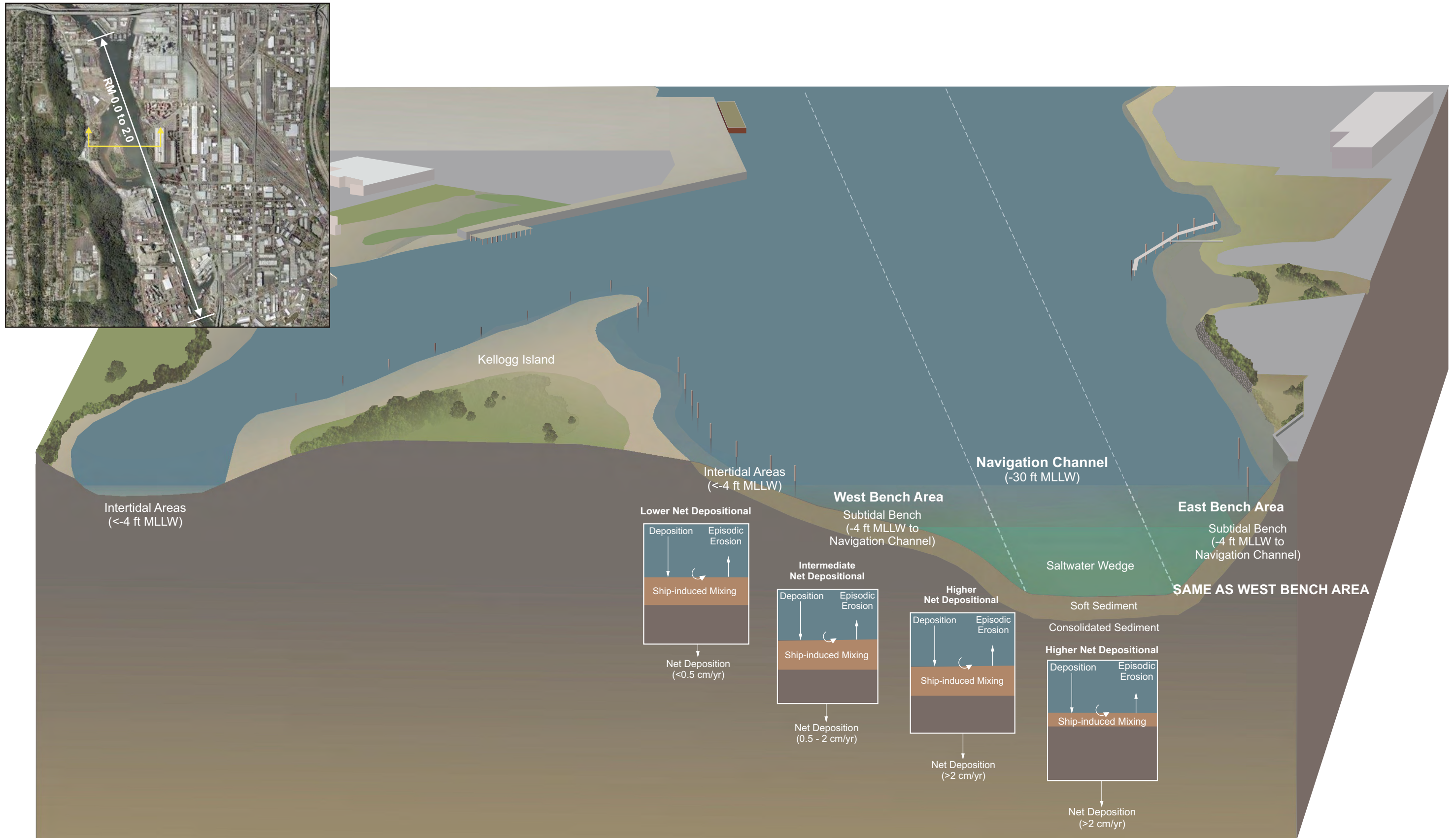
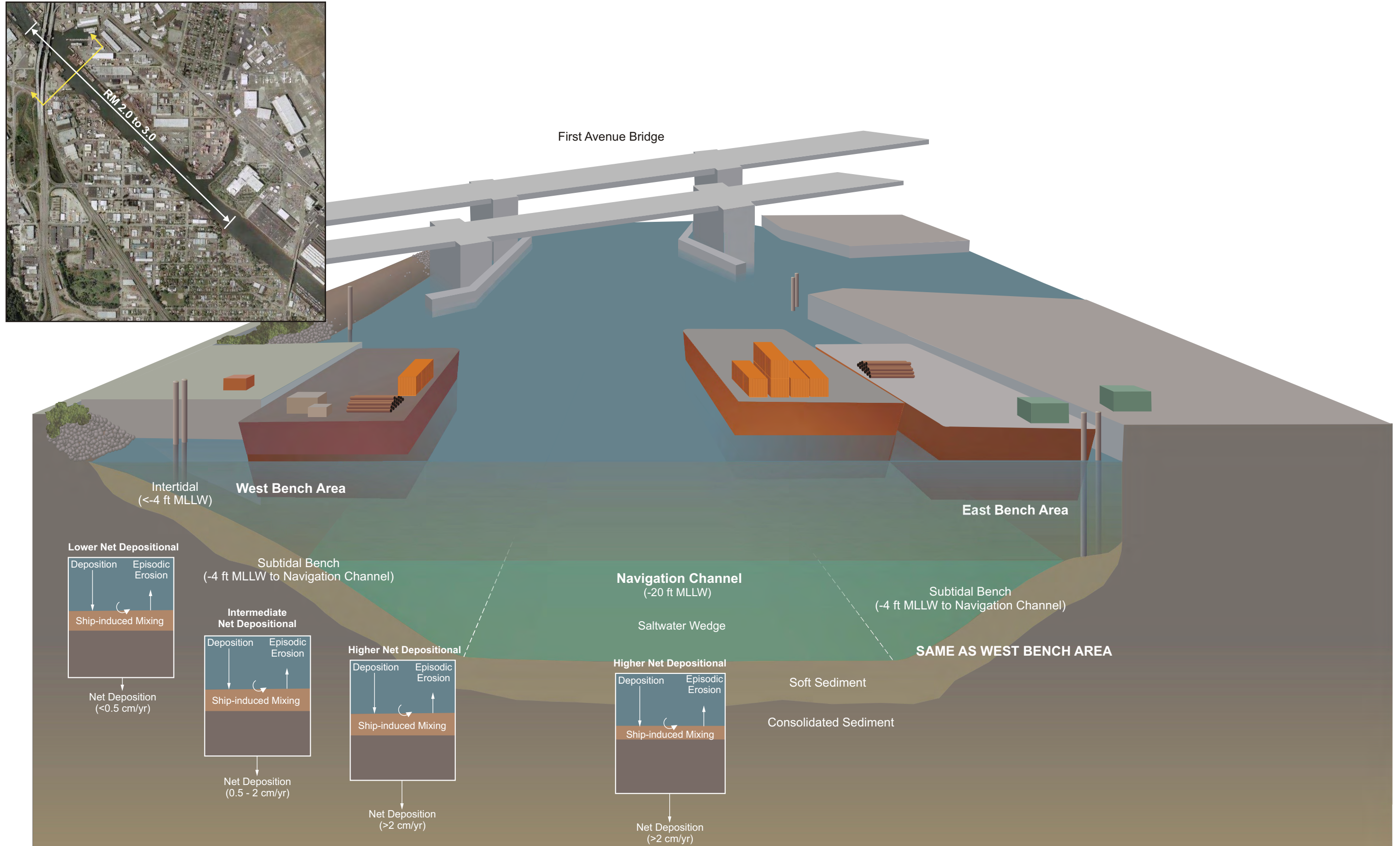


Figure ES-1. LDW Conceptual Site Model for Reach 1 (RM 0.0 - 2.0)



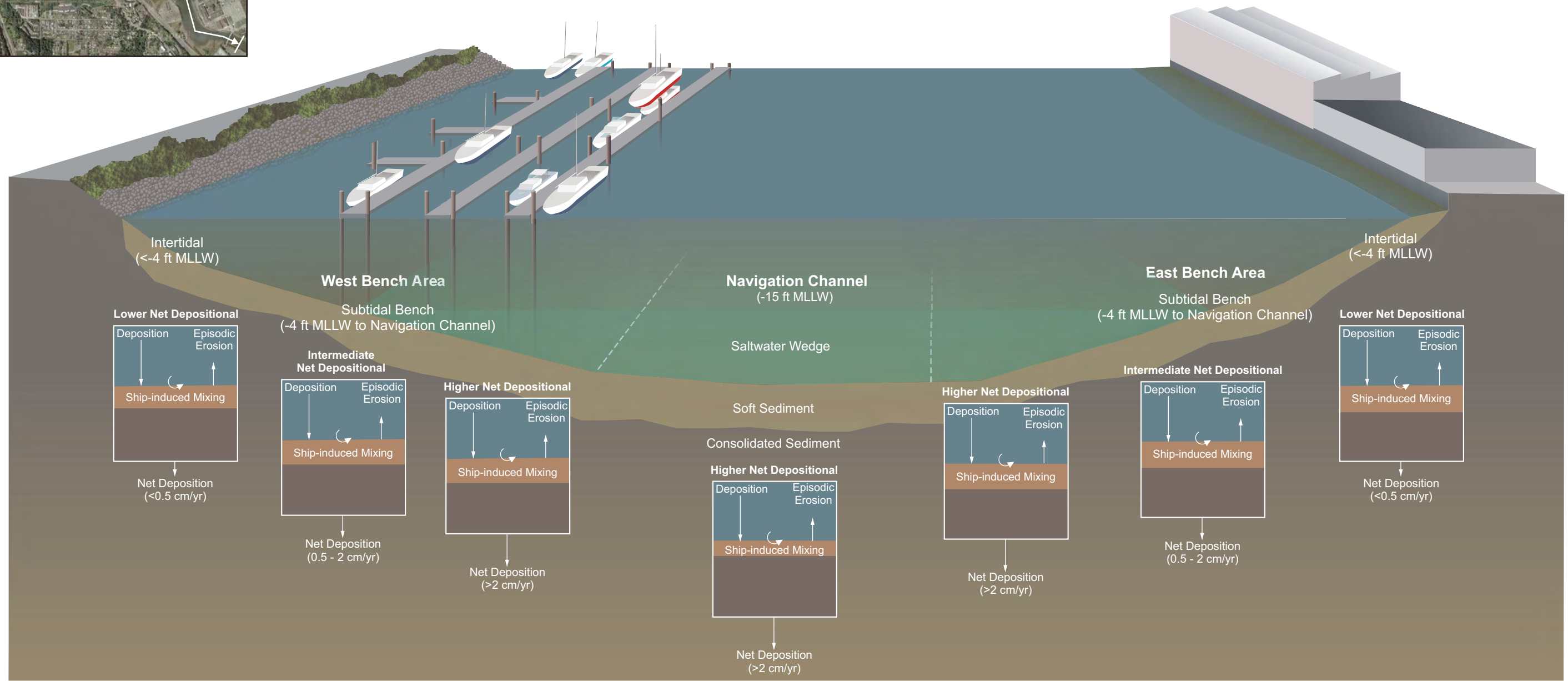
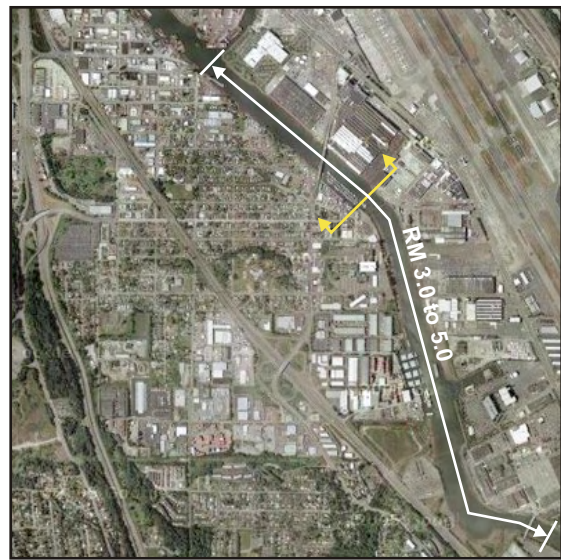
Notes: 1. Approximate net depositional rates from Sediment Transport Analysis Report, Windward and QEA 2006.
 2. Inserts are qualitative illustrations and are not to scale.

Figure ES-2. LDW Conceptual Site Model for Reach 2 (RM 2.0 - 3.0)



Notes: 1. Approximate net depositional rates from Sediment Transport Analysis Report, Windward and QEA 2006.
2. Inserts are qualitative illustrations and are not to scale.

Figure ES-3. LDW Conceptual Site Model for Reach 3 (RM 3.0 - 5.0)



Notes: 1. Approximate net depositional rates from Sediment Transport Analysis Report, Windward and QEA 2006.
2. Inserts are qualitative illustrations and are not to scale.

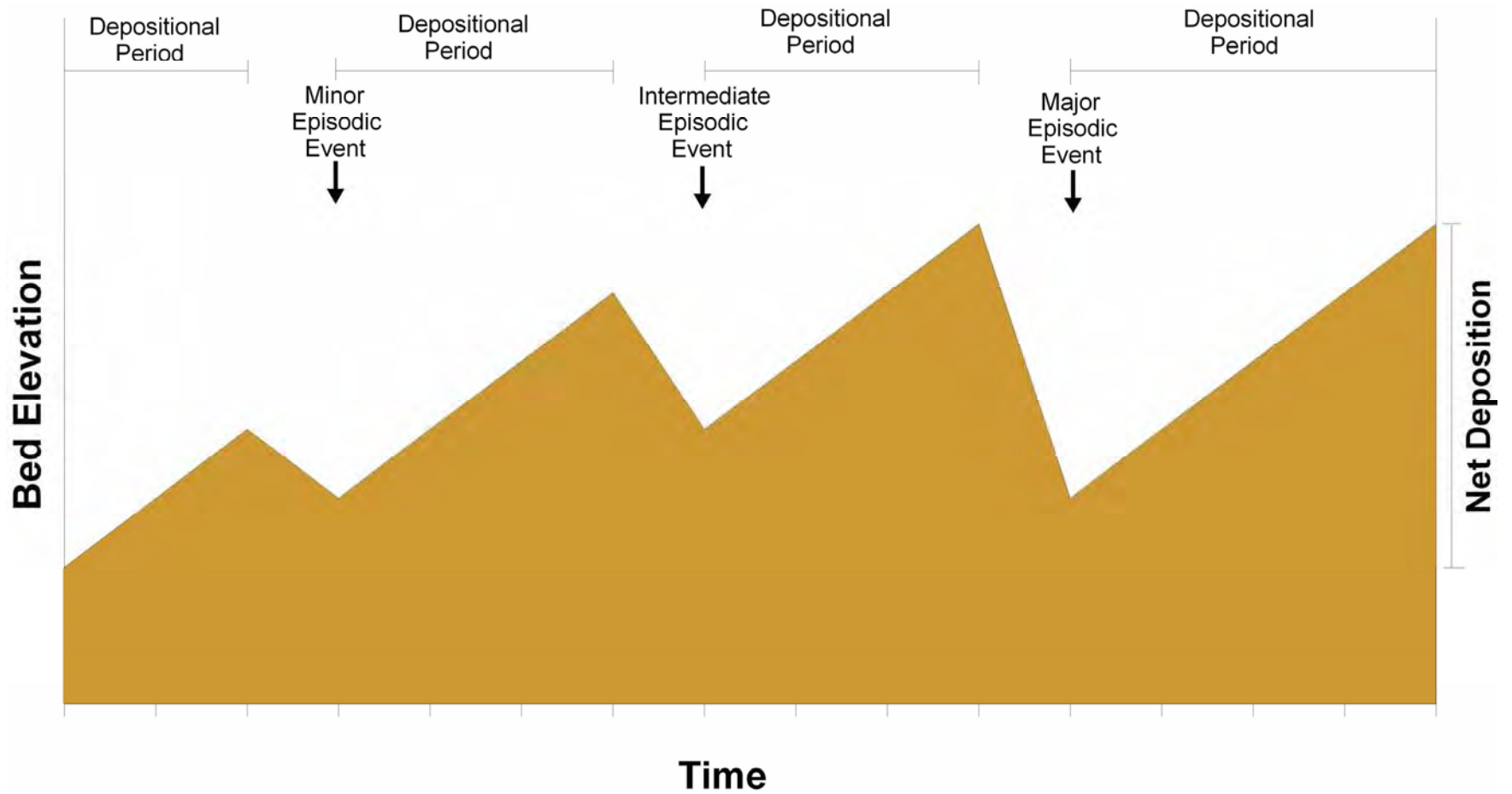


Figure 1-1. Example of net depositional bed with episodic erosion during high-flow events.

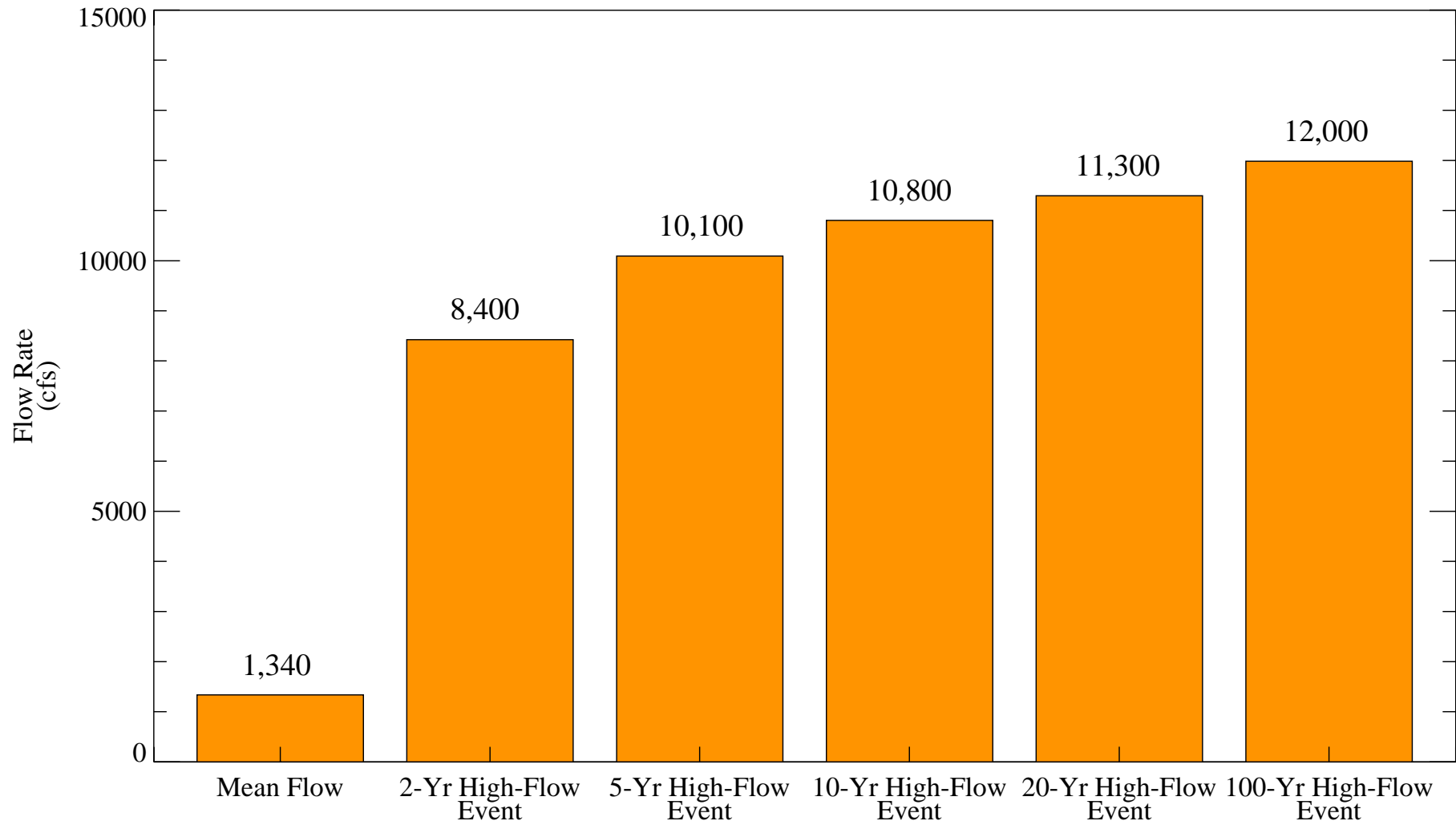


Figure 2-1. Comparison of flow rates for various discharge conditions in the Green River.

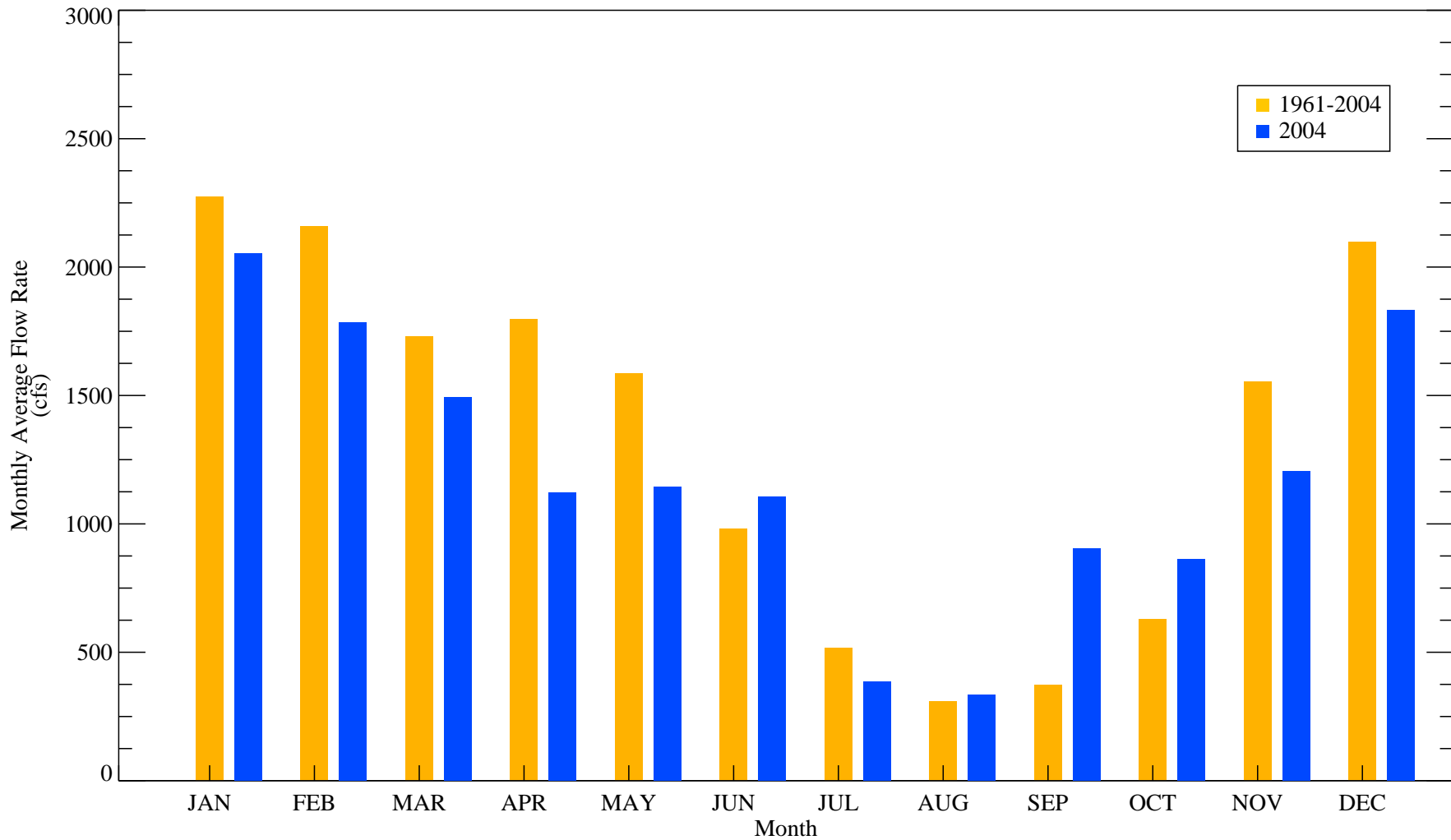


Figure 2-2. Comparison of monthly-average flow rate in Green River during 2004 to historical monthly-average (1961 through 2004).

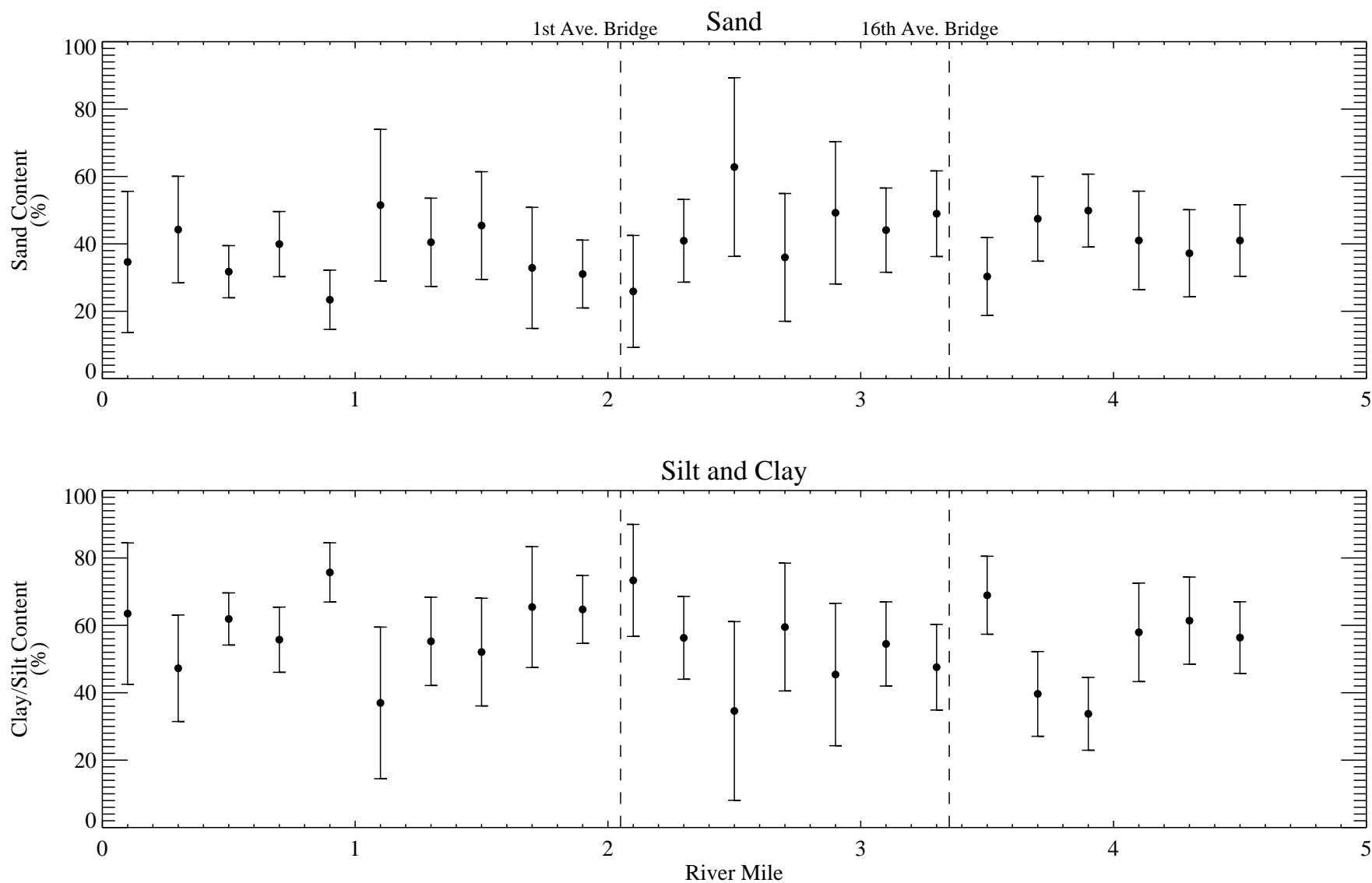


Figure 2-3. Spatial distribution of clay/silt and sand content in surface layer of LDW sediments in west bench area. Raw data are binned in 0.2 mile segments and presented as mean (solid circle) and 2 standard errors about the mean (bar).

Grain size data represent historic sampling results between 1991 and 2005.

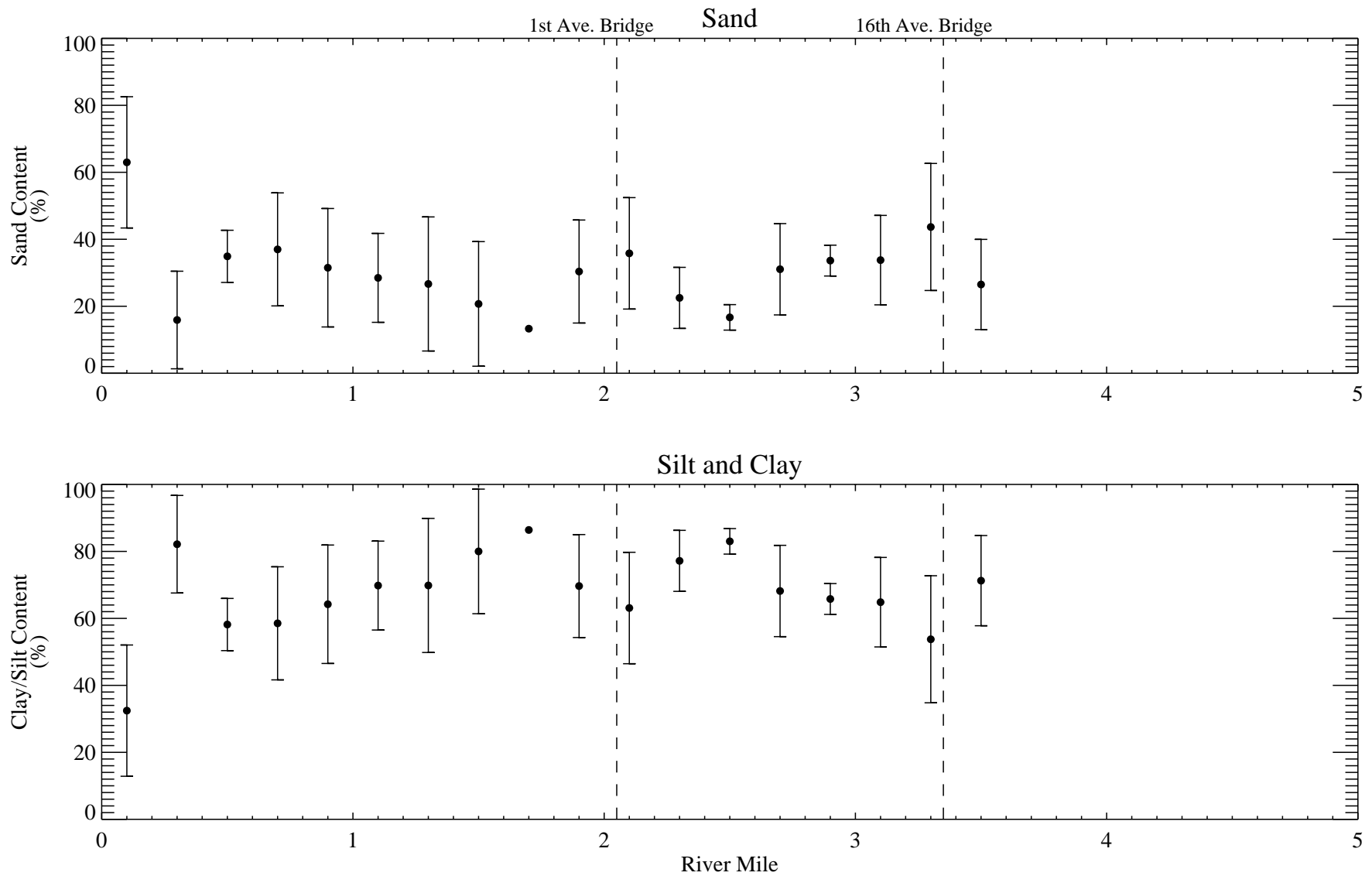


Figure 2-4. Spatial distribution of clay/silt and sand content in surface layer of LDW sediments in navigation channel. Raw data are binned in 0.2 mile segments and presented as mean (solid circle) and 2 standard errors about the mean (bar).

Grain size data represent historic sampling results between 1991 and 2005.

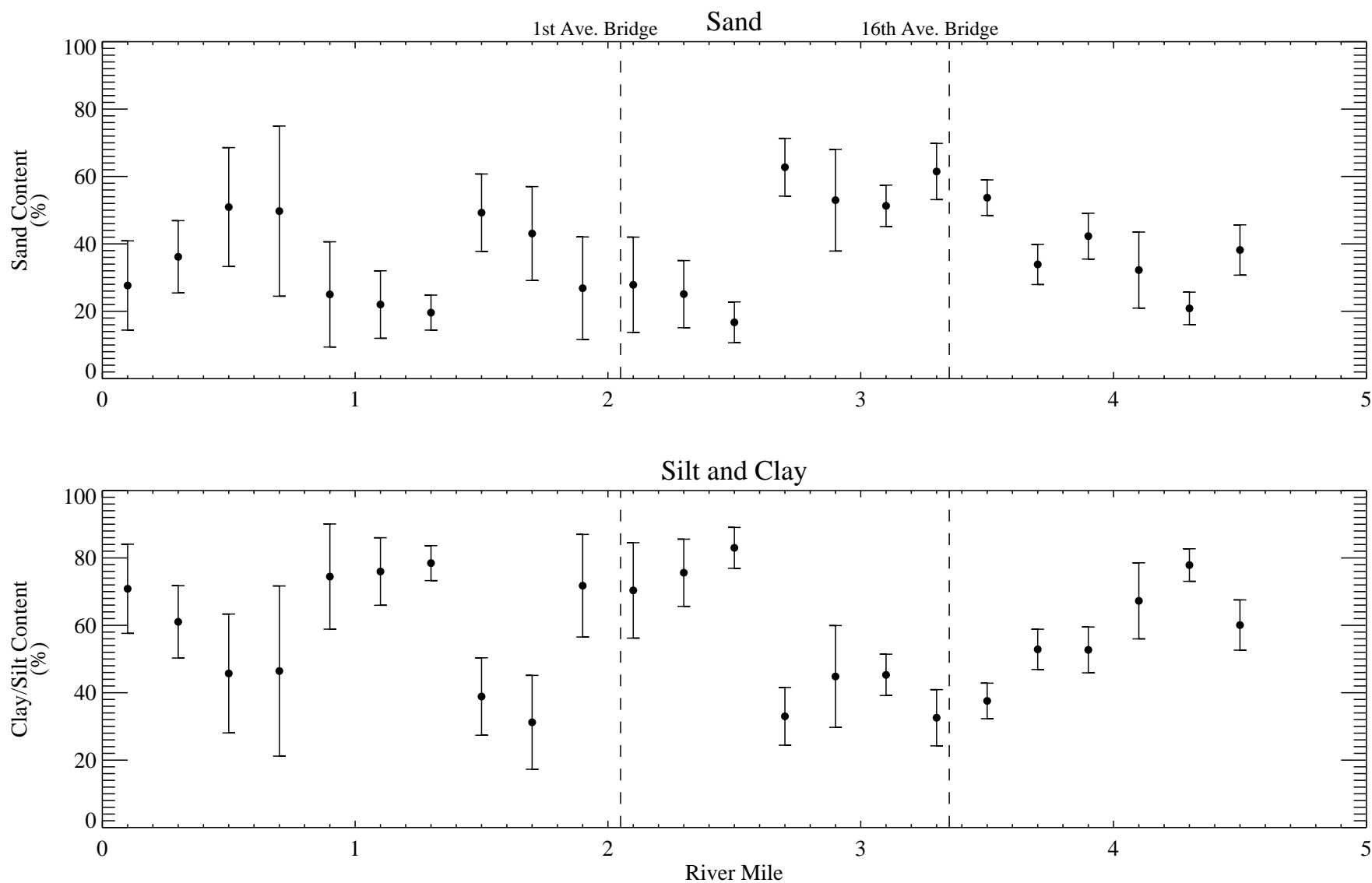


Figure 2-5. Spatial distribution of clay/silt and sand content in surface layer of LDW sediments in east bench area. Raw data are binned in 0.2 mile segments and presented as mean (solid circle) and 2 standard errors about the mean (bar).

Grain size data represent historic sampling results between 1991 and 2005.

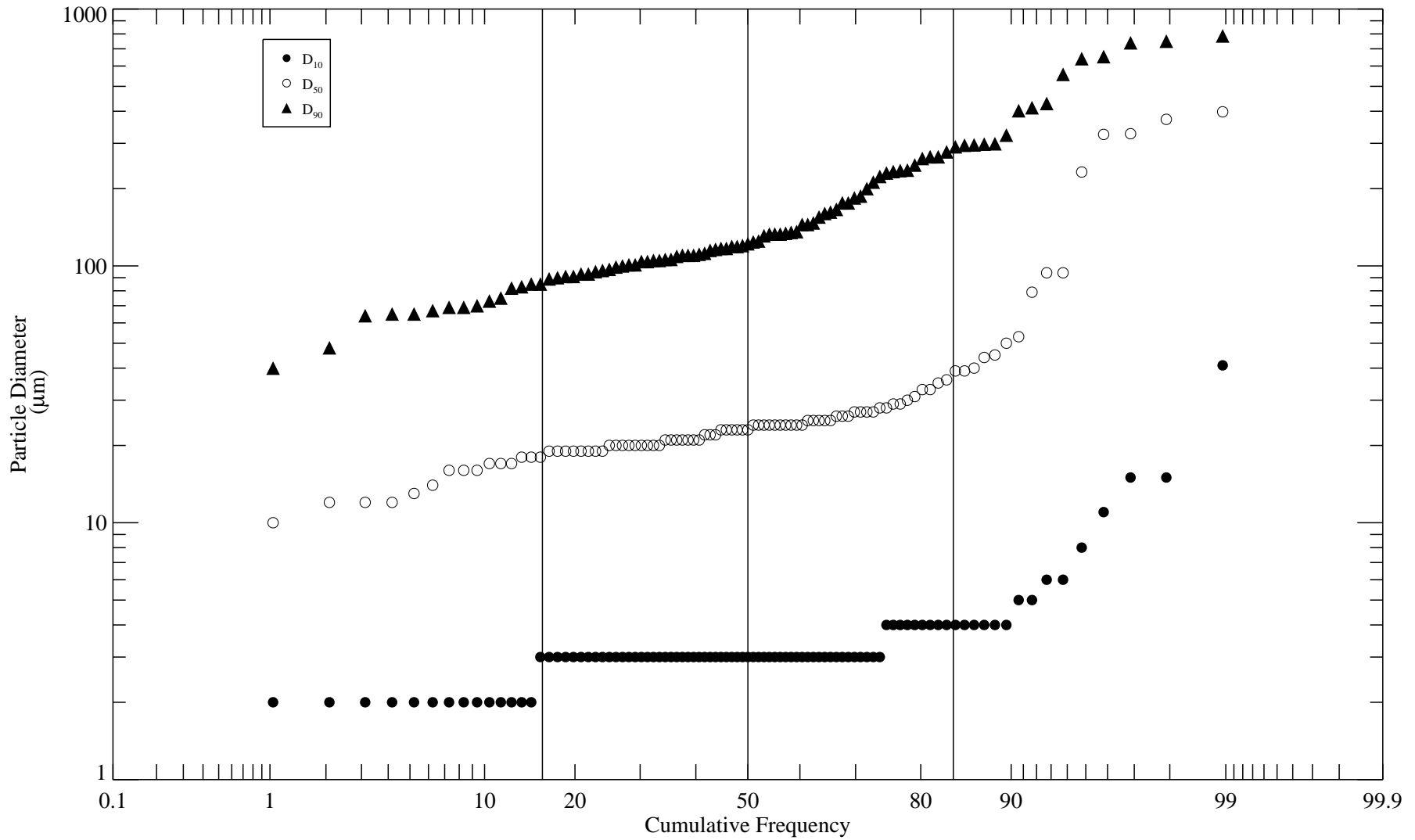


Figure 2-6. Cumulative frequency distribution of particle size measurements obtained during Sedflume study.

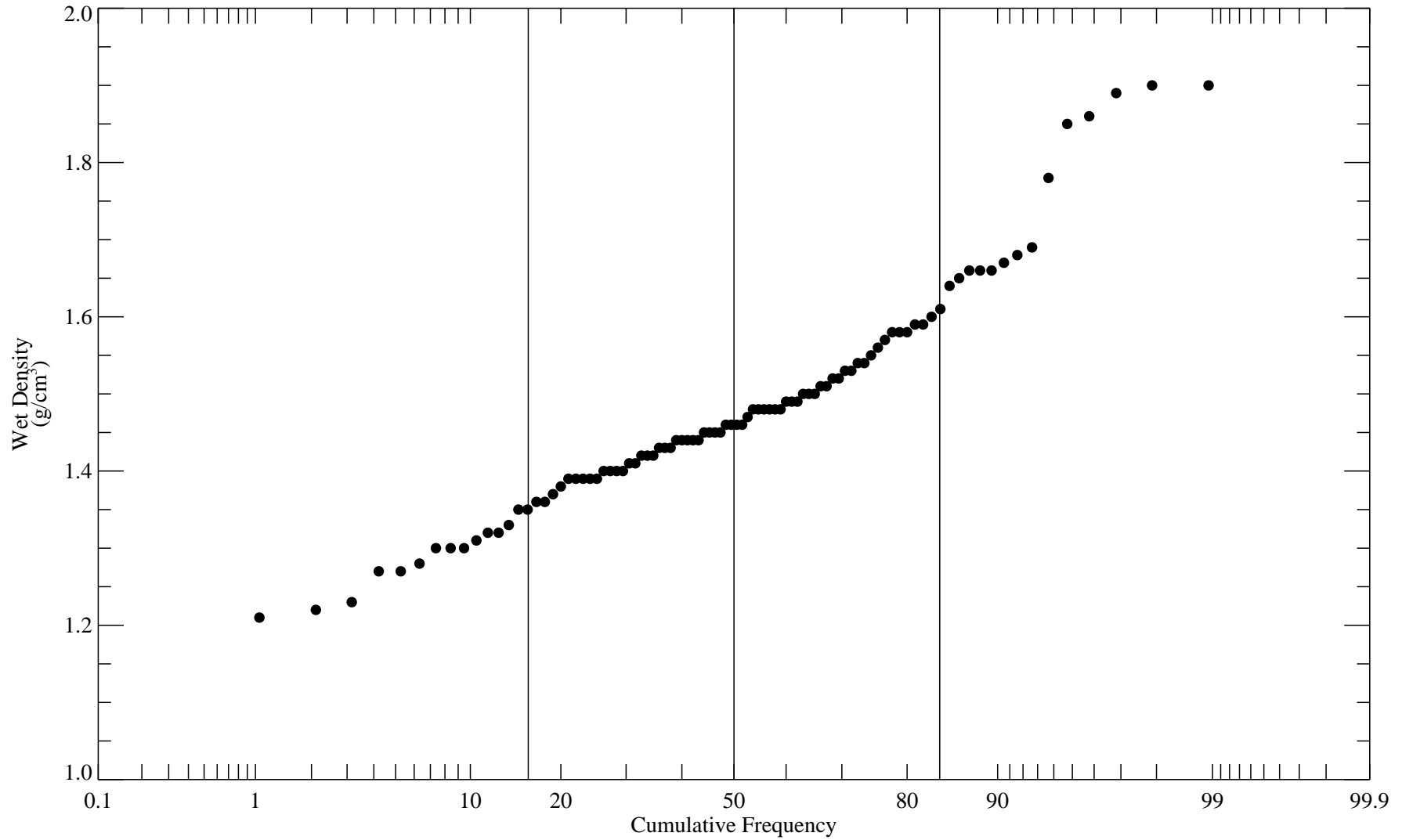


Figure 2-7. Cumulative frequency distribution of wet density measurements obtained during Sedflume study.

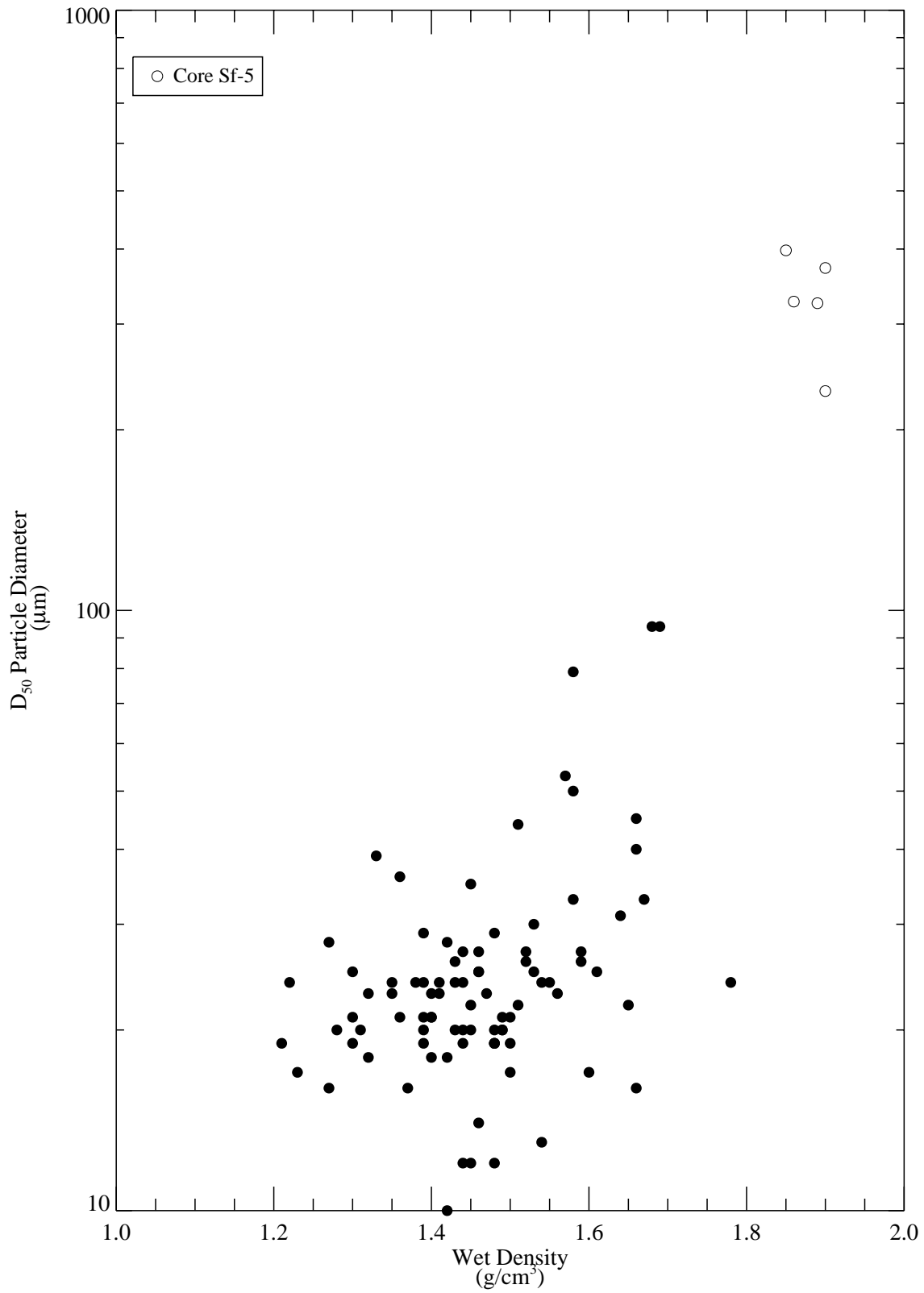


Figure 2-8. Correlation between particle diameter and wet density measurements obtained during Sedflume study.

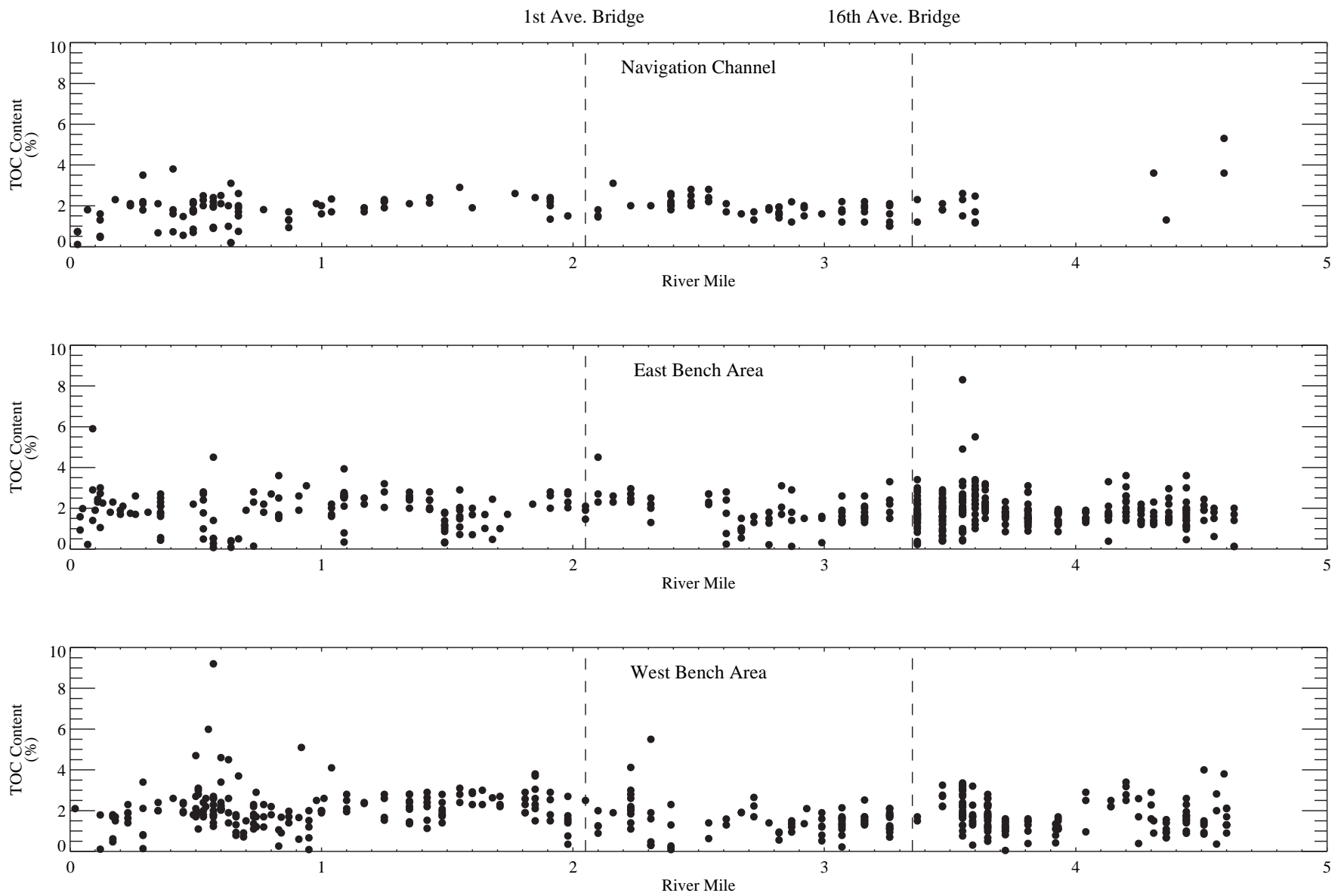


Figure 2-9. Spatial distribution of total organic carbon (TOC) content in surface layer of sediments located in bench areas and navigation channel.

Values represent historic sampling between 1997 and 2005.

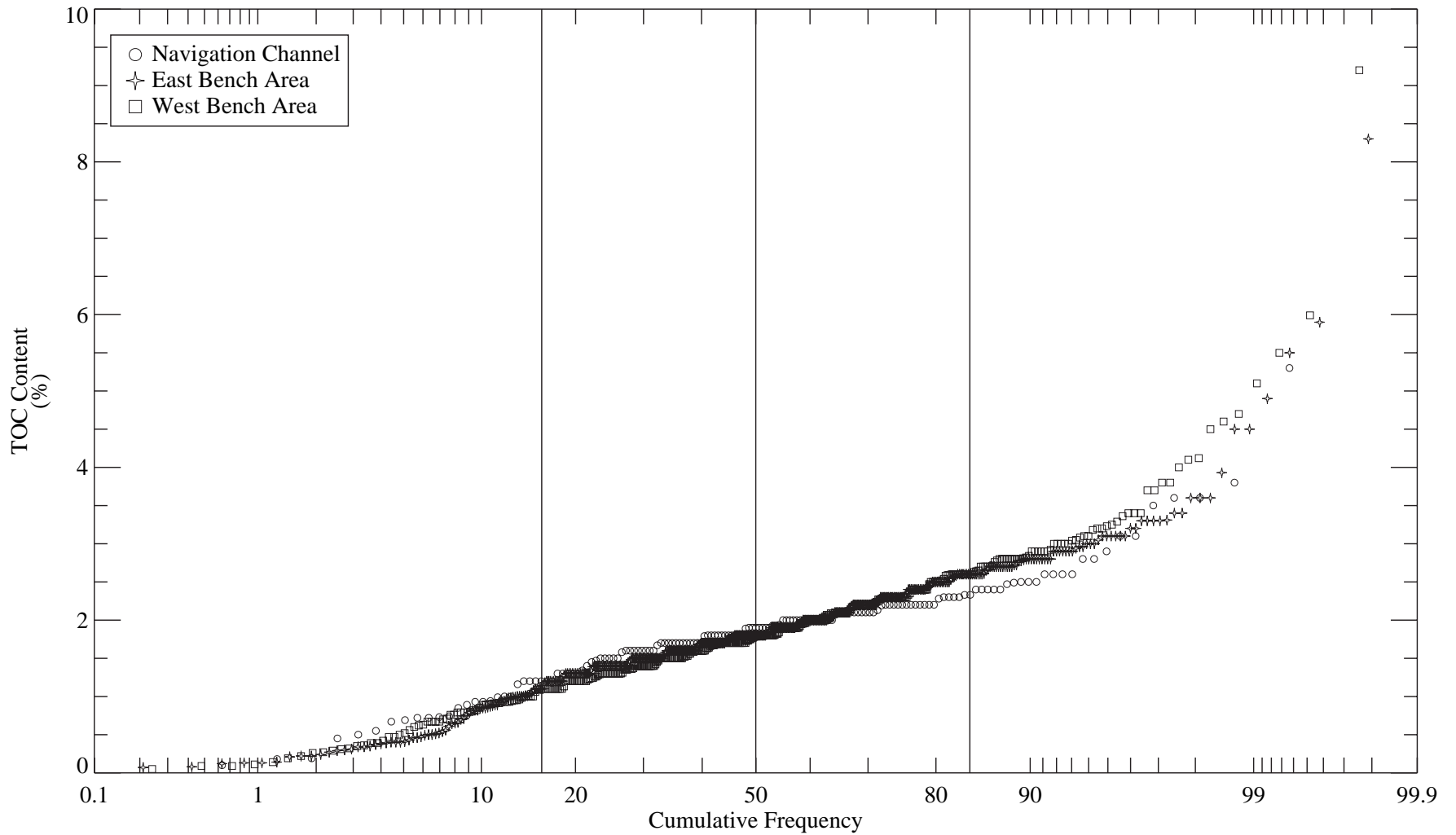


Figure 2-10. Cumulative frequency distribution of TOC content in surface layer of sediments located in bench areas and navigation channel.

Values represent historic sampling between 1997 and 2005.

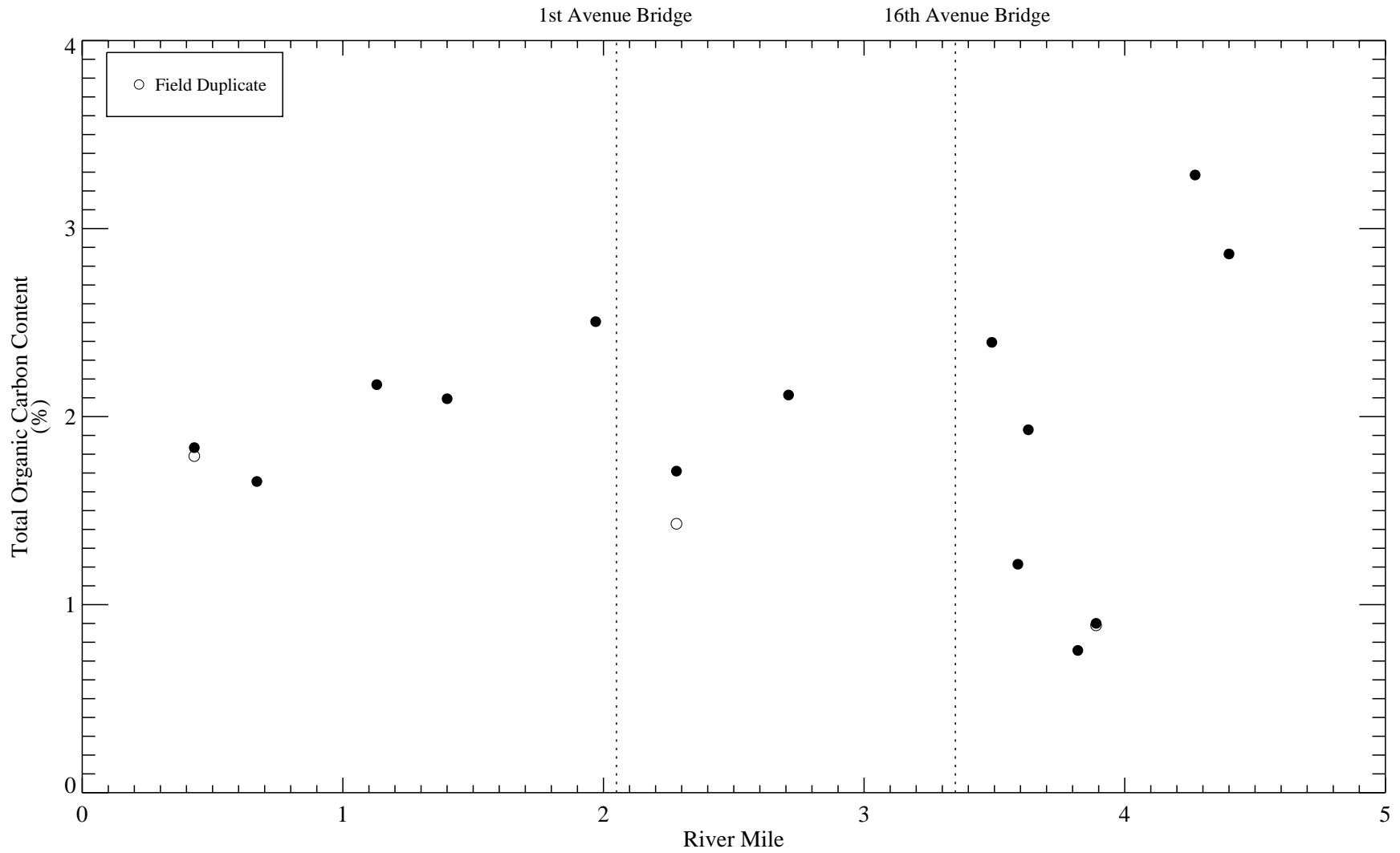
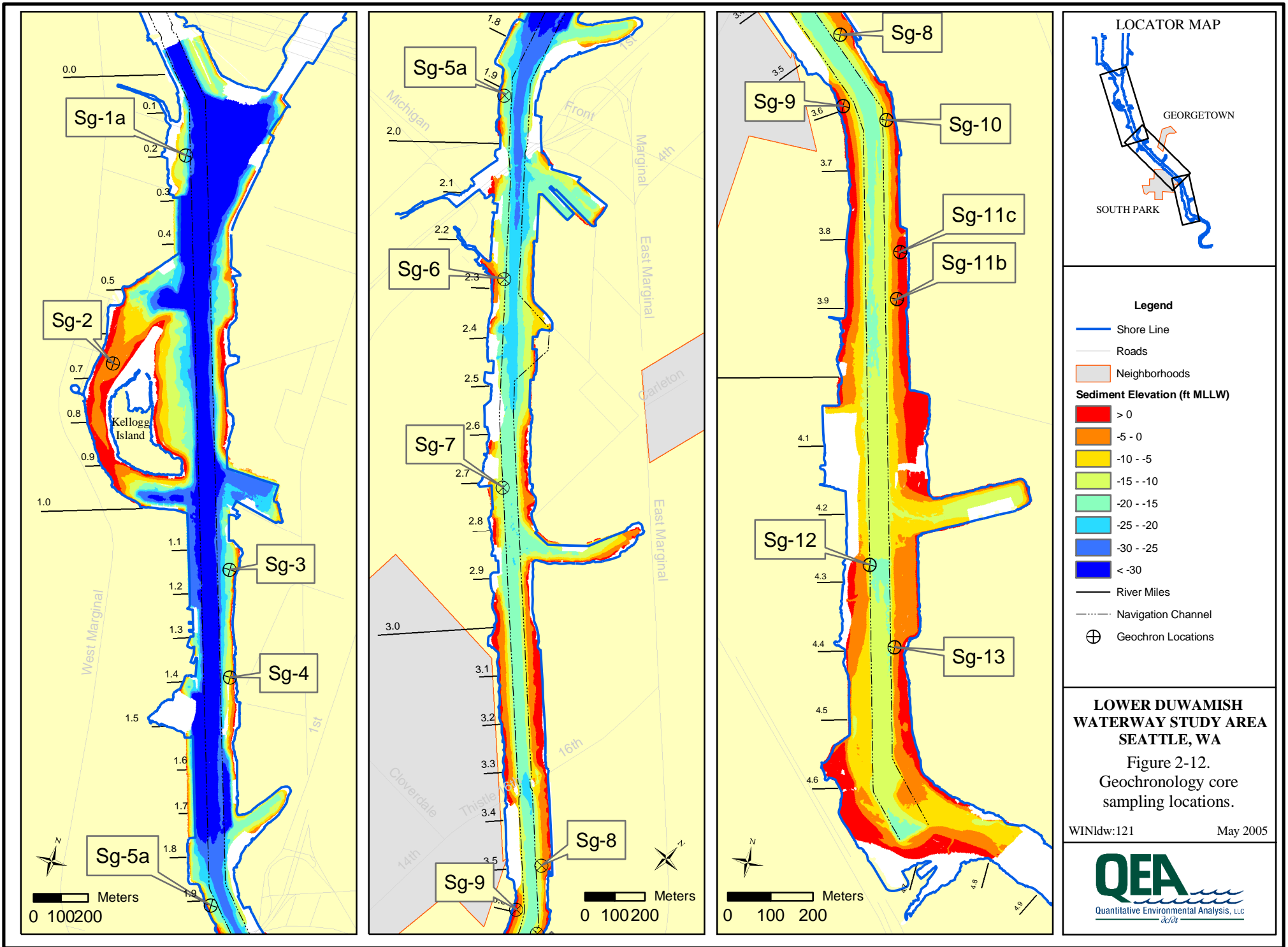


Figure 2-11. Spatial distribution of TOC content in surface layer of geochronology cores.



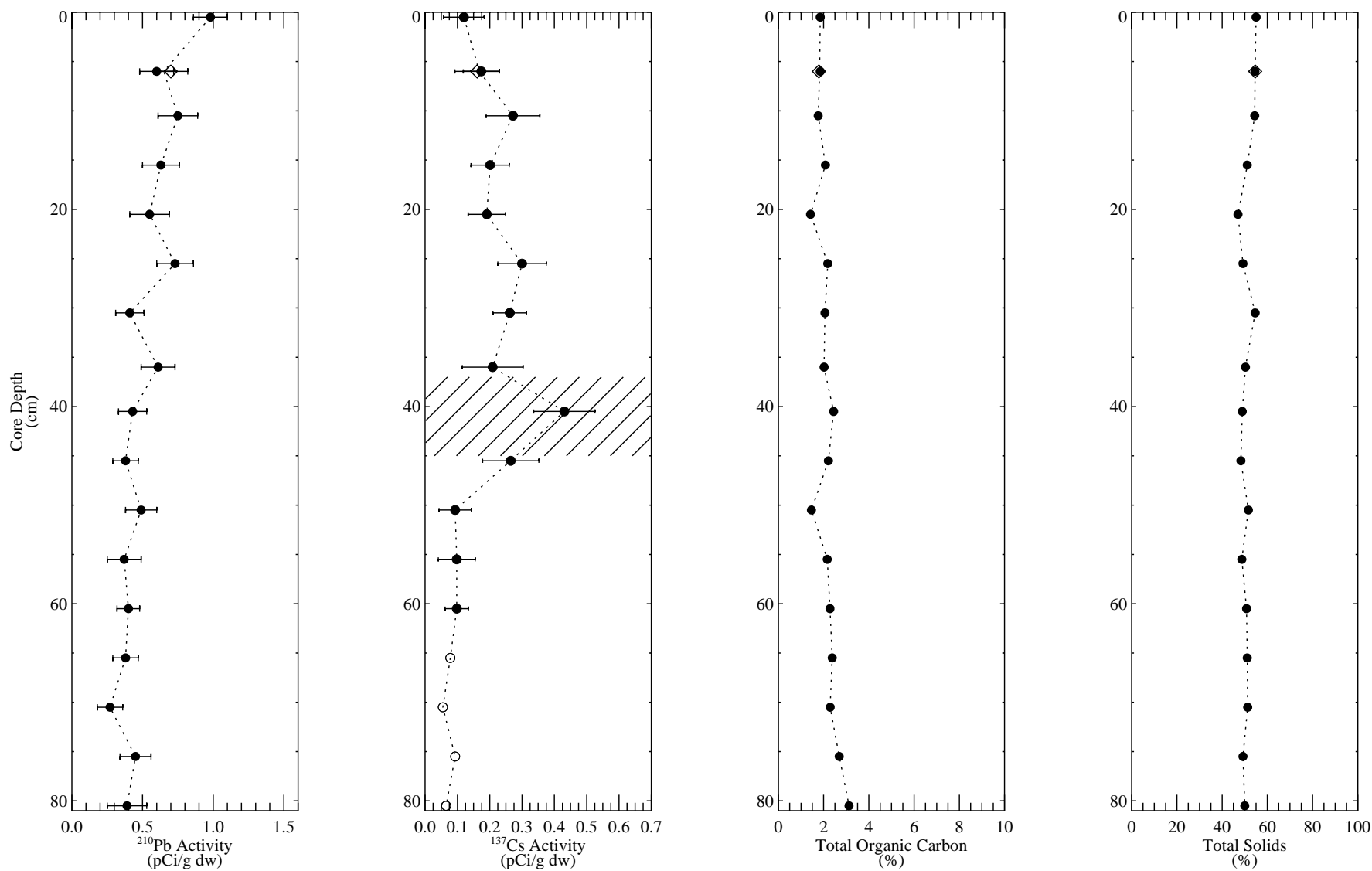


Figure 2-13. Vertical profiles of ^{210}Pb and ^{137}Cs activity, total organic carbon and total solids for core Sg-1a.

Error bars on ^{210}Pb and ^{137}Cs panels represent 95% confidence intervals around the best estimate as reported by the laboratory.

Cross-hatching represents approximate range of ^{137}Cs peak.

Orange square symbols represent samples analyzed from archive.

- Below Detection Limit
- ◇ Field Duplicate
- Archive Samples

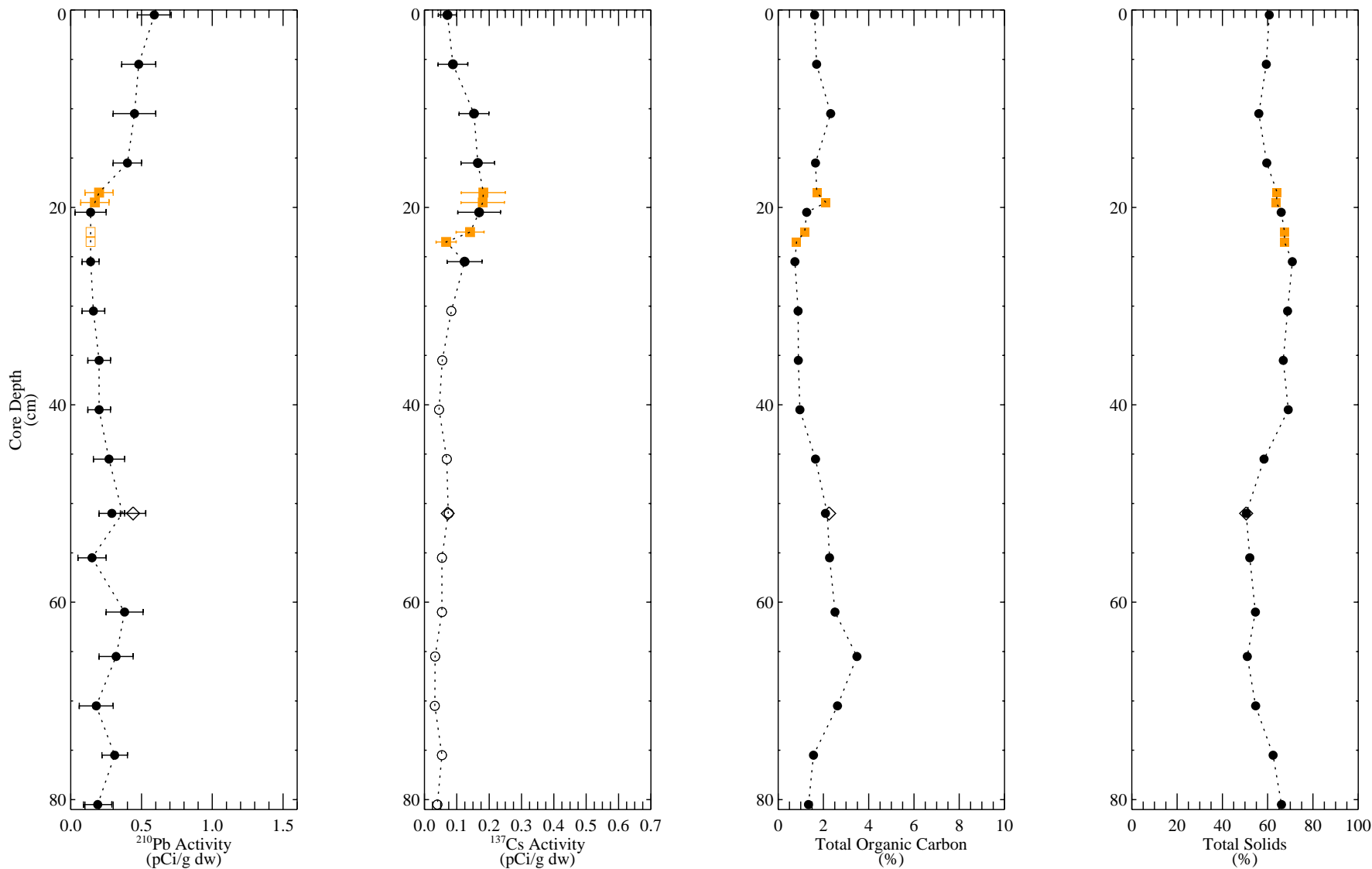


Figure 2-14. Vertical profiles of ^{210}Pb and ^{137}Cs activity, total organic carbon and total solids for core Sg-2.

Error bars on ^{210}Pb and ^{137}Cs panels represent 95% confidence intervals around the best estimate as reported by the laboratory.

Cross-hatching represents approximate range of ^{137}Cs peak.

Orange square symbols represent samples analyzed from archive.

- Below Detection Limit
- ◇ Field Duplicate
- Archive Samples

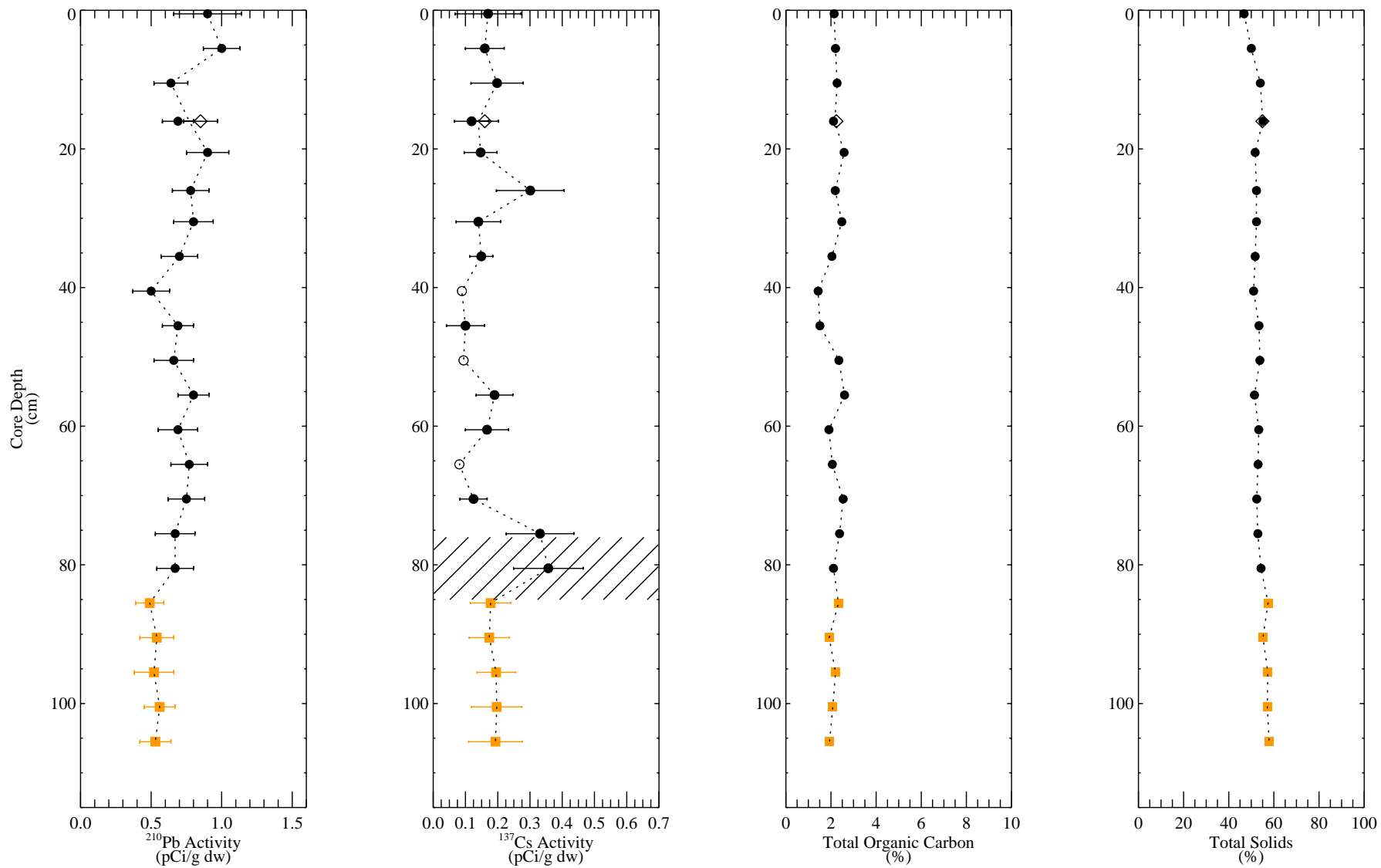


Figure 2-15. Vertical profiles of ^{210}Pb and ^{137}Cs activity, total organic carbon and total solids for core Sg-3.

Error bars on ^{210}Pb and ^{137}Cs panels represent 95% confidence intervals around the best estimate as reported by the laboratory.

Cross-hatching represents approximate range of ^{137}Cs peak.

Orange square symbols represent samples analyzed from archive.

- Below Detection Limit
- ◇ Field Duplicate
- Archive Samples

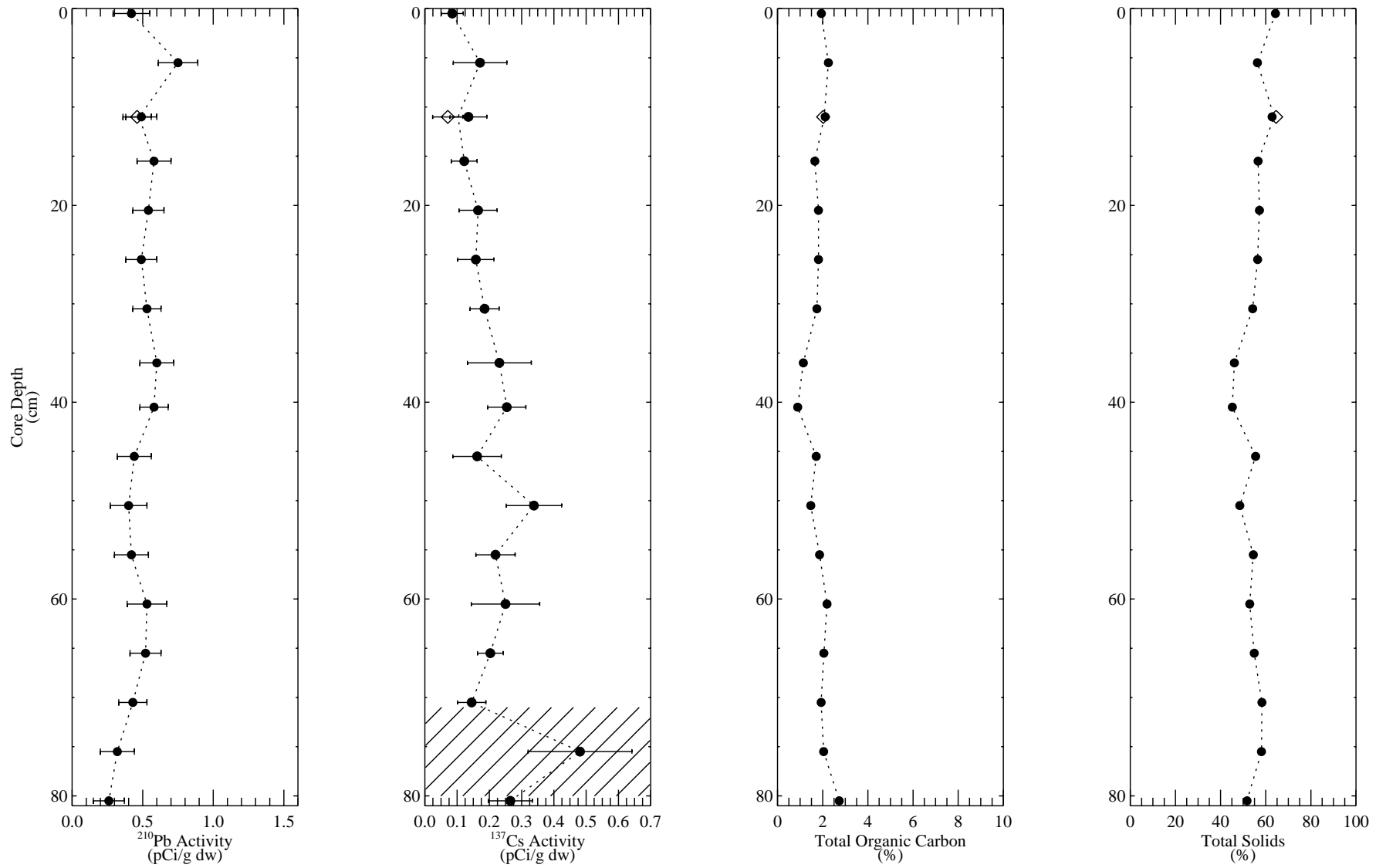


Figure 2-16. Vertical profiles of ^{210}Pb and ^{137}Cs activity, total organic carbon and total solids for core Sg-4.

Error bars on ^{210}Pb and ^{137}Cs panels represent 95% confidence intervals around the best estimate as reported by the laboratory.

Cross-hatching represents approximate range of ^{137}Cs peak.

Orange square symbols represent samples analyzed from archive.

- Below Detection Limit
- ◇ Field Duplicate
- Archive Samples

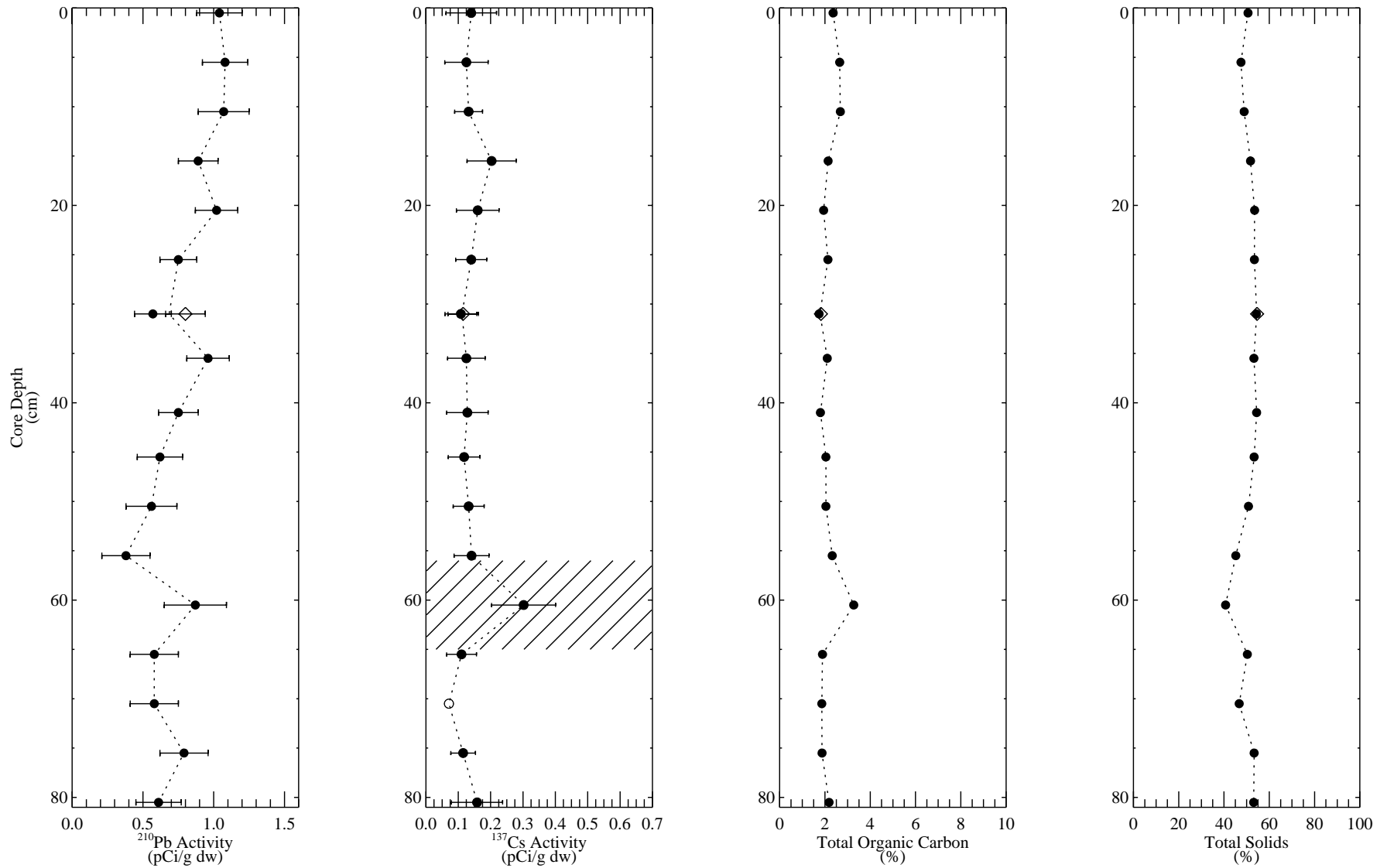
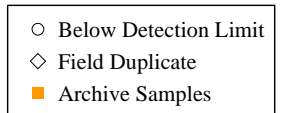


Figure 2-17. Vertical profiles of ^{210}Pb and ^{137}Cs activity, total organic carbon and total solids for core Sg-5a.

Error bars on ^{210}Pb and ^{137}Cs panels represent 95% confidence intervals around the best estimate as reported by the laboratory.

Cross-hatching represents approximate range of ^{137}Cs peak.

Orange square symbols represent samples analyzed from archive.



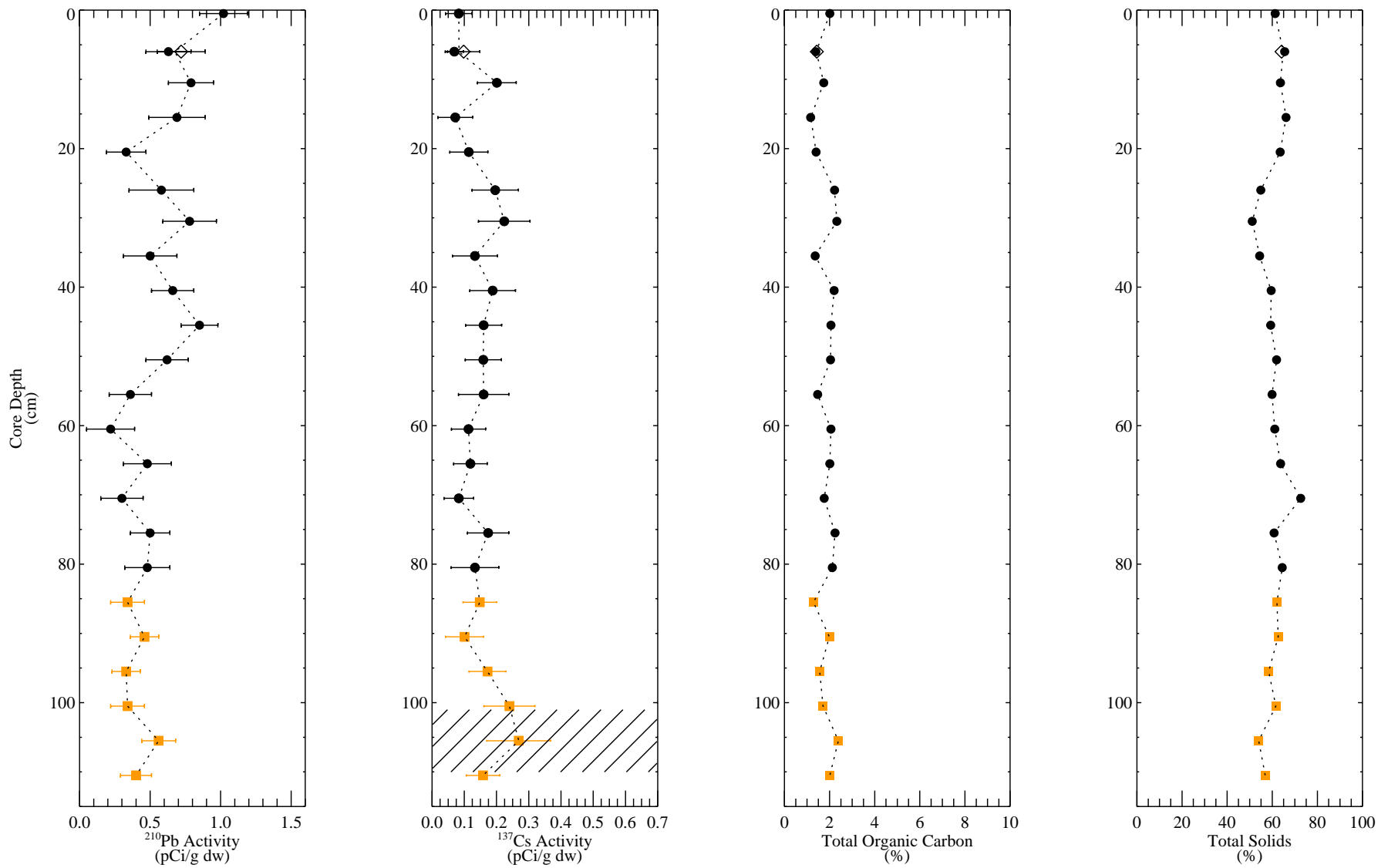
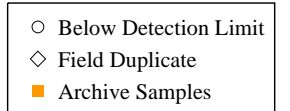


Figure 2-18. Vertical profiles of ^{210}Pb and ^{137}Cs activity, total organic carbon and total solids for core Sg-6.

Error bars on ^{210}Pb and ^{137}Cs panels represent 95% confidence intervals around the best estimate as reported by the laboratory.

Cross-hatching represents approximate range of ^{137}Cs peak.

Orange square symbols represent samples analyzed from archive.



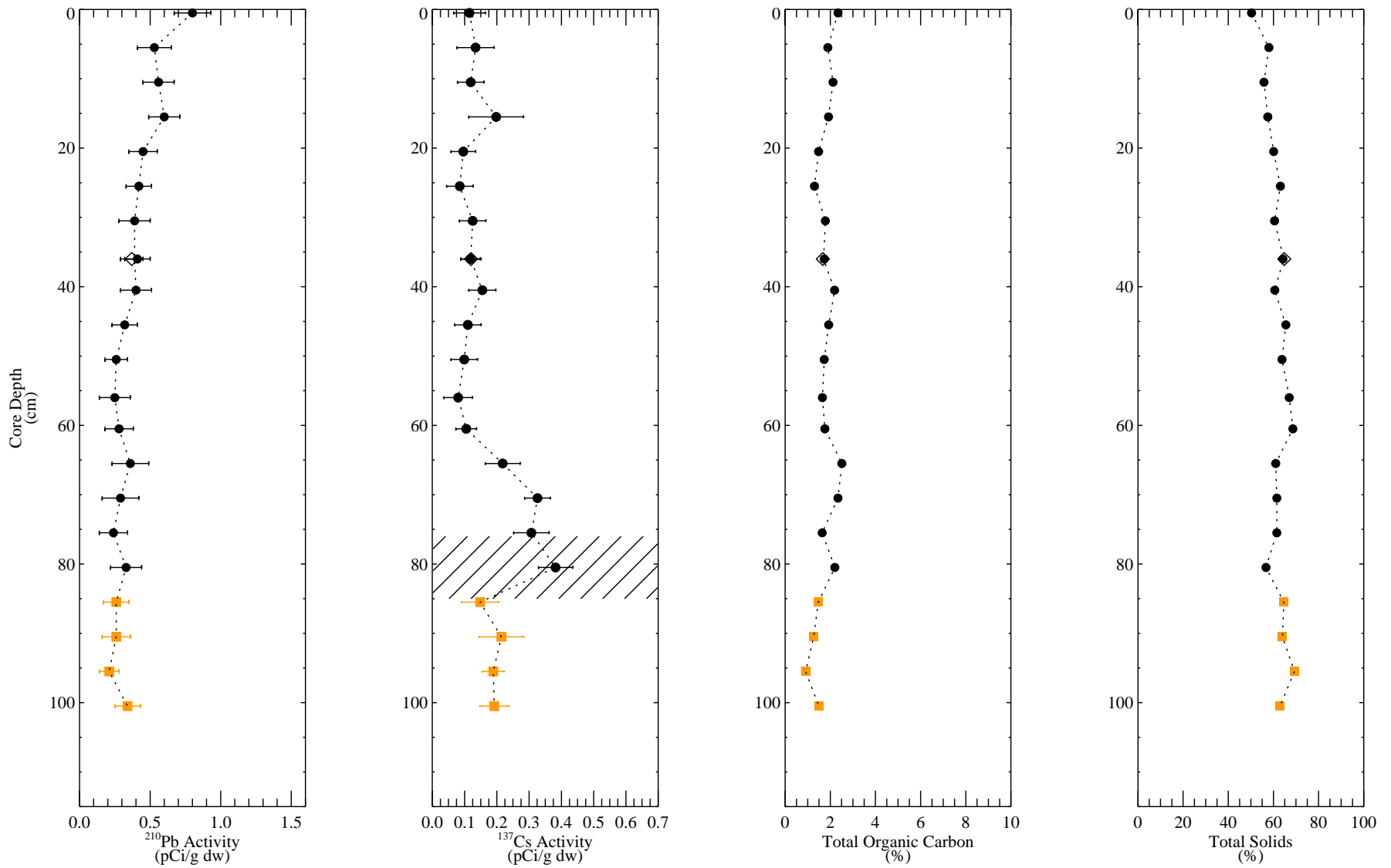


Figure 2-19. Vertical profiles of ^{210}Pb and ^{137}Cs activity, total organic carbon and total solids for core Sg-7.

Error bars on ^{210}Pb and ^{137}Cs panels represent 95% confidence intervals around the best estimate as reported by the laboratory.

Cross-hatching represents approximate range of ^{137}Cs peak.

Orange square symbols represent samples analyzed from archive.

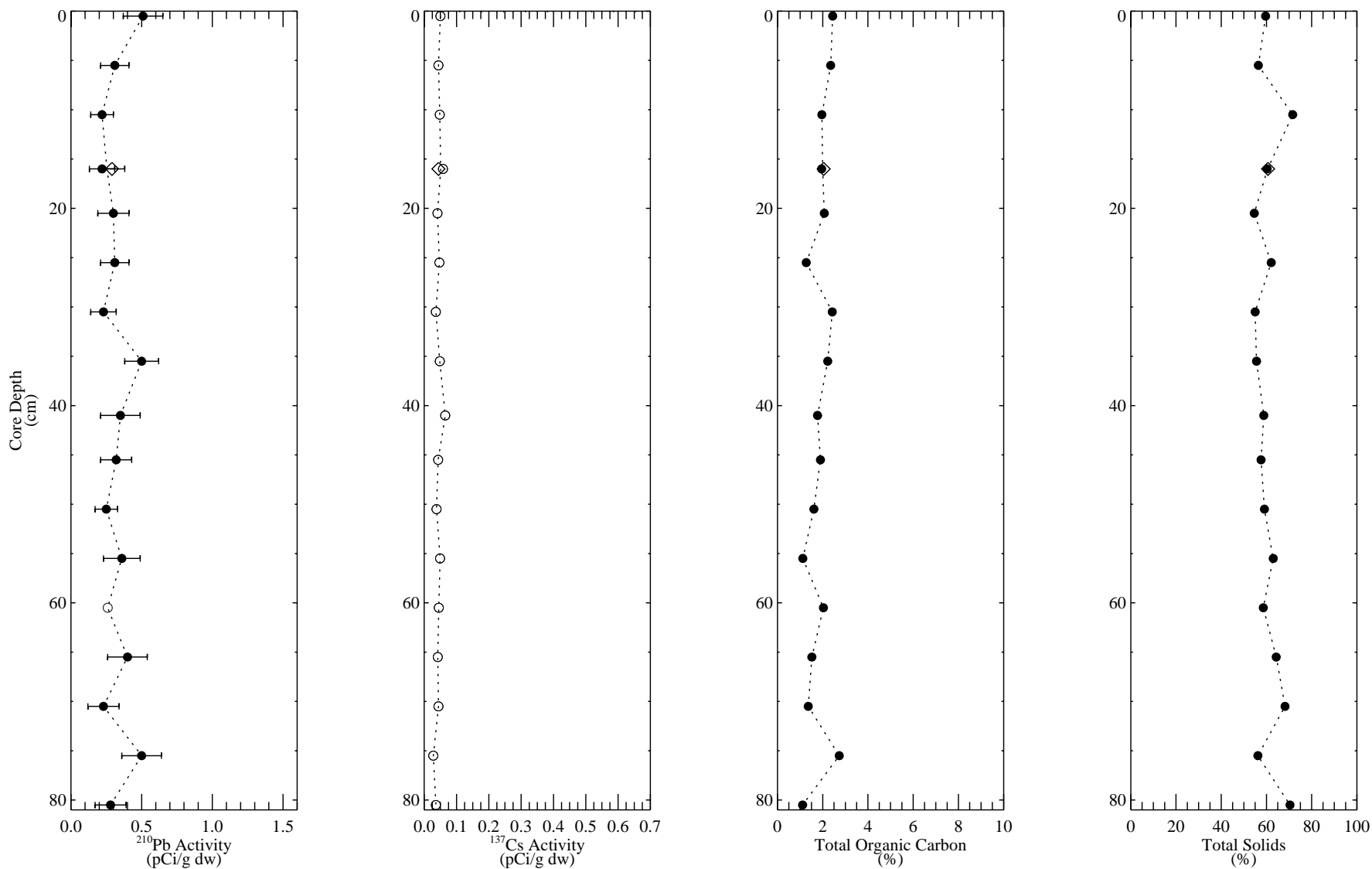


Figure 2-20. Vertical profiles of ^{210}Pb and ^{137}Cs activity, total organic carbon and total solids for core Sg-8.

Error bars on ^{210}Pb and ^{137}Cs panels represent 95% confidence intervals around the best estimate as reported by the laboratory.

Cross-hatching represents approximate range of ^{137}Cs peak.

Orange square symbols represent samples analyzed from archive.

- Below Detection Limit
- ◇ Field Duplicate
- Archive Samples

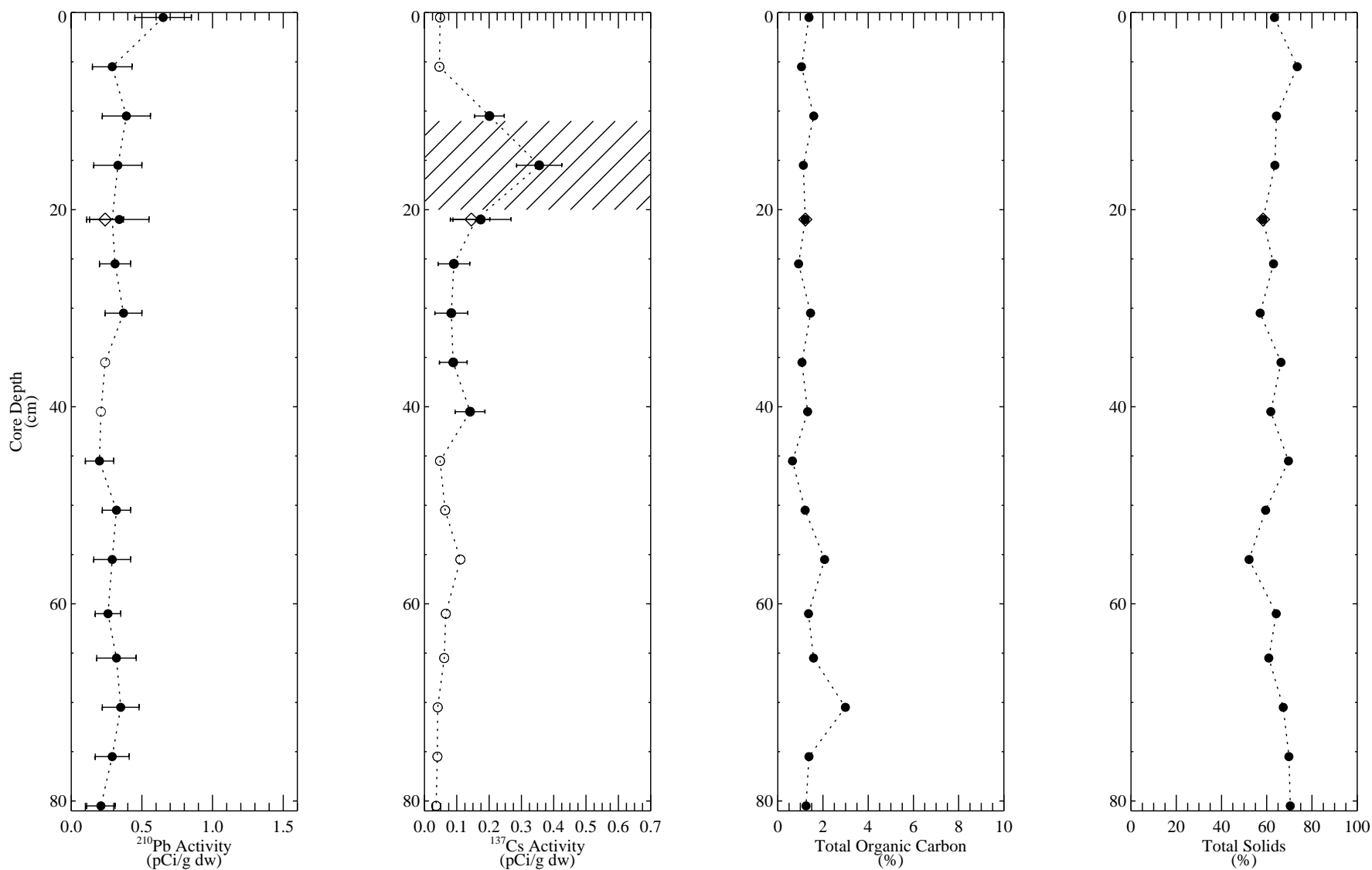


Figure 2-21. Vertical profiles of ^{210}Pb and ^{137}Cs activity, total organic carbon and total solids for core Sg-9.

Error bars on ^{210}Pb and ^{137}Cs panels represent 95% confidence intervals around the best estimate as reported by the laboratory.

Cross-hatching represents approximate range of ^{137}Cs peak.

Orange square symbols represent samples analyzed from archive.

- Below Detection Limit
- ◇ Field Duplicate
- Archive Samples

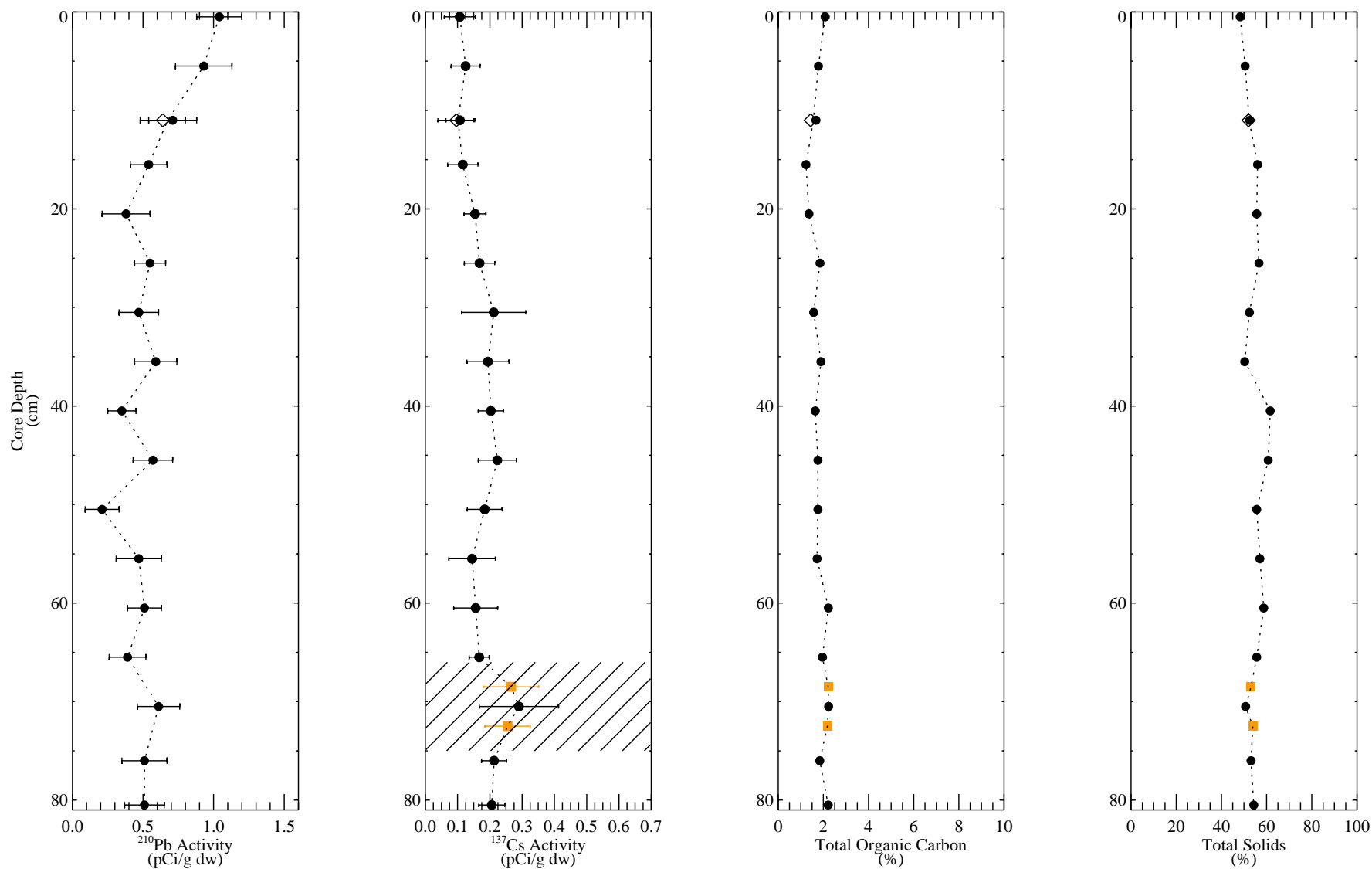


Figure 2-22. Vertical profiles of ^{210}Pb and ^{137}Cs activity, total organic carbon and total solids for core Sg-10.

Error bars on ^{210}Pb and ^{137}Cs panels represent 95% confidence intervals around the best estimate as reported by the laboratory.

Cross-hatching represents approximate range of ^{137}Cs peak.

Orange square symbols represent samples analyzed from archive.

- Below Detection Limit
- ◇ Field Duplicate
- Archive Samples

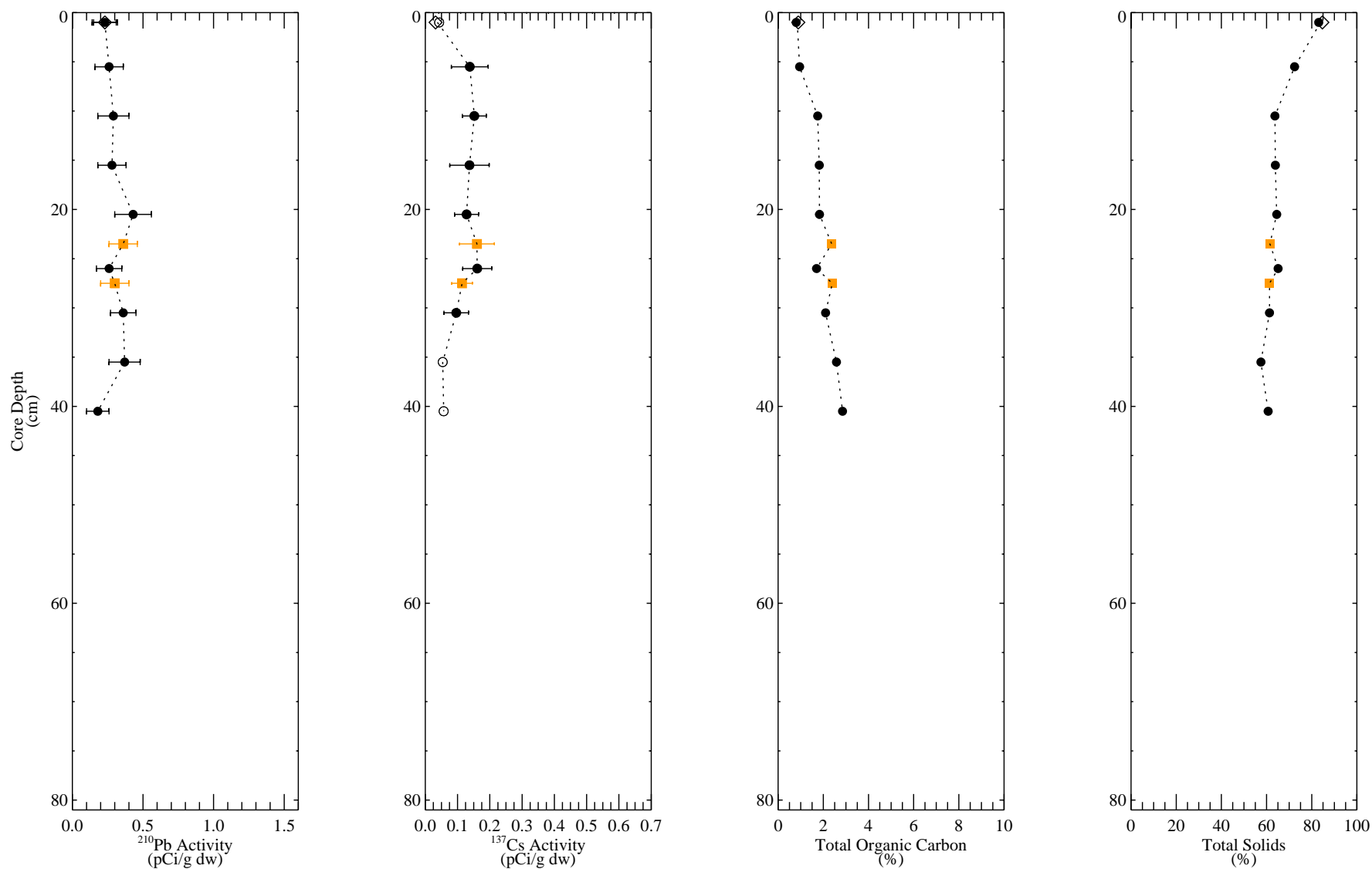
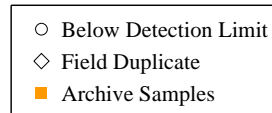


Figure 2-23. Vertical profiles of ^{210}Pb and ^{137}Cs activity, total organic carbon and total solids for core Sg-11b.

Error bars on ^{210}Pb and ^{137}Cs panels represent 95% confidence intervals around the best estimate as reported by the laboratory.

Cross-hatching represents approximate range of ^{137}Cs peak.

Orange square symbols represent samples analyzed from archive.



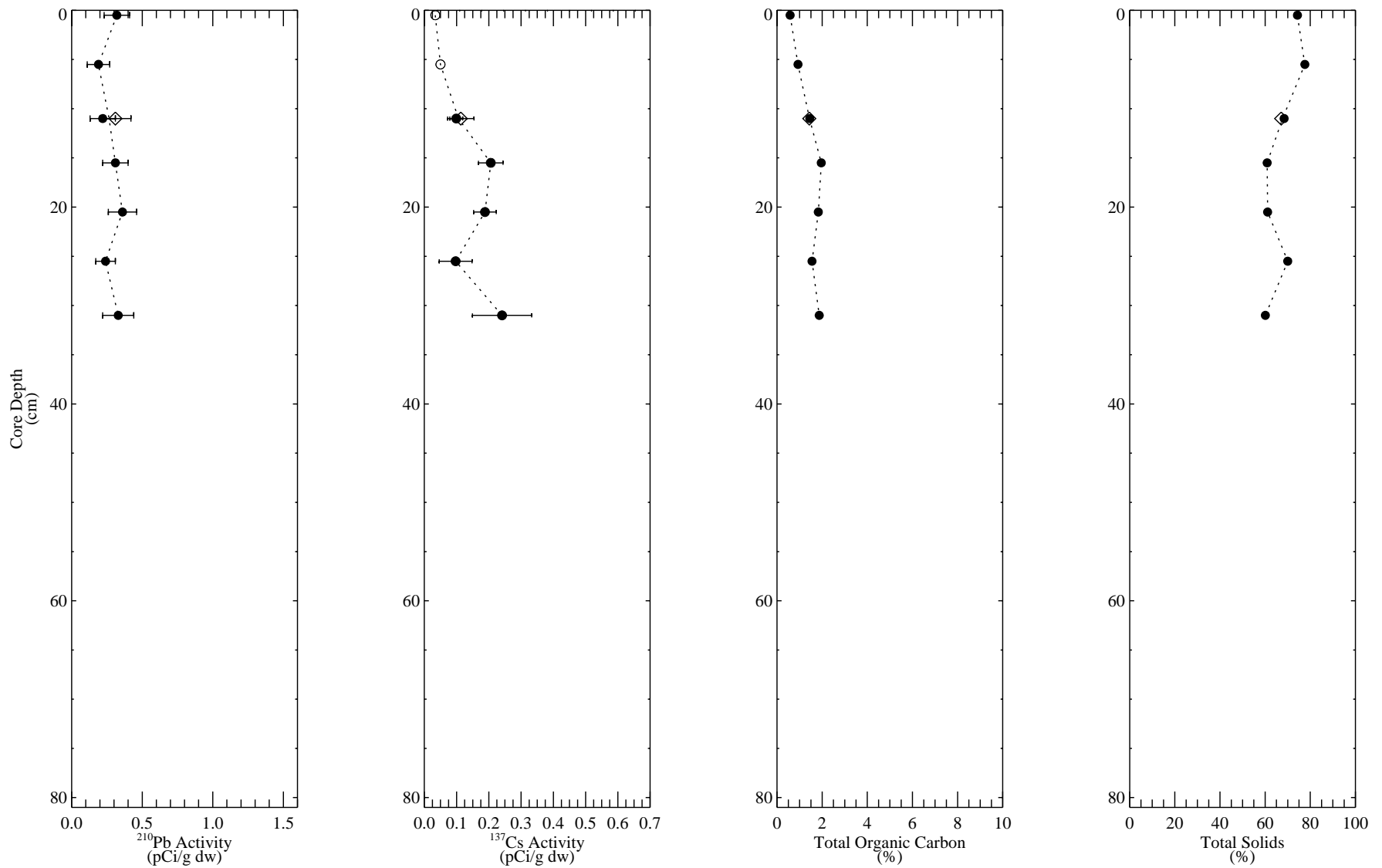


Figure 2-24. Vertical profiles of ^{210}Pb and ^{137}Cs activity, total organic carbon and total solids for core Sg-11c.

Error bars on ^{210}Pb and ^{137}Cs panels represent 95% confidence intervals around the best estimate as reported by the laboratory.

Cross-hatching represents approximate range of ^{137}Cs peak.

Orange square symbols represent samples analyzed from archive.

- Below Detection Limit
- ◇ Field Duplicate
- Archive Samples

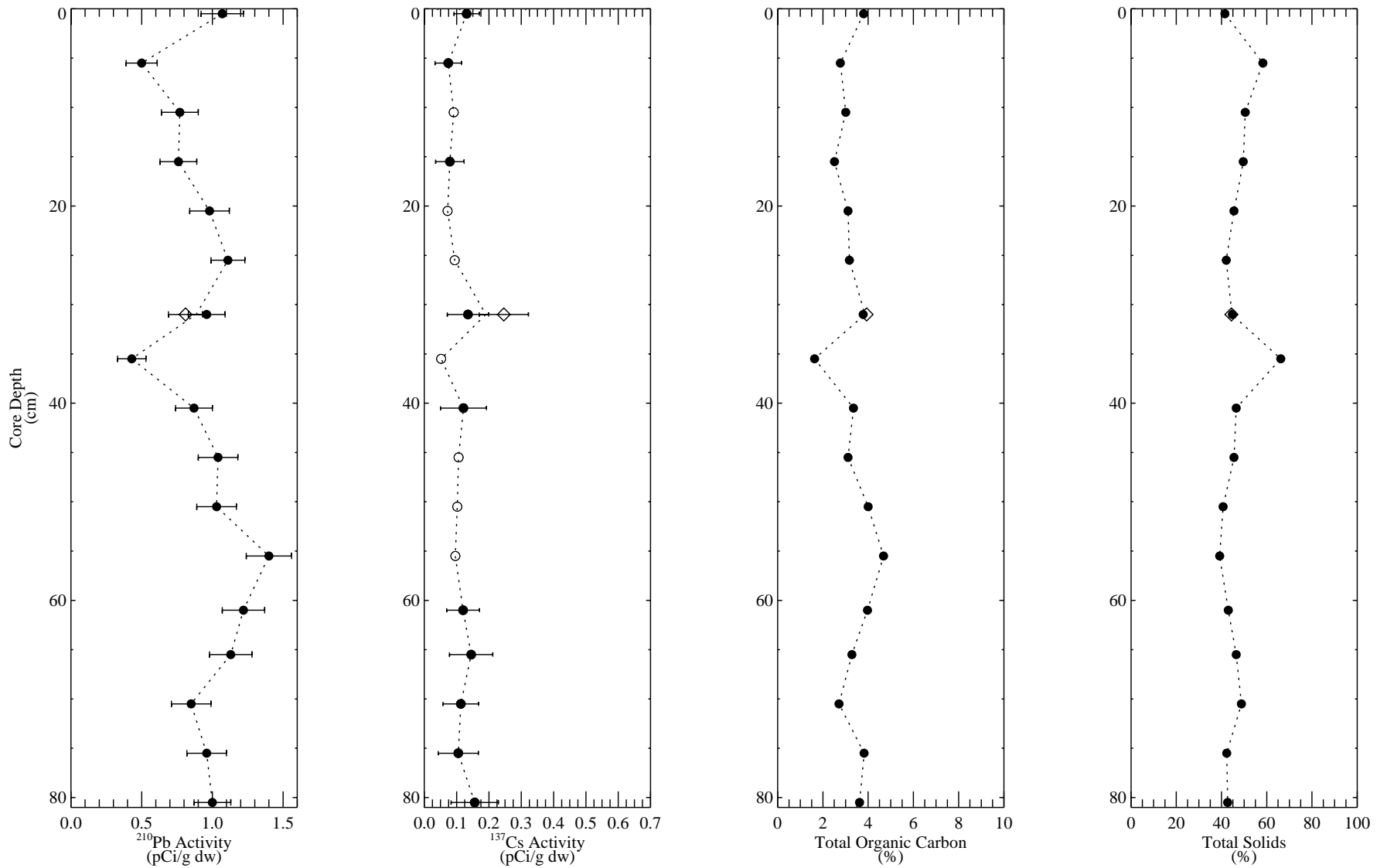
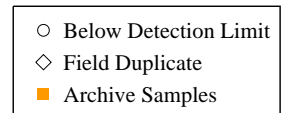


Figure 2-25. Vertical profiles of ^{210}Pb and ^{137}Cs activity, total organic carbon and total solids for core Sg-12.

Error bars on ^{210}Pb and ^{137}Cs panels represent 95% confidence intervals around the best estimate as reported by the laboratory.

Cross-hatching represents approximate range of ^{137}Cs peak.

Orange square symbols represent samples analyzed from archive.



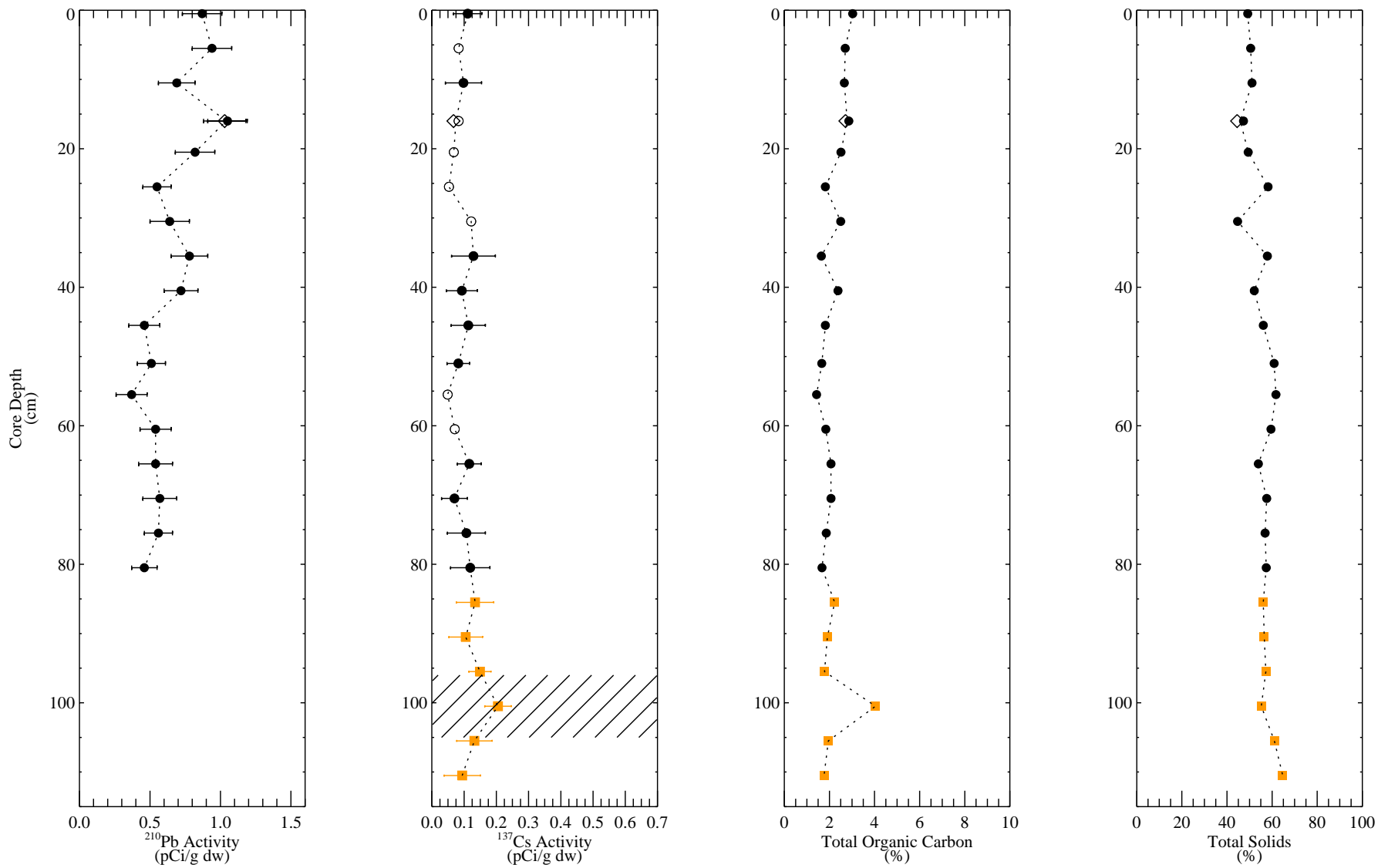
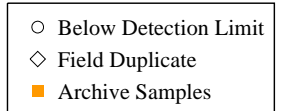


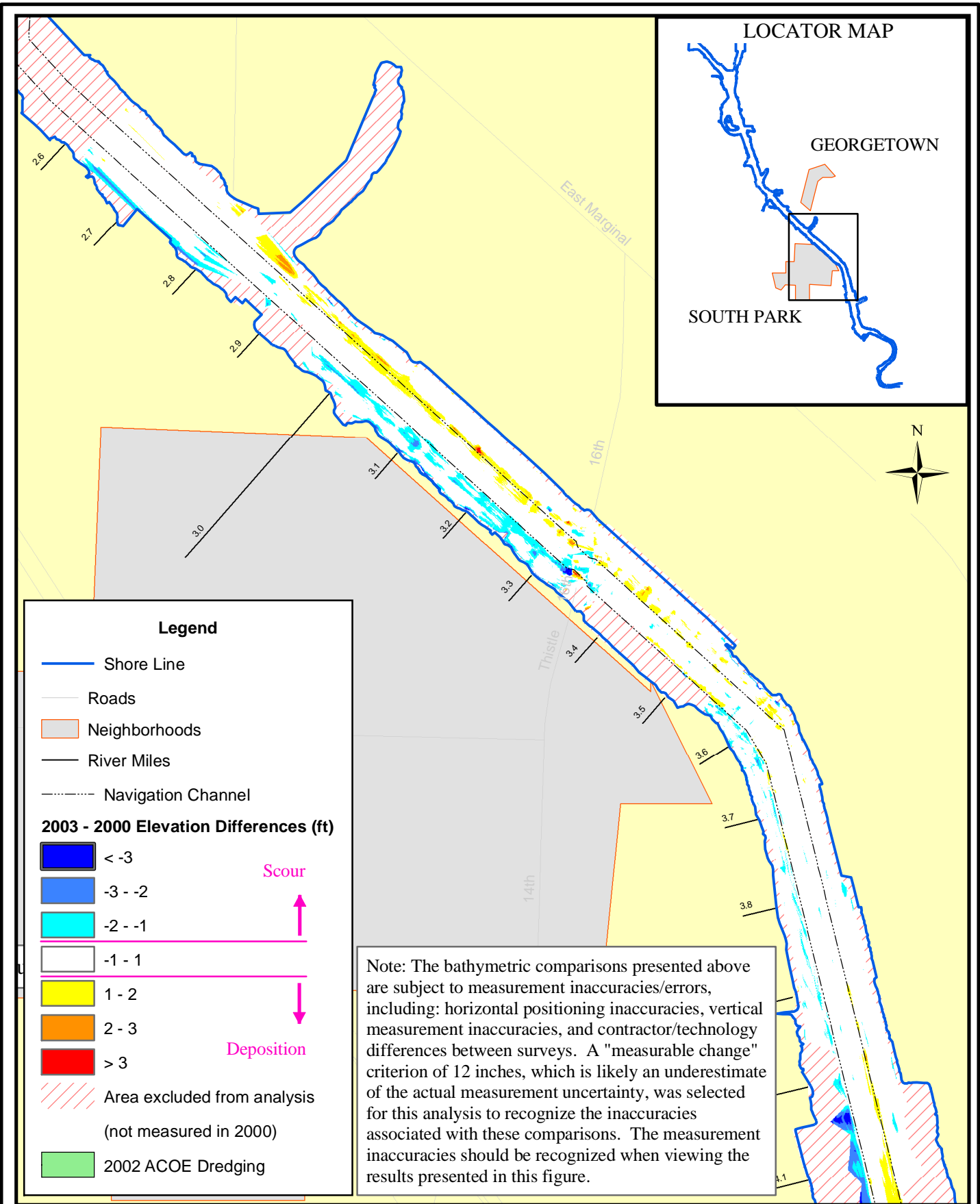
Figure 2-26. Vertical profiles of ^{210}Pb and ^{137}Cs activity, total organic carbon and total solids for core Sg-13.

Error bars on ^{210}Pb and ^{137}Cs panels represent 95% confidence intervals around the best estimate as reported by the laboratory.

Cross-hatching represents approximate range of ^{137}Cs peak.

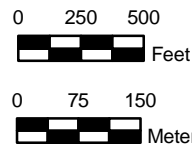
Orange square symbols represent samples analyzed from archive.

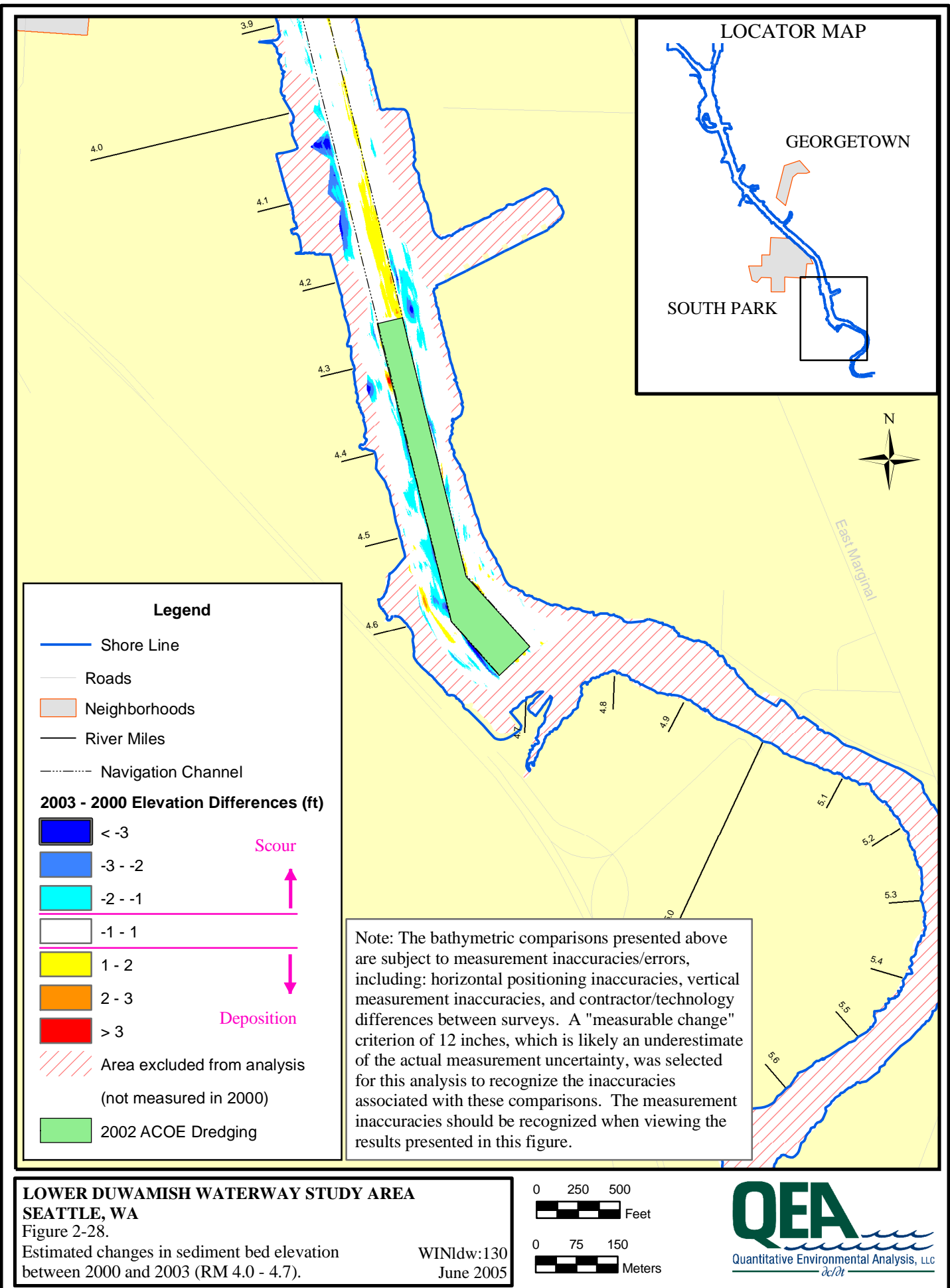


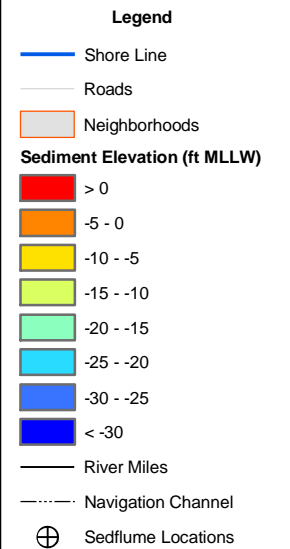
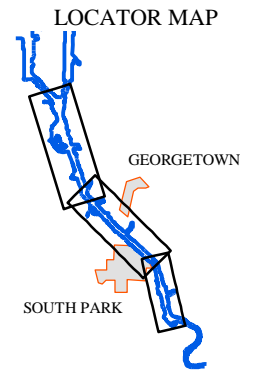
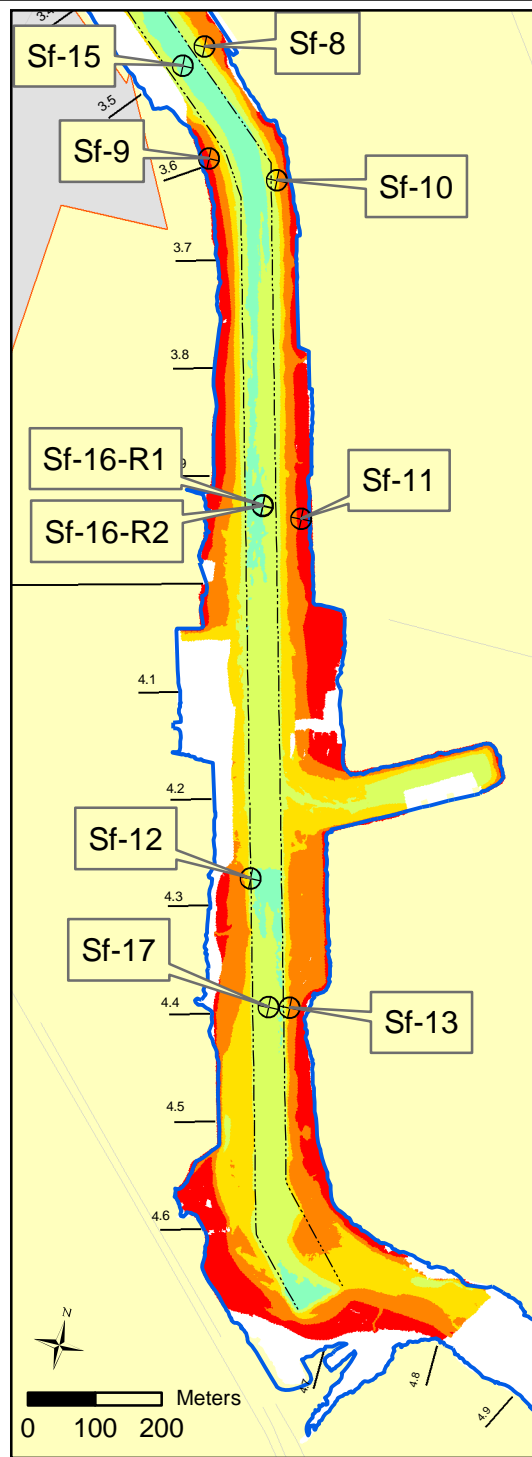
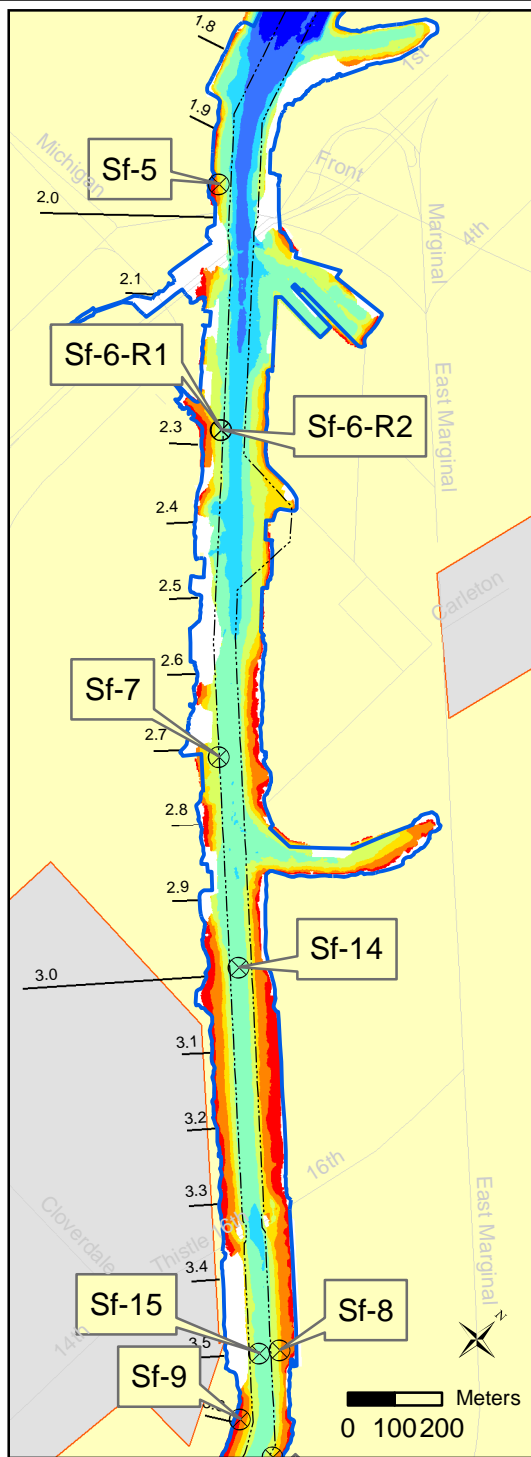
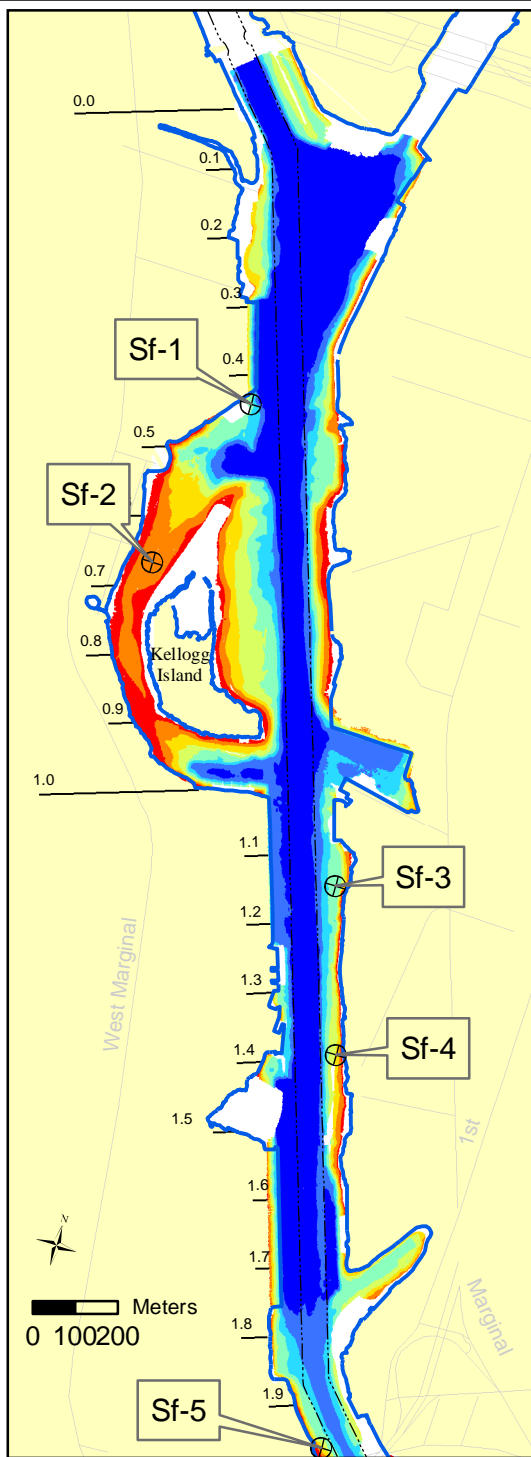


LOWER DUWAMISH WATERWAY STUDY AREA
SEATTLE, WA
 Figure 2-27.
 Estimated changes in sediment bed elevation
 between 2000 and 2003 (RM 2.6 - 4.0).

WINldw:130
 June 2005







LOWER DUWAMISH WATERWAY STUDY AREA SEATTLE, WA
 Figure 3-1. Sedflume core sampling locations.

WINldw:130 October 2005



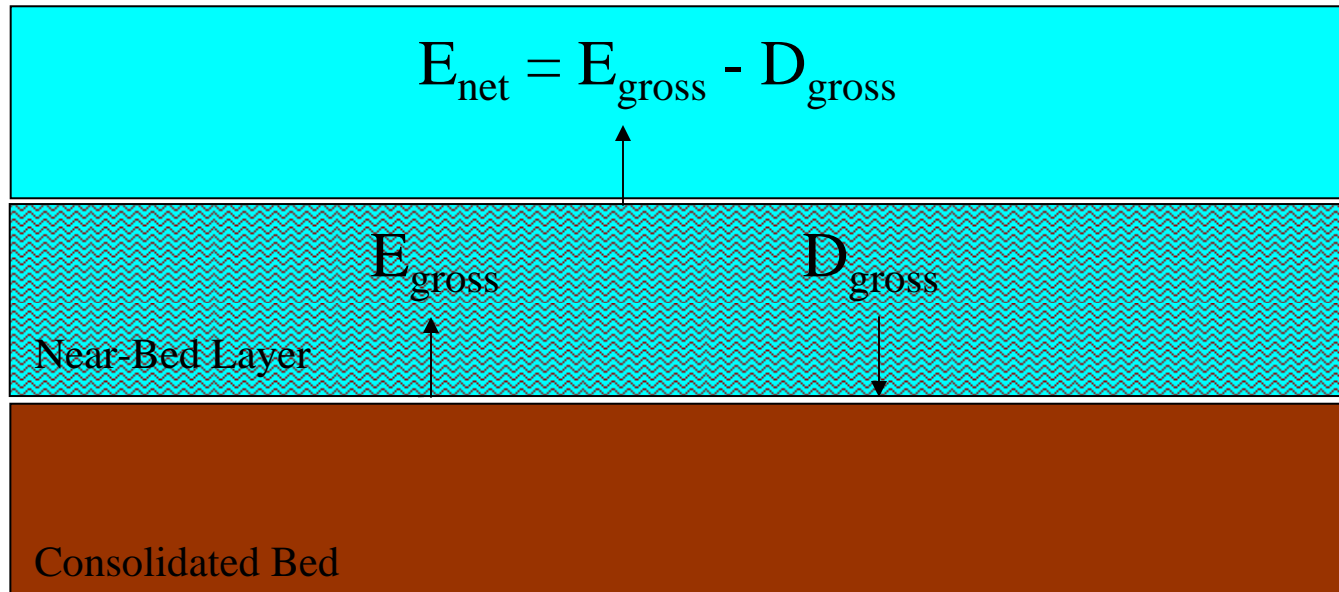


Figure 3-2. Relationship between net (E_{net}) and gross (E_{gross}) erosion rates and gross deposition rate (D_{gross}).

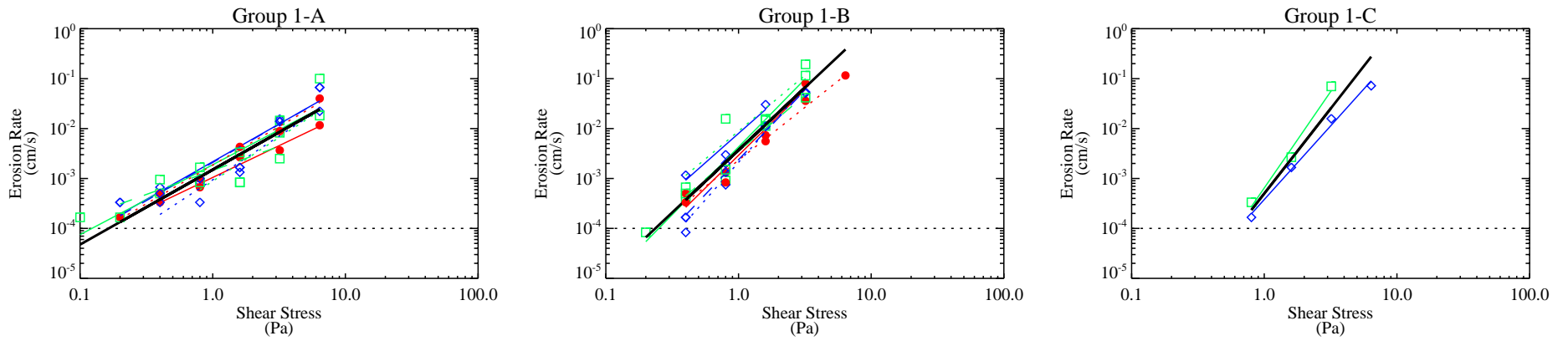


Figure 3-3. Erosion rate data (symbols) and corresponding log-linear regression results (dashed lines) for individual cores in each core group for 0-5 cm layer. Solid line represents average log-linear regression line for the group.

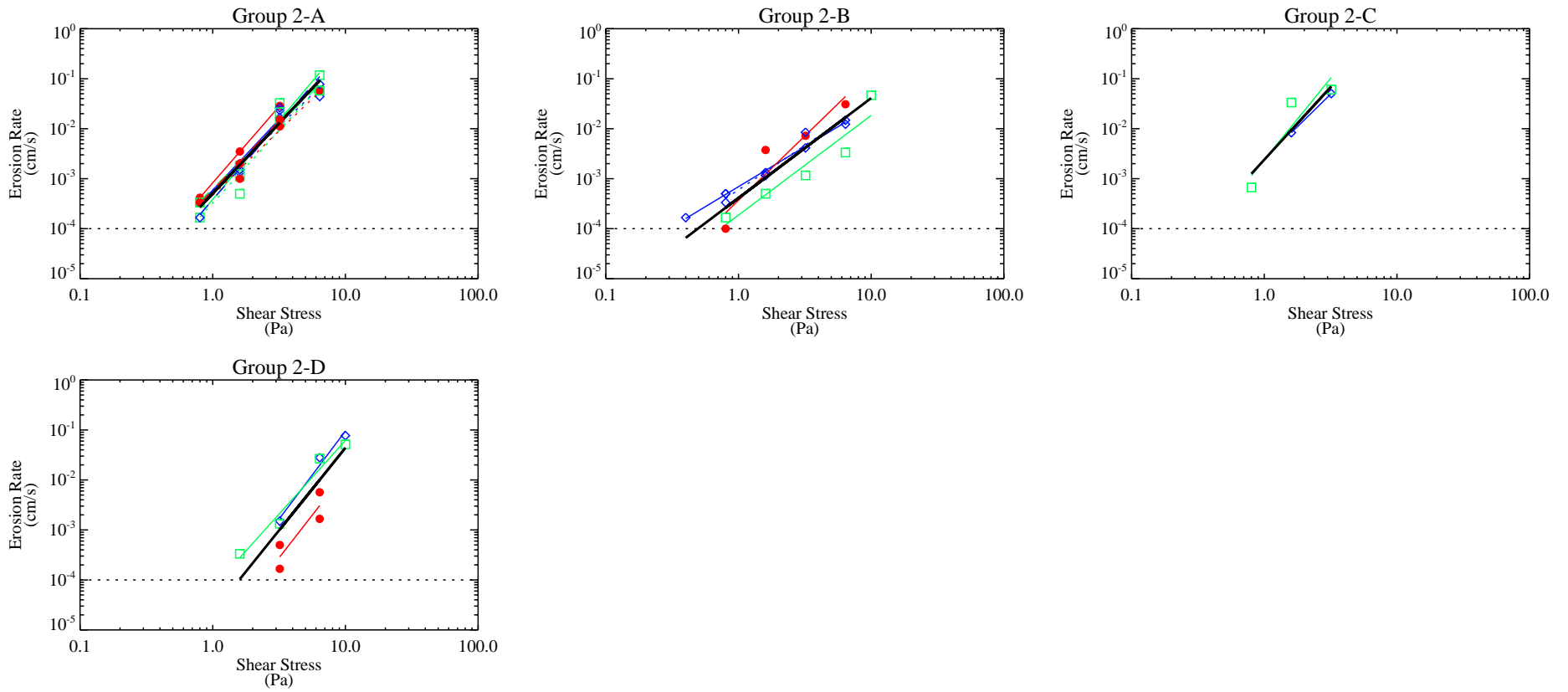


Figure 3-4. Erosion rate data (symbols) and corresponding log-linear regression results (dashed lines) for individual cores in each core group for 5-10 cm layer. Solid line represents average log-linear regression line for the group.

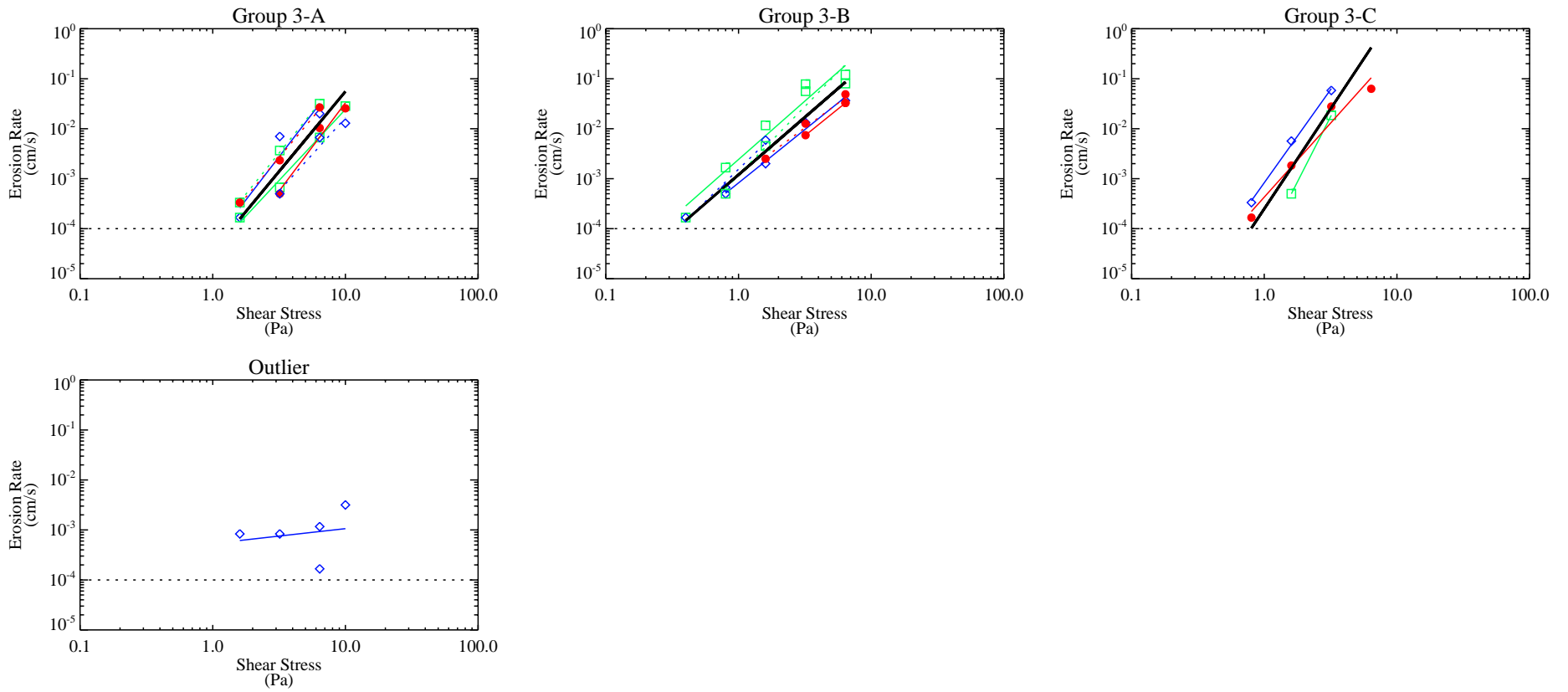


Figure 3-5. Erosion rate data (symbols) and corresponding log-linear regression results (dashed lines) for individual cores in each core group for 10-15 cm layer. Solid line represents average log-linear regression line for the group.

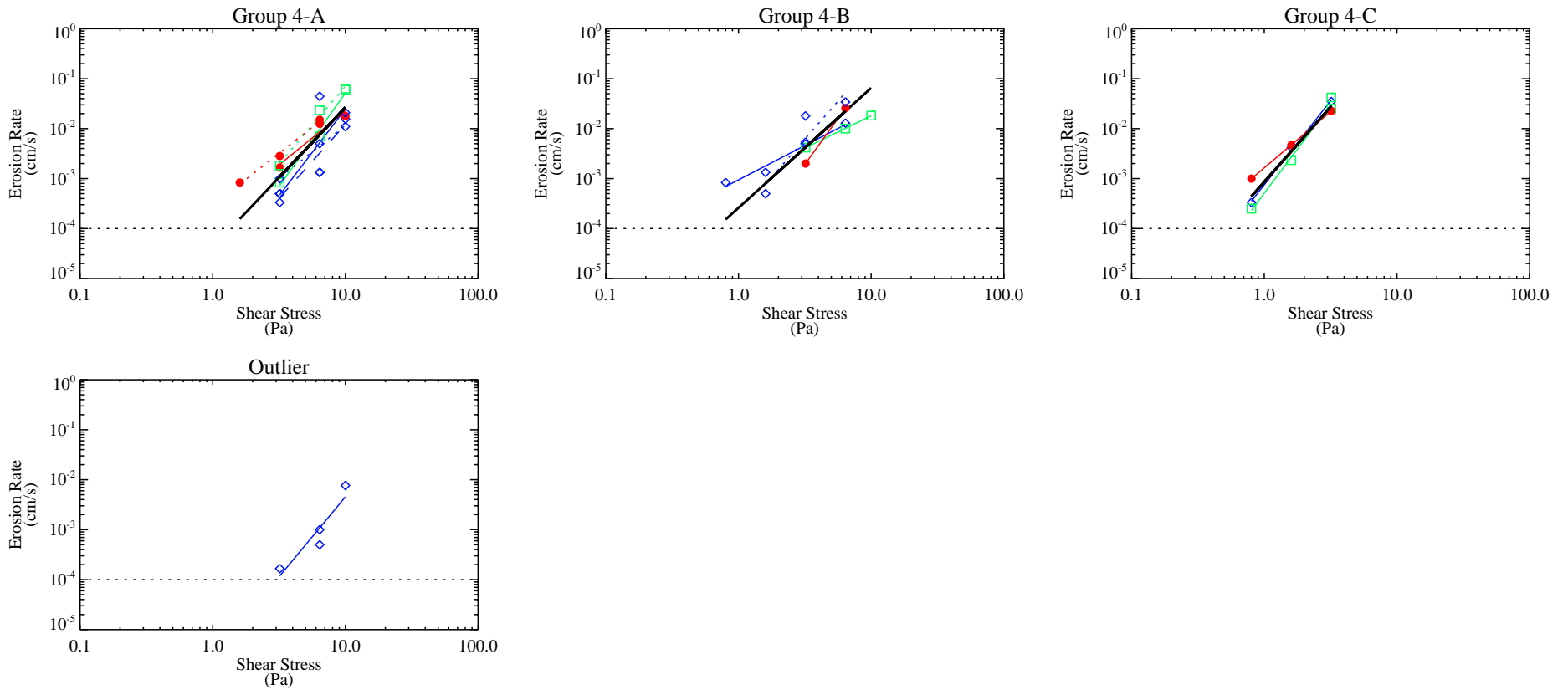


Figure 3-6. Erosion rate data (symbols) and corresponding log-linear regression results (dashed lines) for individual cores in each core group for 15-20 cm layer. Solid line represents average log-linear regression line for the group.

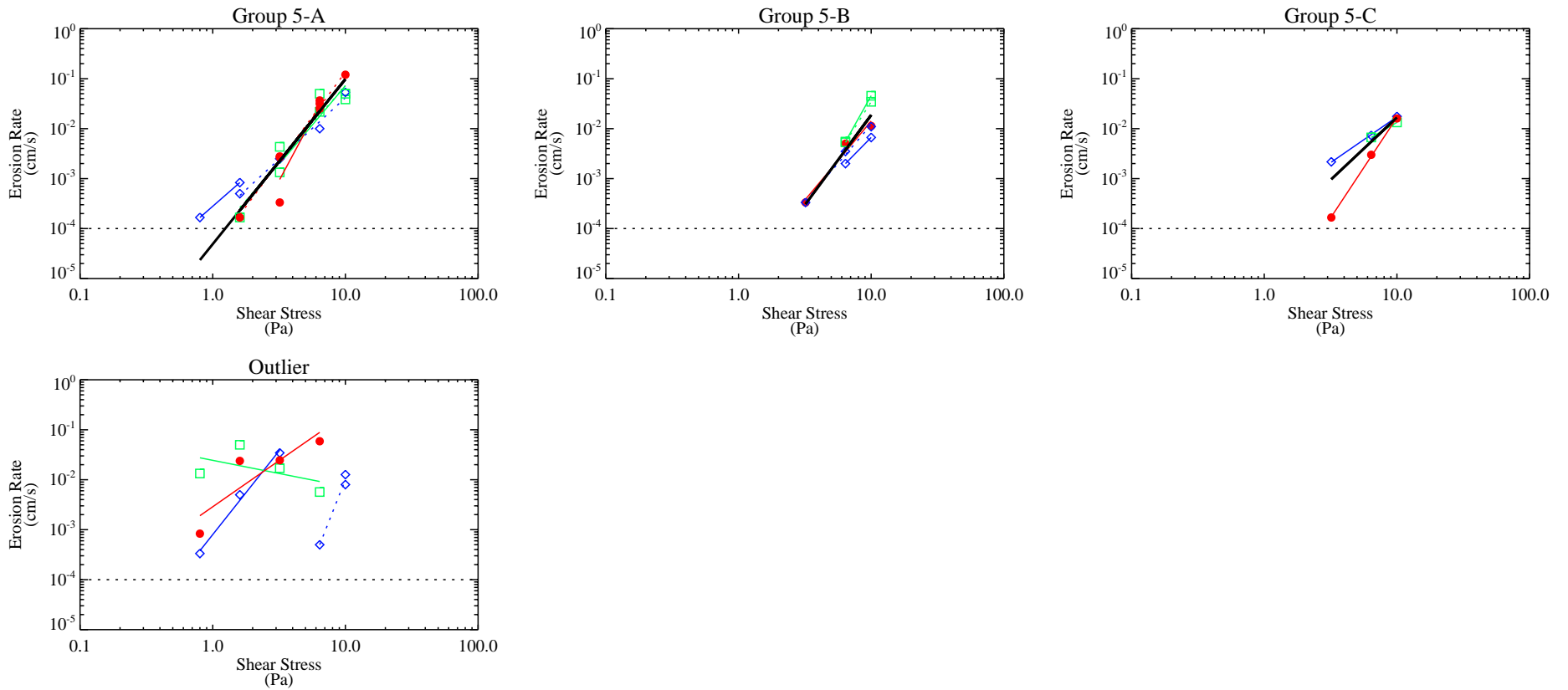


Figure 3-7. Erosion rate data (symbols) and corresponding log-linear regression results (dashed lines) for individual cores in each core group for 20-25 cm layer. Solid line represents average log-linear regression line for the group.

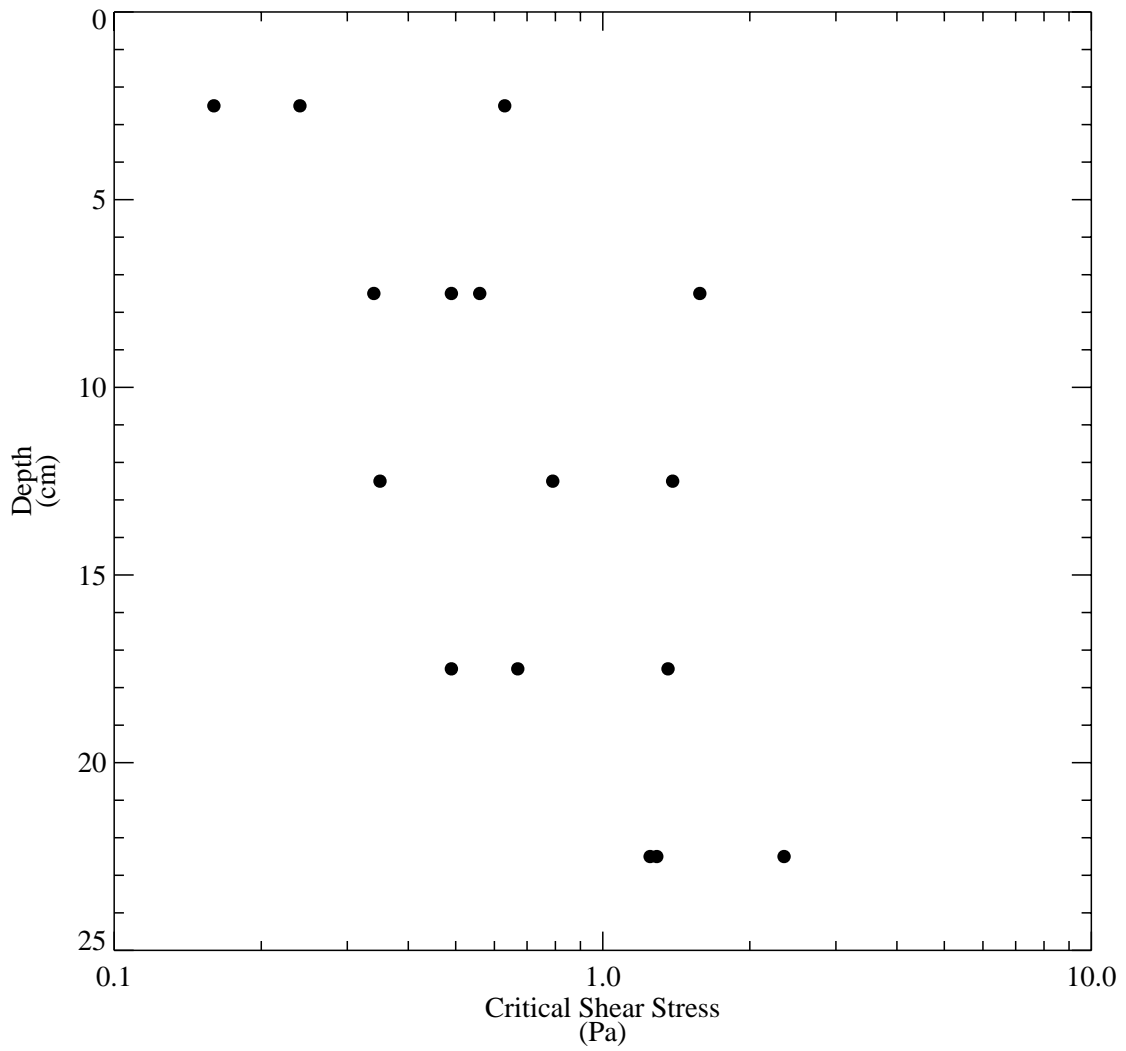


Figure 3-8. Vertical distribution of group-average critical shear stress values.

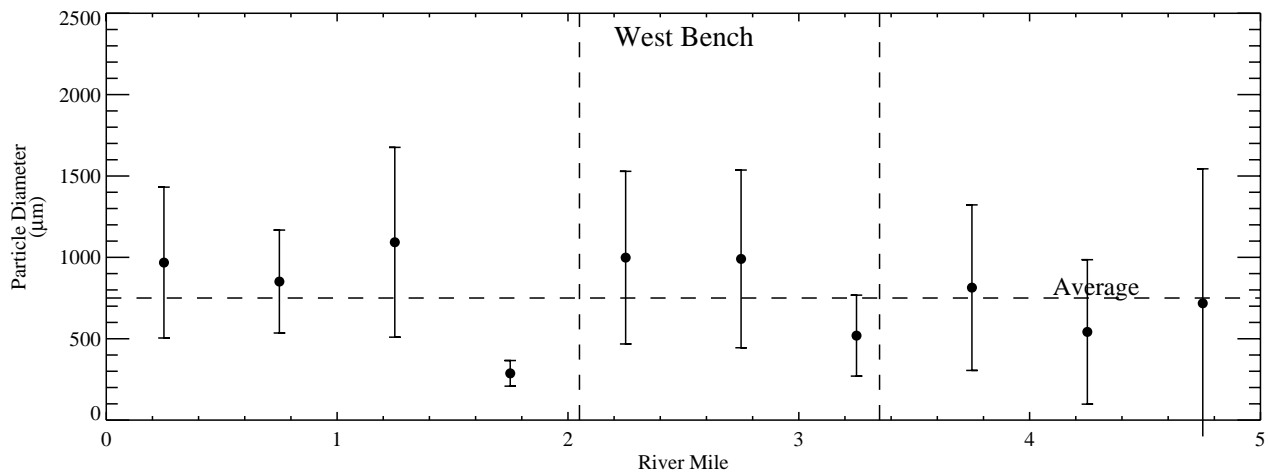
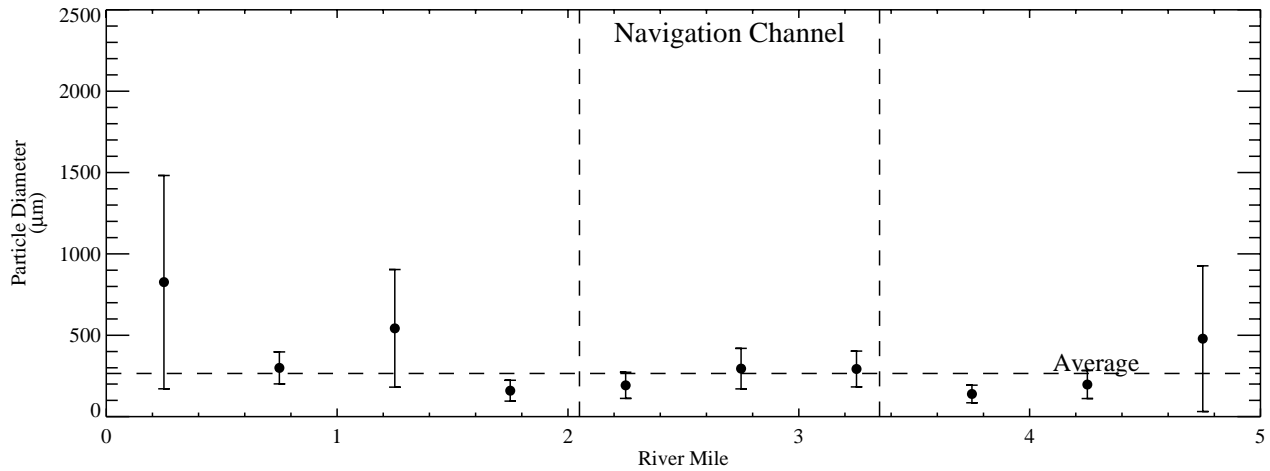
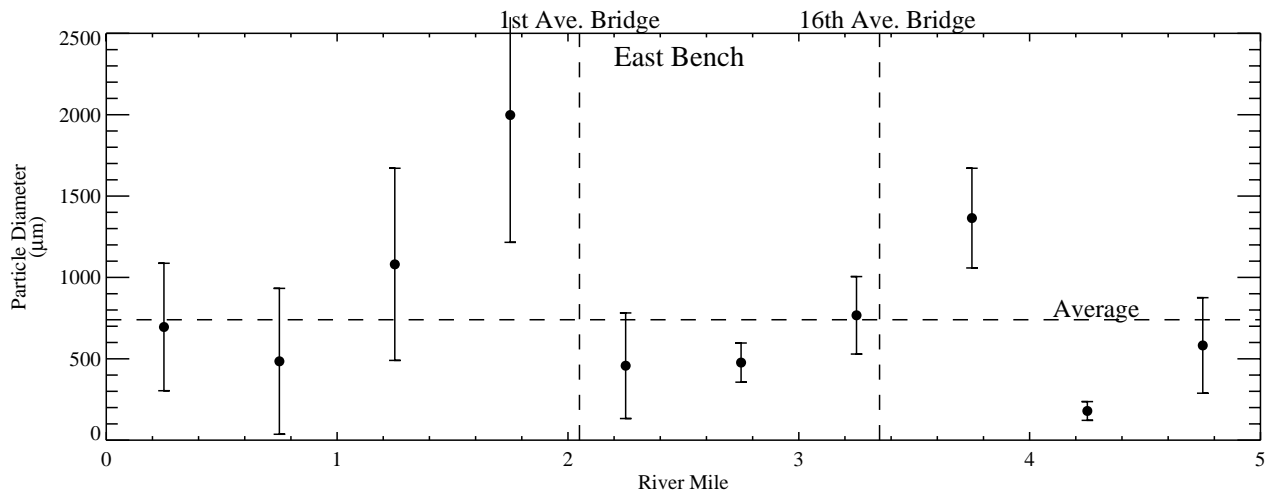
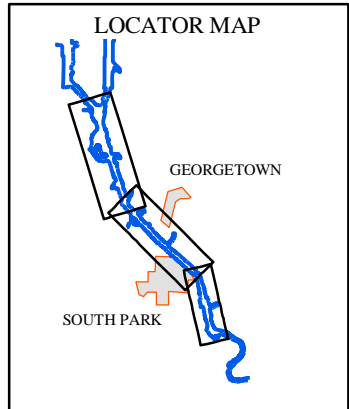
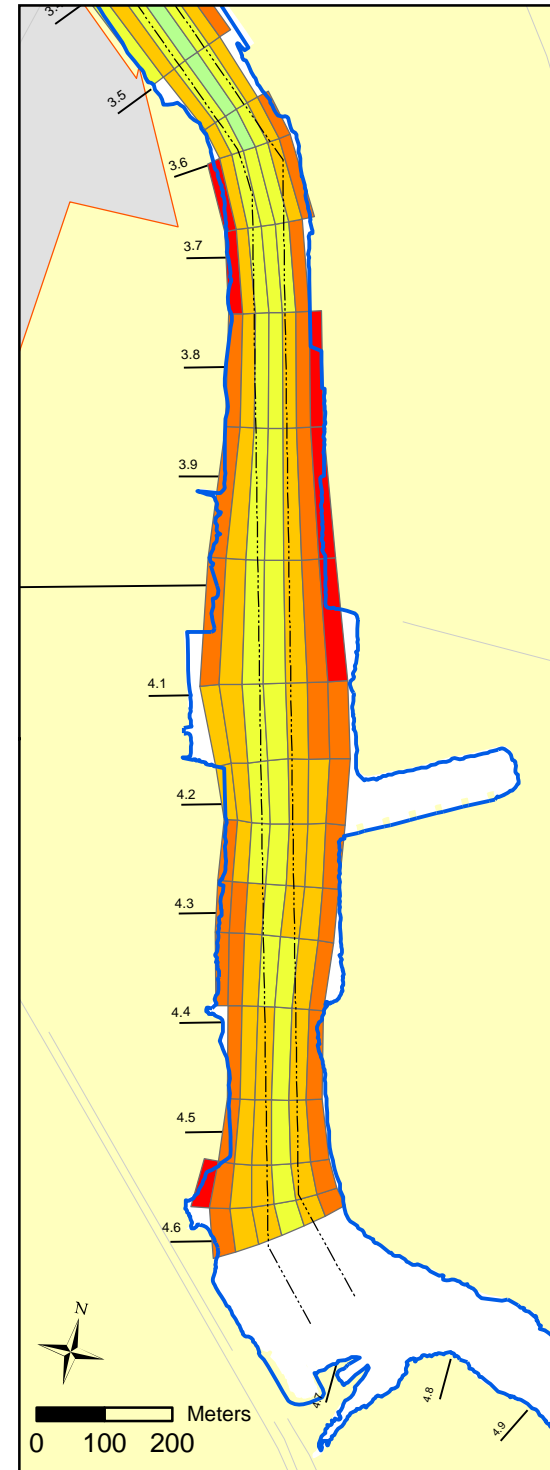
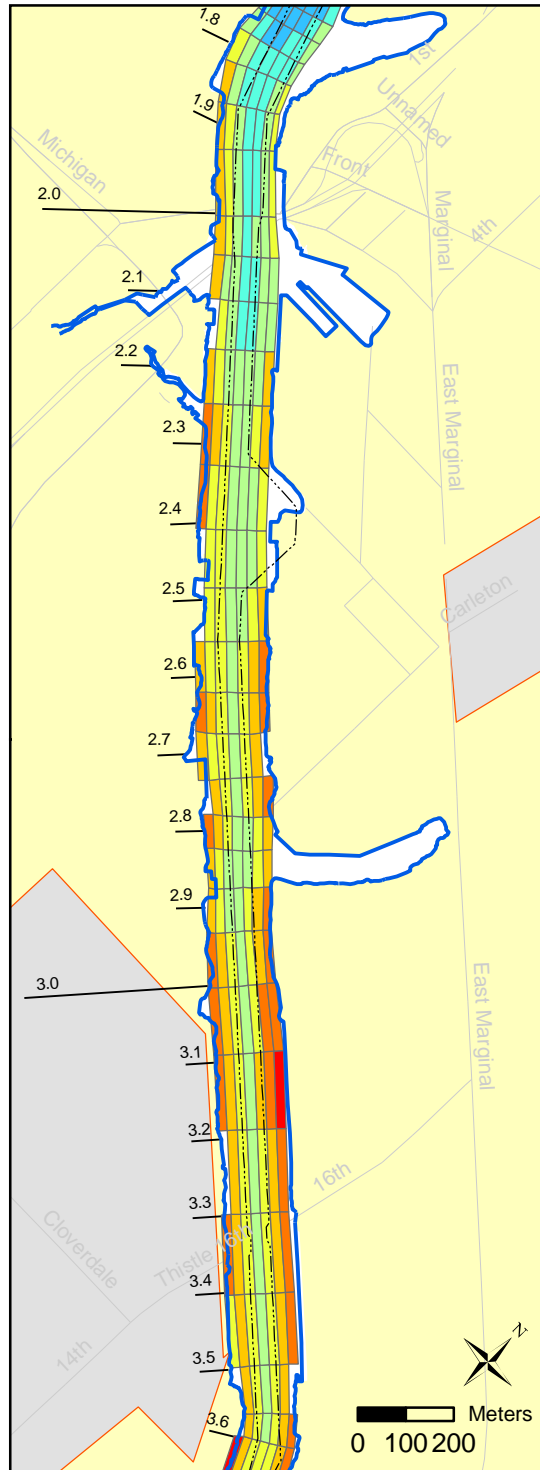
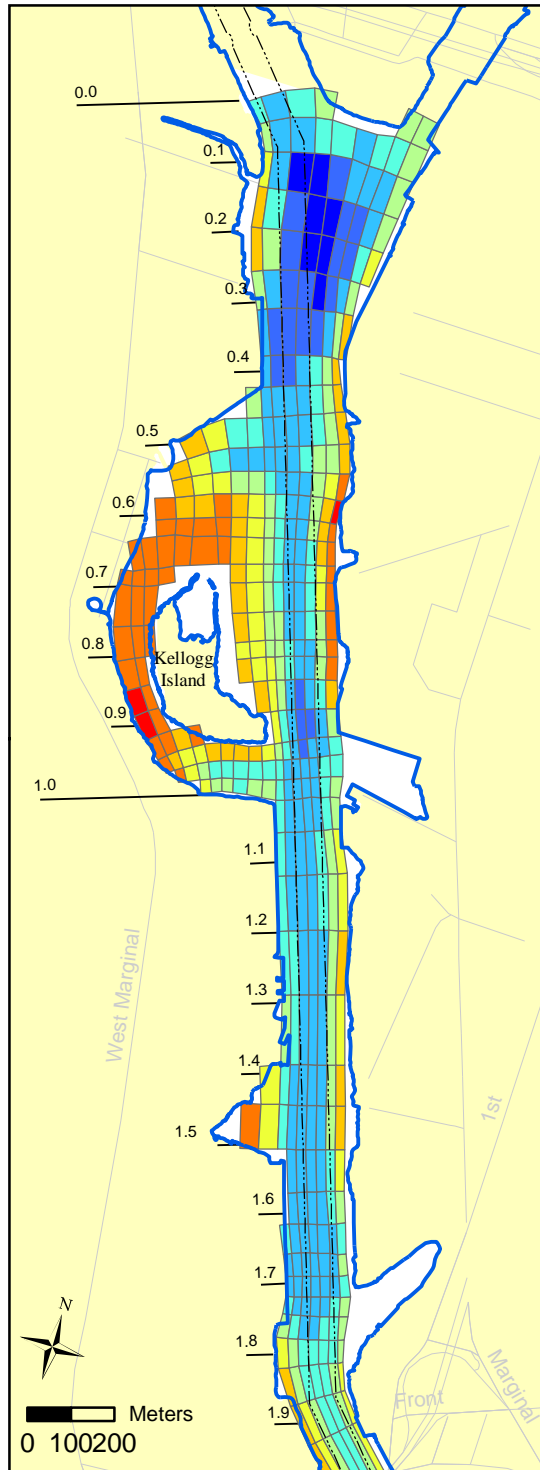


Figure 3-9. Spatial distribution of D_{90} in surface layer (0 - 1 ft) of LDW sediment. Raw data are binned in 0.5 mile segments and presented as mean (solid circle) and 2 standard errors about the mean (bar).

Grain size data collected from September 1991 to February 2006.

Source 1: \\Daleel\D_DRIVE\WIN\ldw\Data\PCB\050919\BaselineSurface-2005-12-23-AveragedToSampleLevel\BaselineSurface-2005-12-23-AveragedToSampleLevel.mdb

Source 2: \\Daleel\D_DRIVE\WIN\ldw\Data\Grain_Size\061004\LDWG Subsurface Sediment Final Data-2006-10-03 for QEA.xls



Legend

- Shore Line
- Roads
- Neighborhoods
- River Miles
- Navigation Channel

Water Depth (m MSL)

- < 1
- 1 - 3
- 3 - 5
- 5 - 7
- 7 - 9
- 9 - 11
- 11 - 13
- 13 - 15
- > 15

LOWER DUWAMISH WATERWAY STUDY AREA SEATTLE, WA

Figure 3-10.
 Portion of the numerical grid within LDW study area.

WINldw:130 October 2005



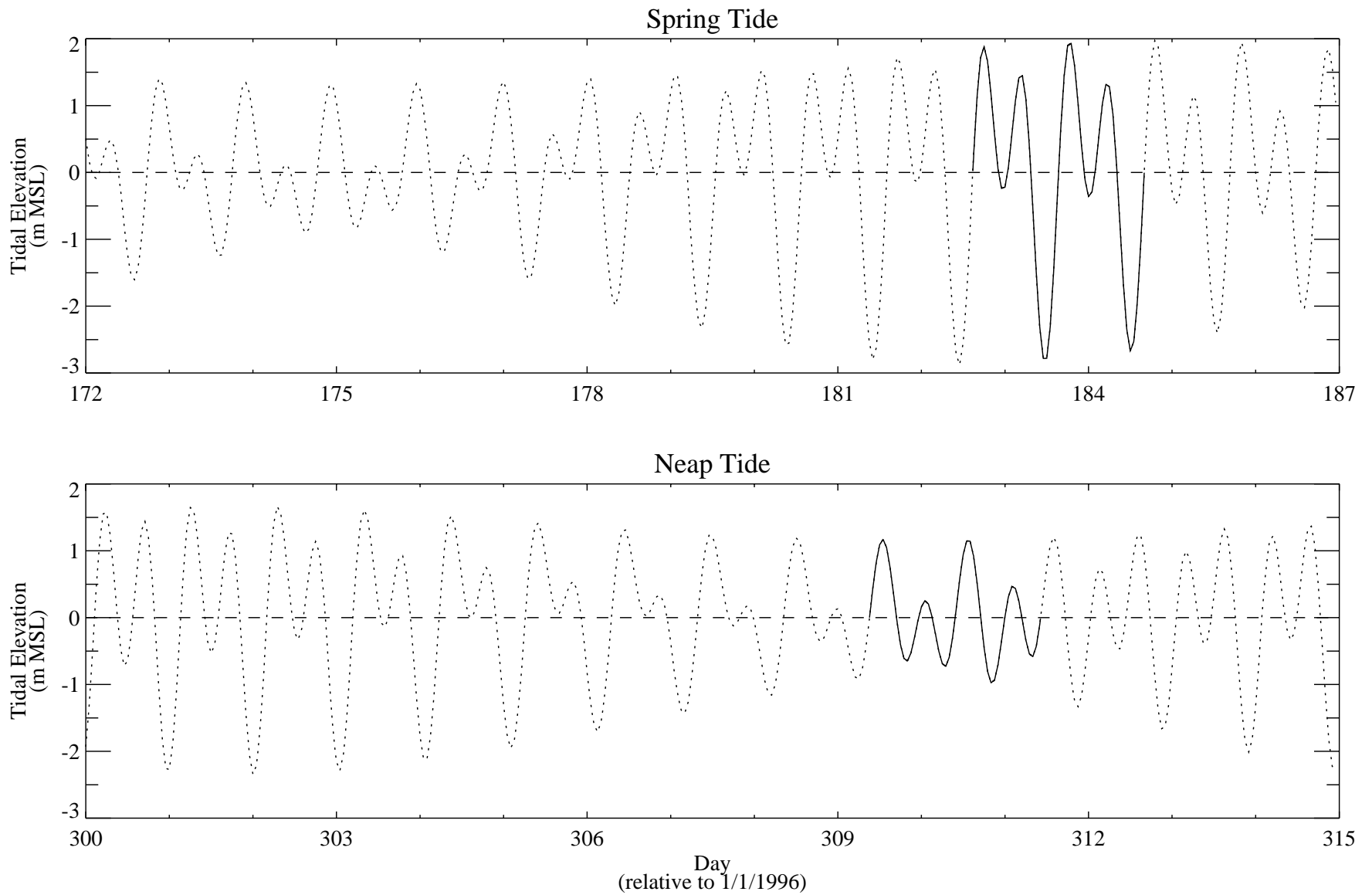


Figure 3-11. Tidal boundary conditions during spring and neap tidal cycles used for high-flow event simulations. Solid line represents 48-hour period used in analysis.

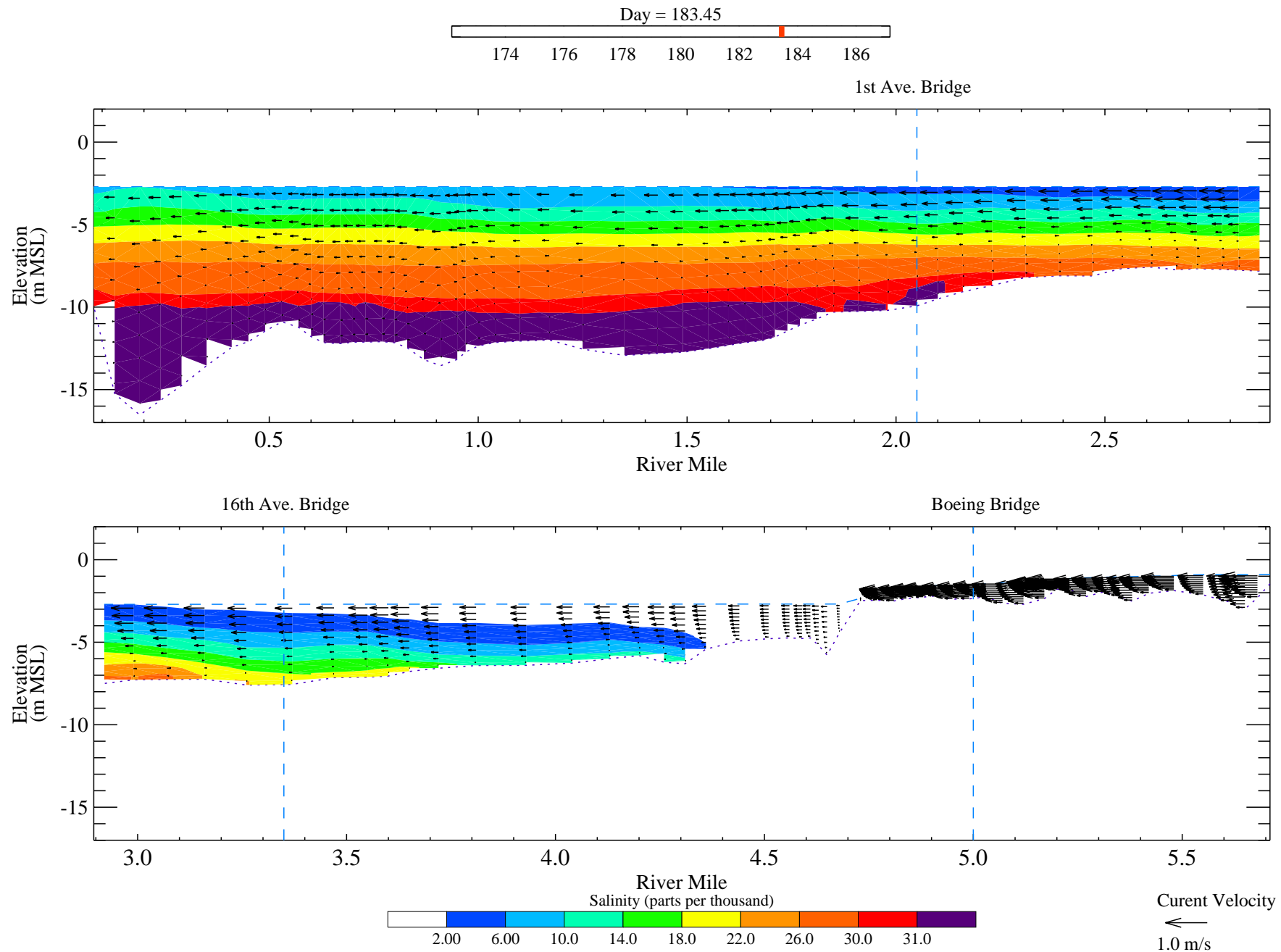


Figure 3-12a. Predicted circulation pattern and salinity distribution in LDW during ebb tide period of average flow (1,340 cfs), spring tide.

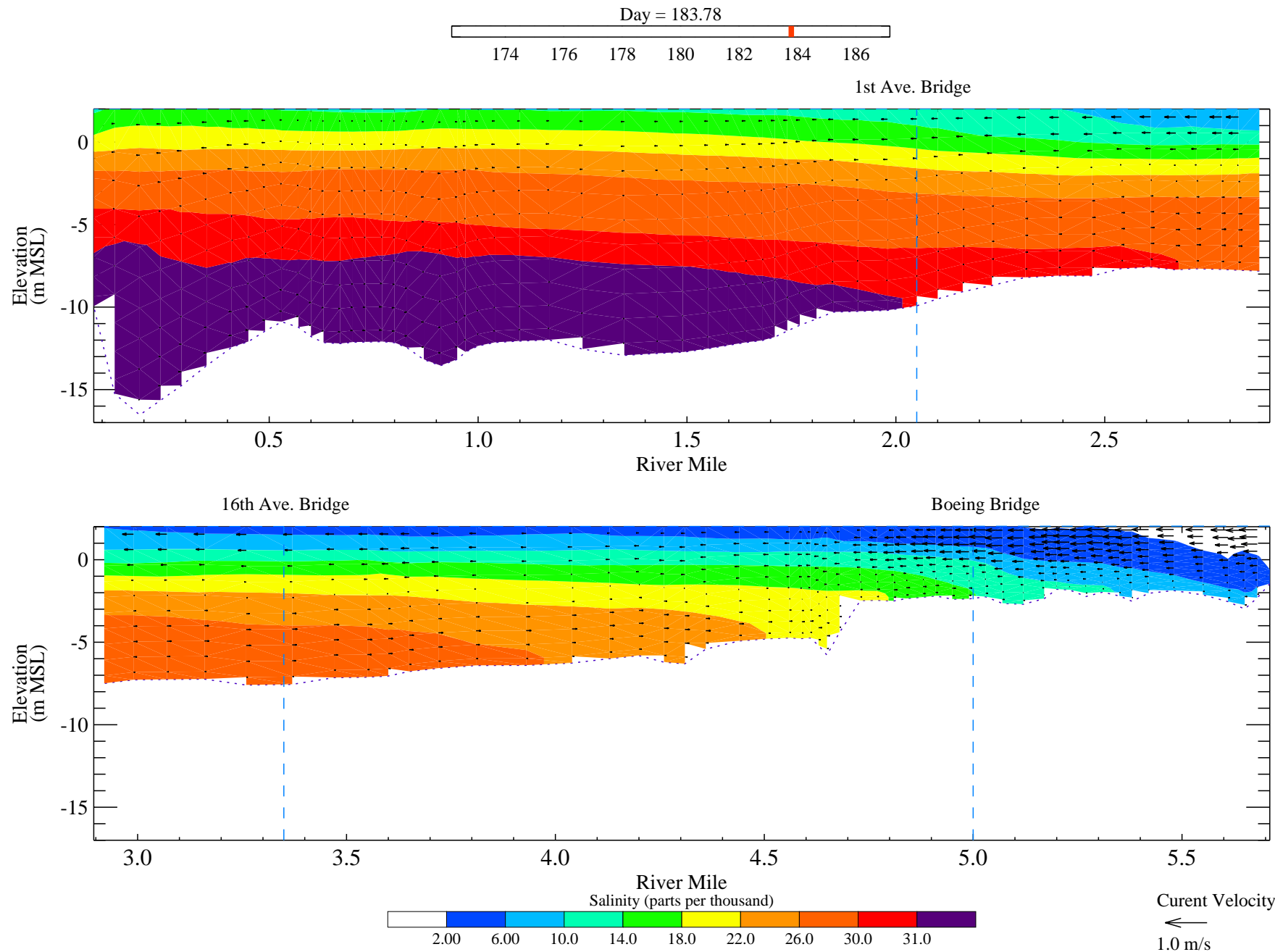


Figure 3-12b. Predicted circulation pattern and salinity distribution in LDW during flood tide period of average flow (1,340 cfs), spring tide.

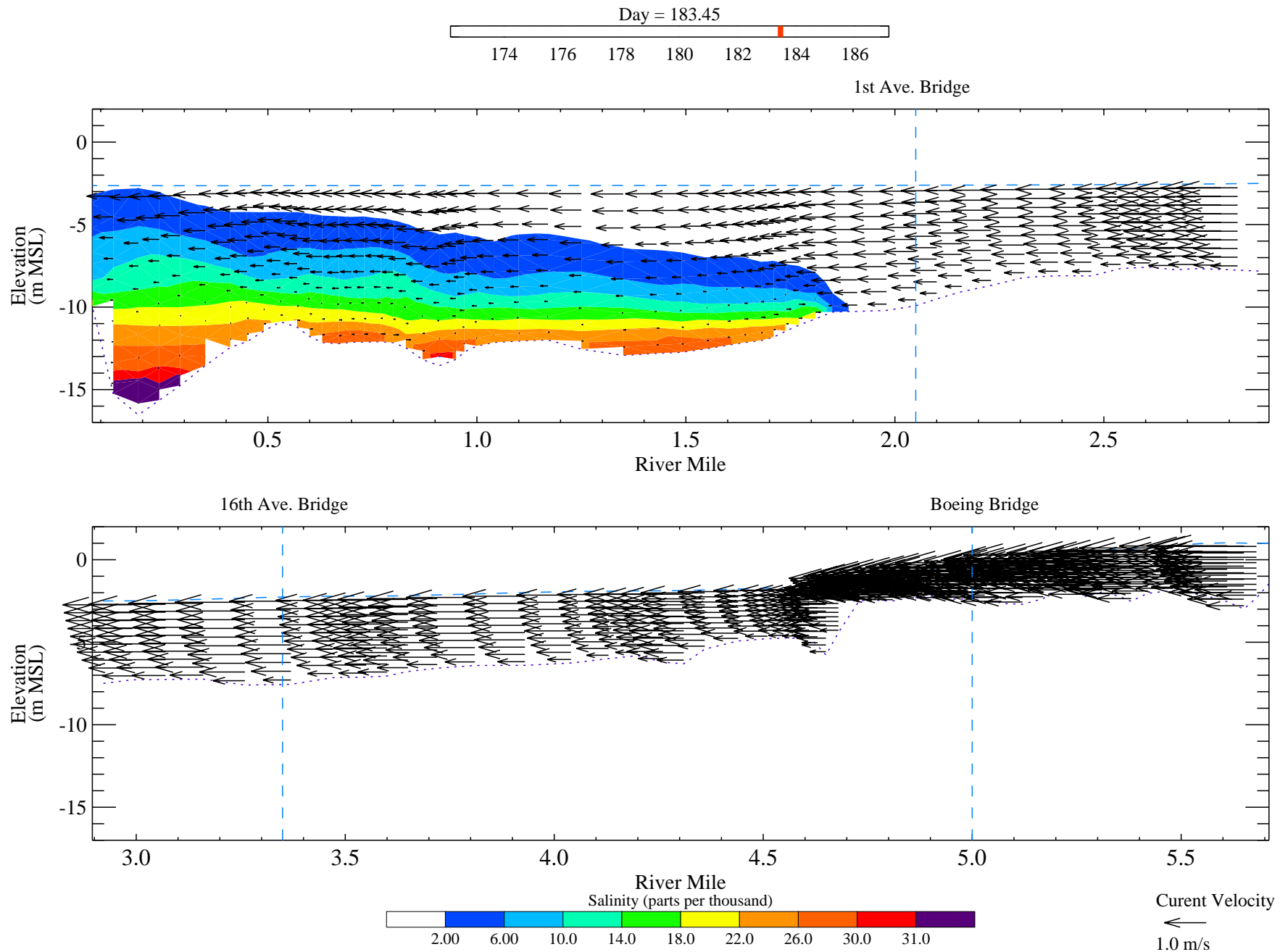


Figure 3-13a. Predicted circulation pattern and salinity distribution in LDW during ebb tide period of 100-yr high flow event (12,000 cfs), spring tide.

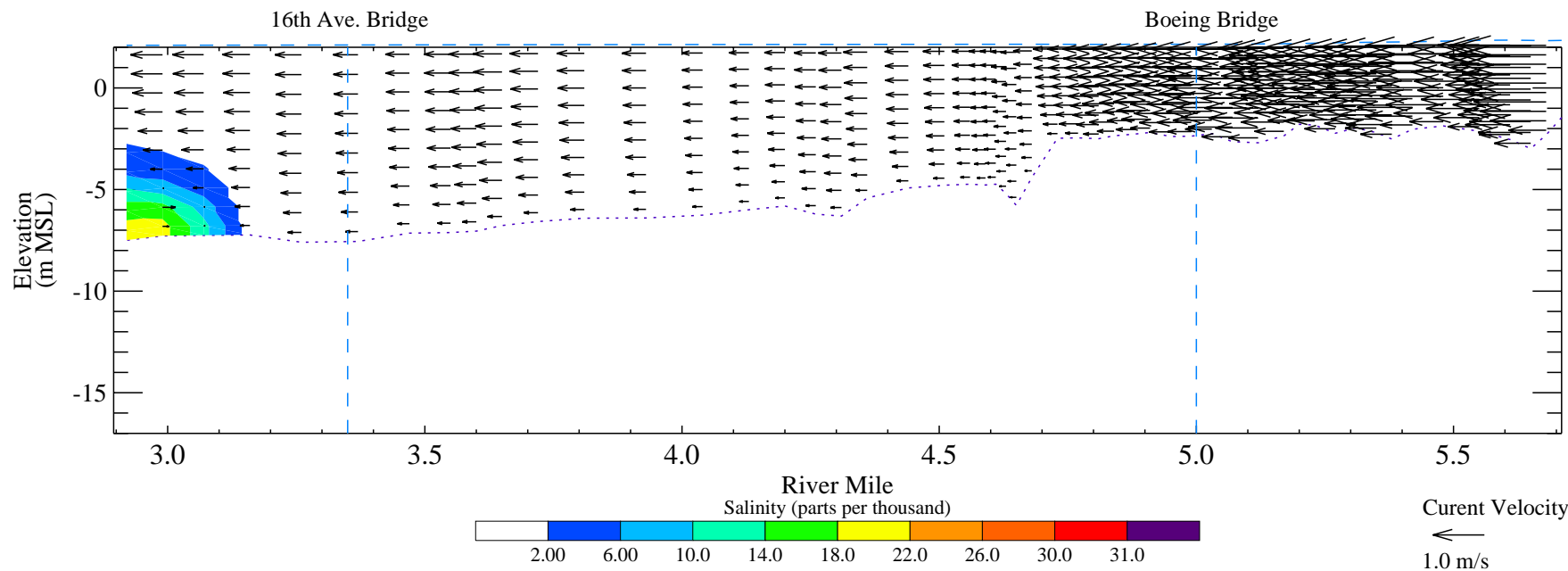
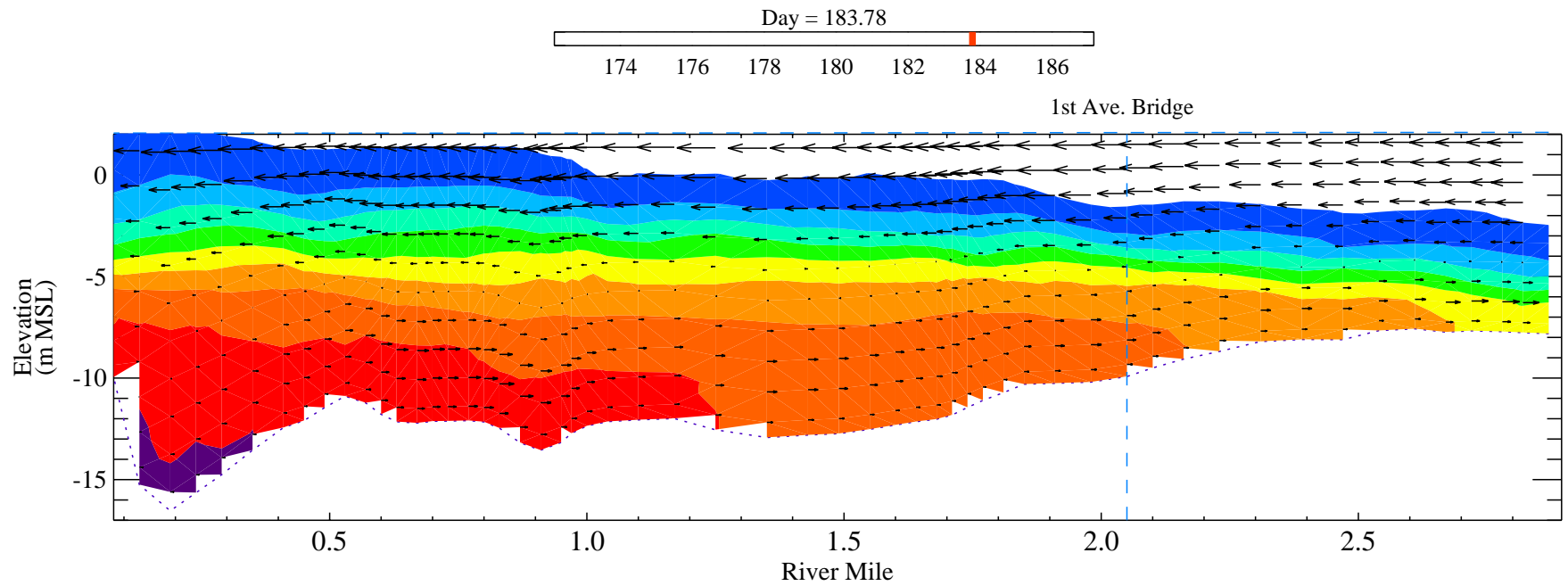
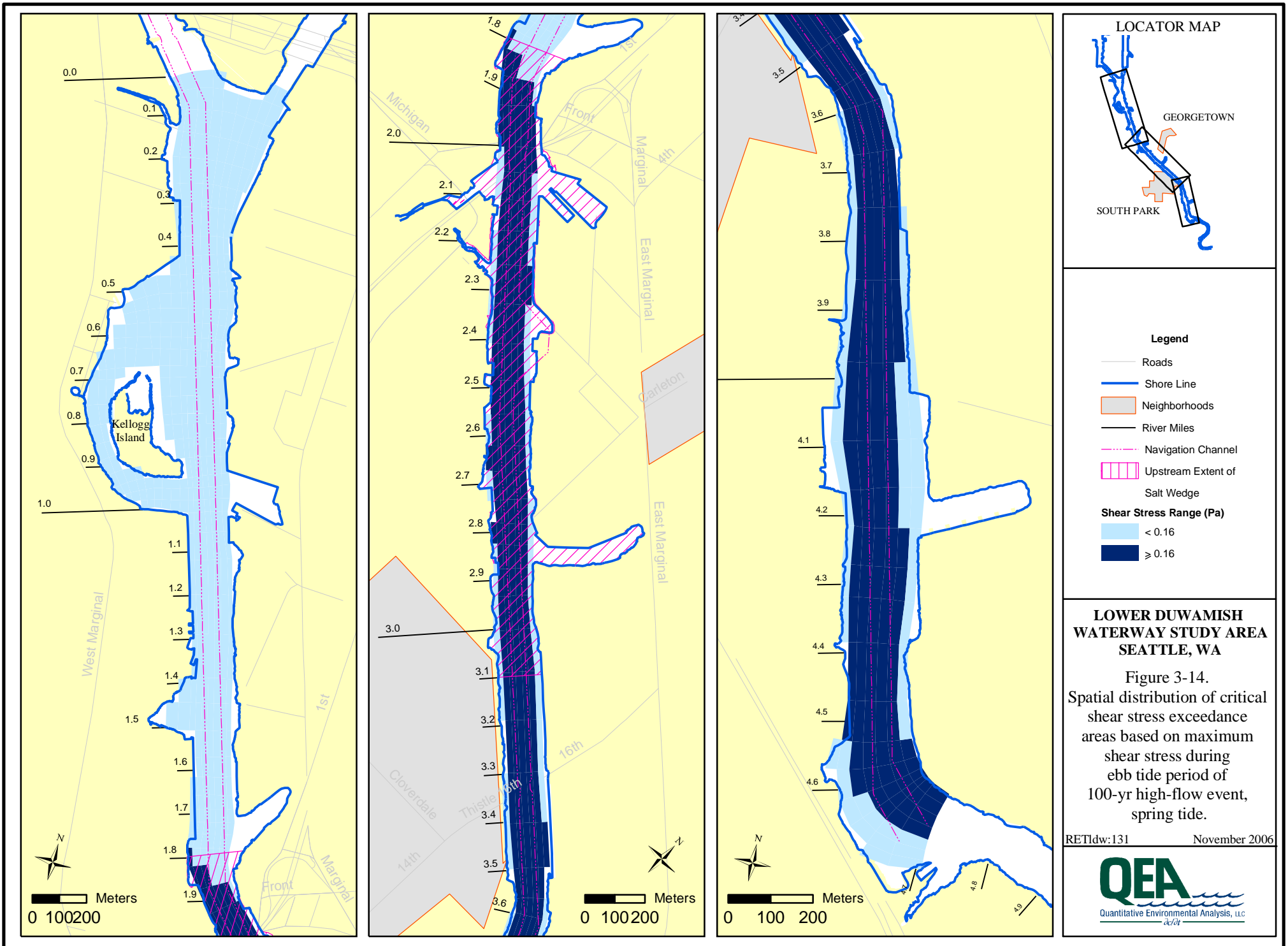
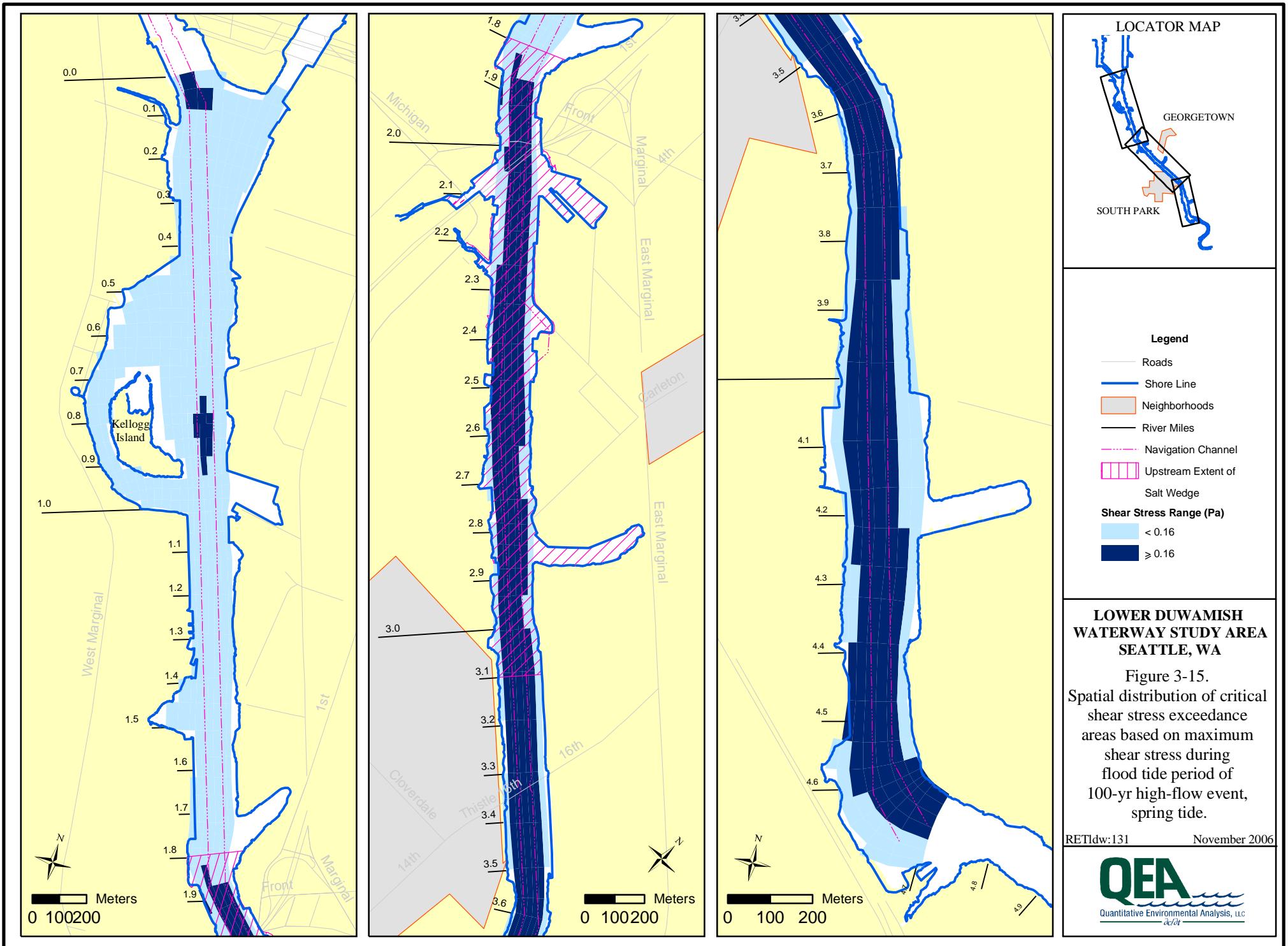
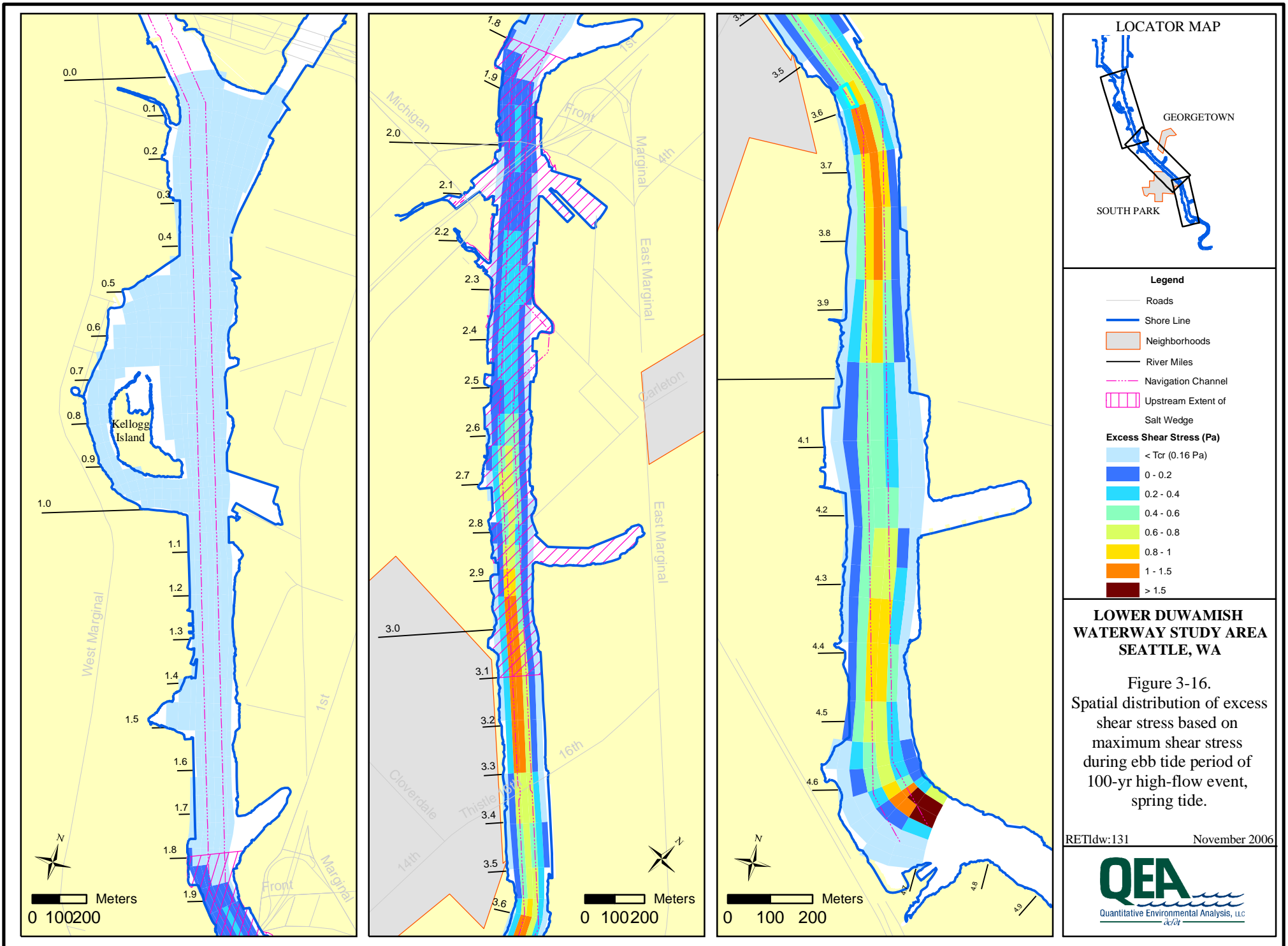
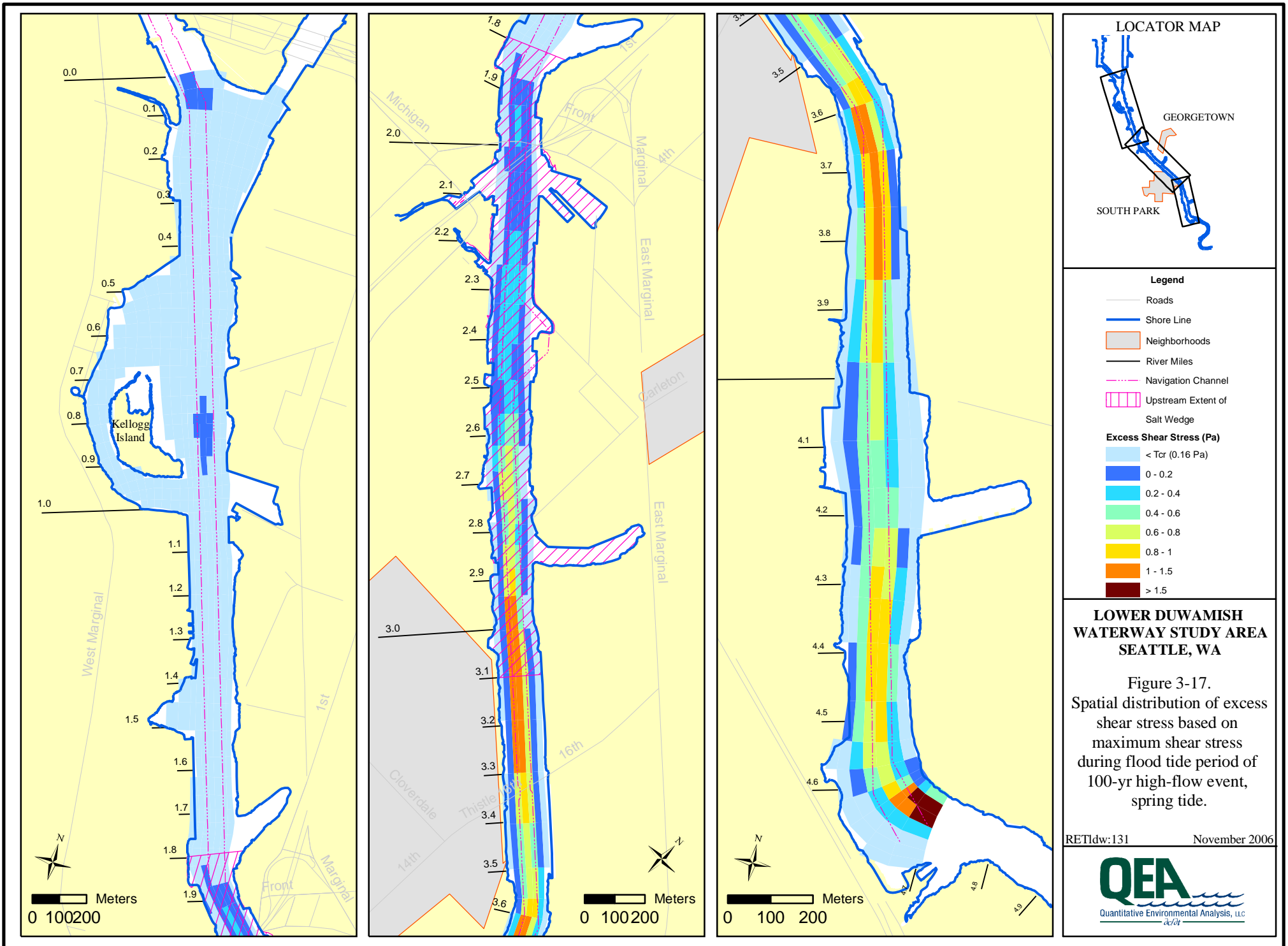


Figure 3-13b. Predicted circulation pattern and salinity distribution in LDW during flood tide period of 100-yr high flow event (12,000 cfs), spring tide.









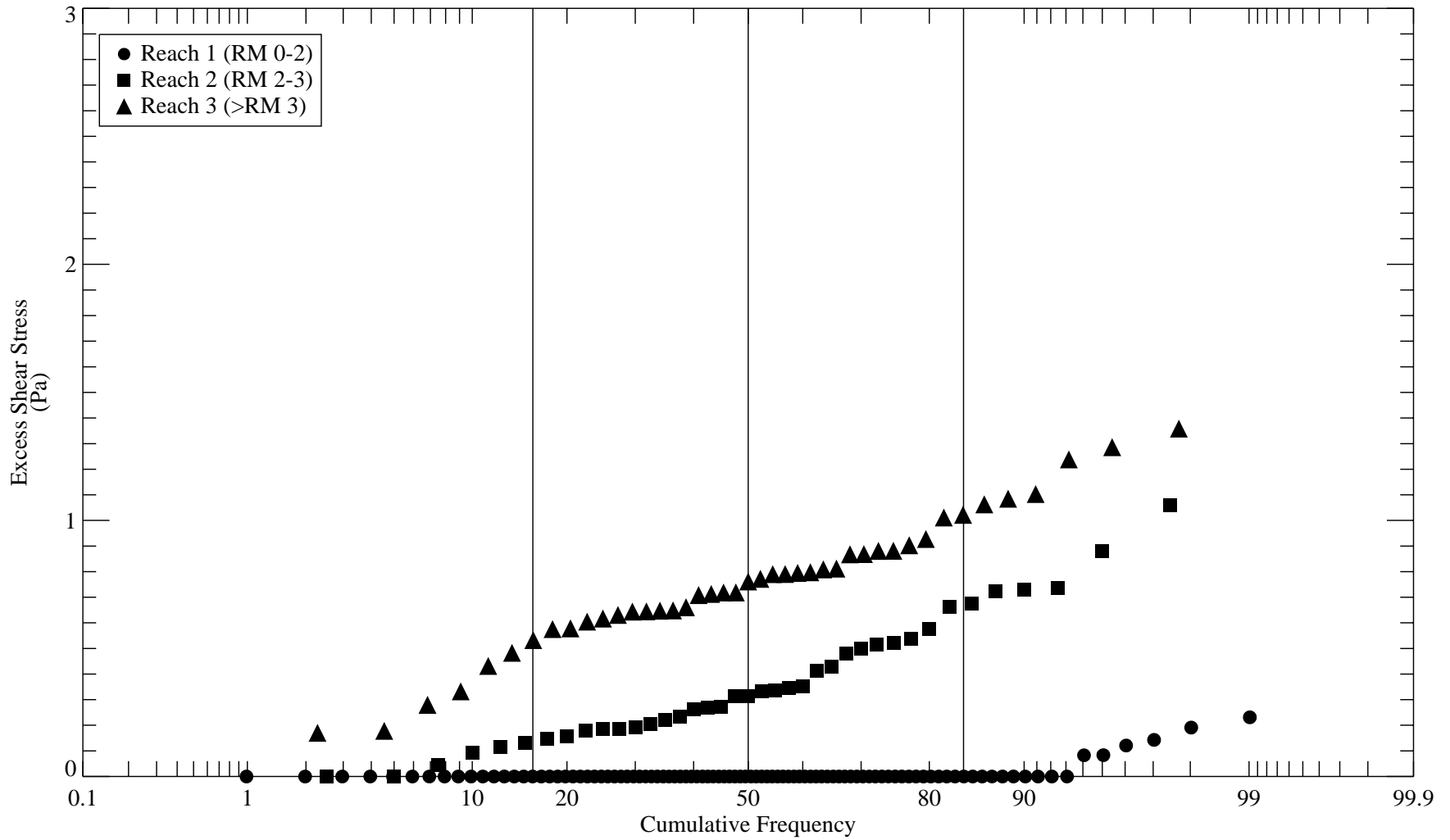


Figure 3-18. Cumulative frequency distributions of excess shear stress (based on maximum shear stress) in three reaches of the navigation channel during ebb tide period for 100-yr high-flow event, spring tide.

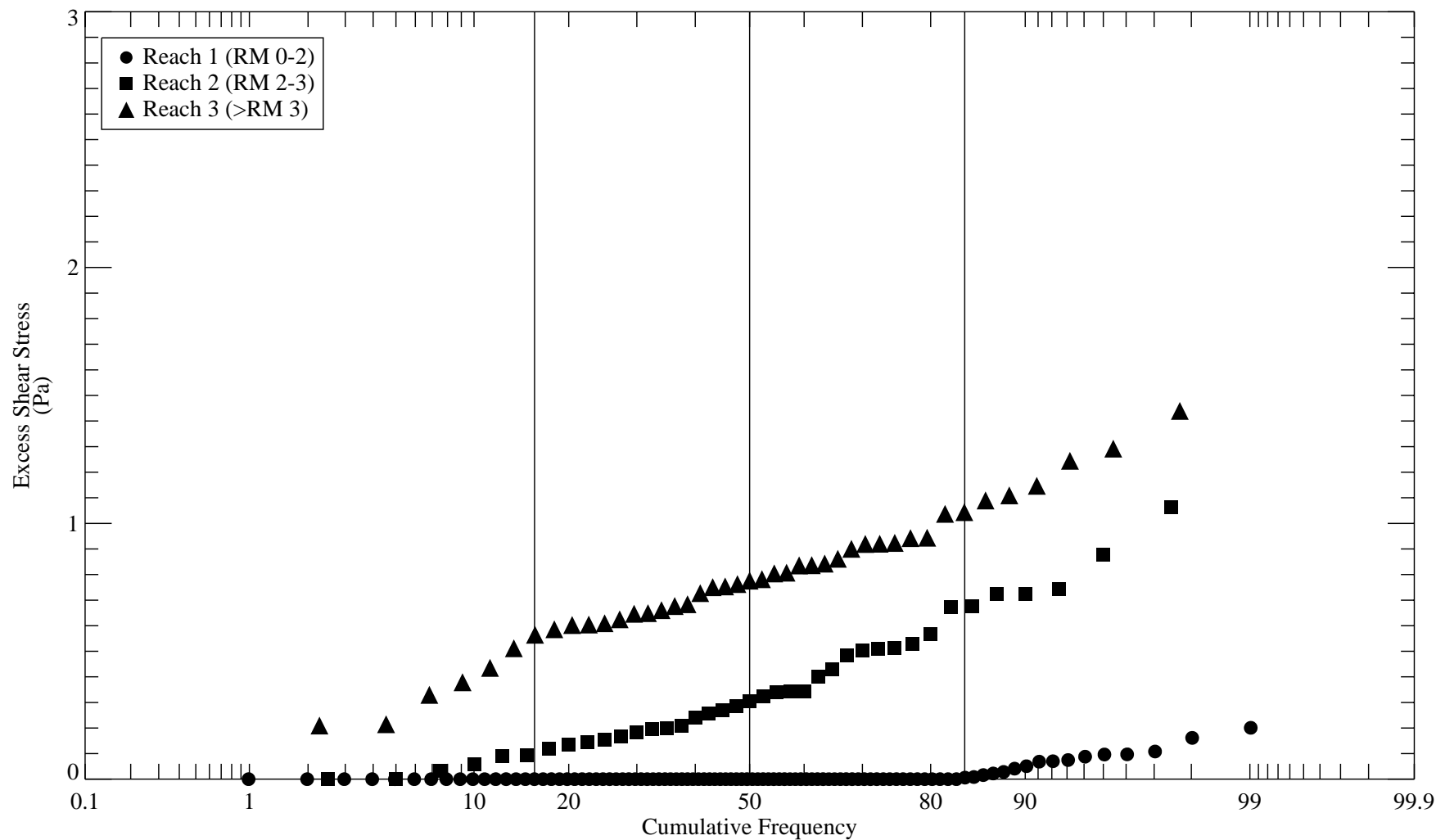


Figure 3-19. Cumulative frequency distributions of excess shear stress (based on maximum shear stress) in three reaches of the navigation channel during flood tide period for 100-yr high-flow event, spring tide.

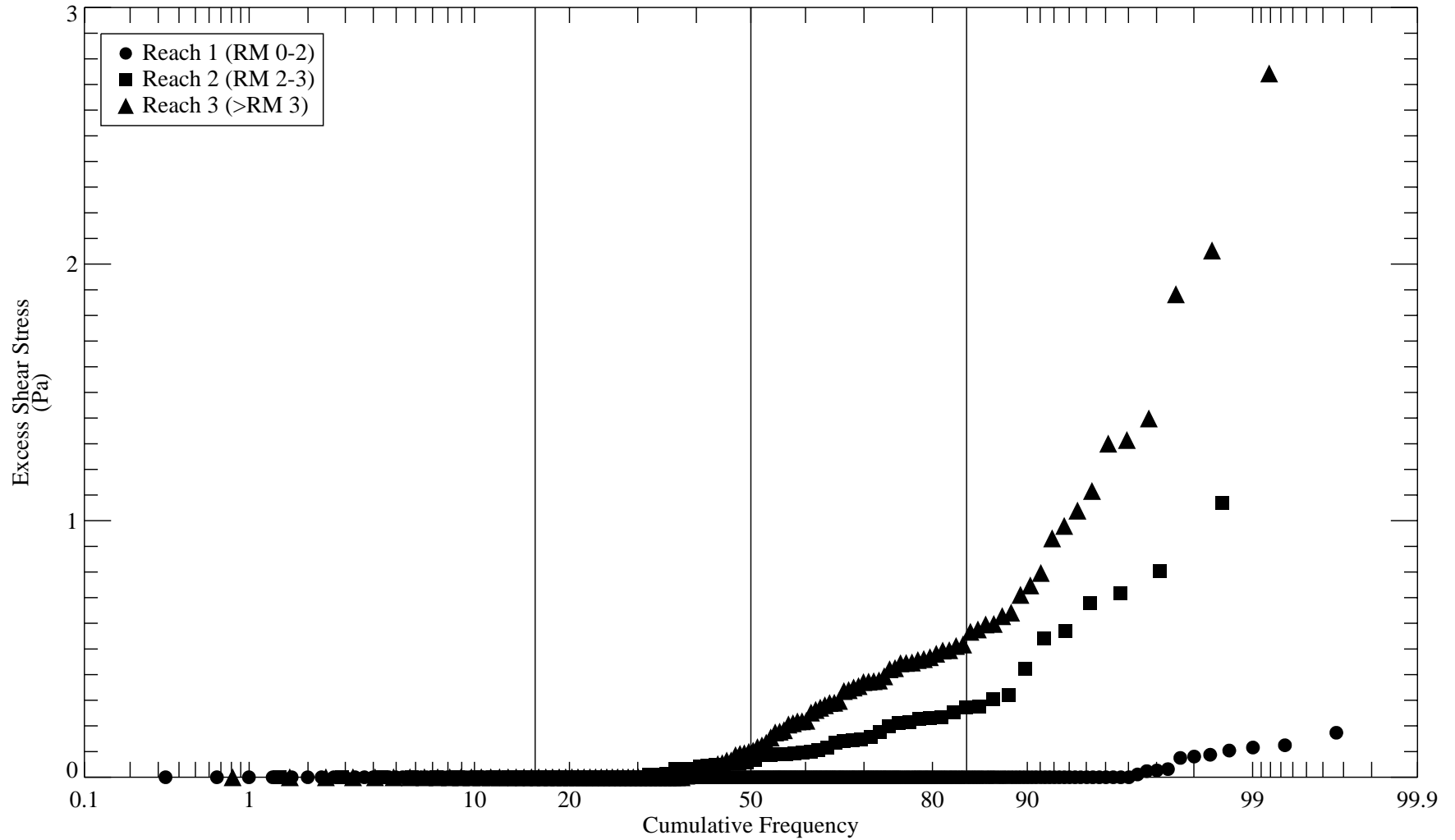


Figure 3-20. Cumulative frequency distributions of excess shear stress (based on maximum shear stress) in three reaches of the bench areas during ebb tide period for 100-yr high-flow event, spring tide.

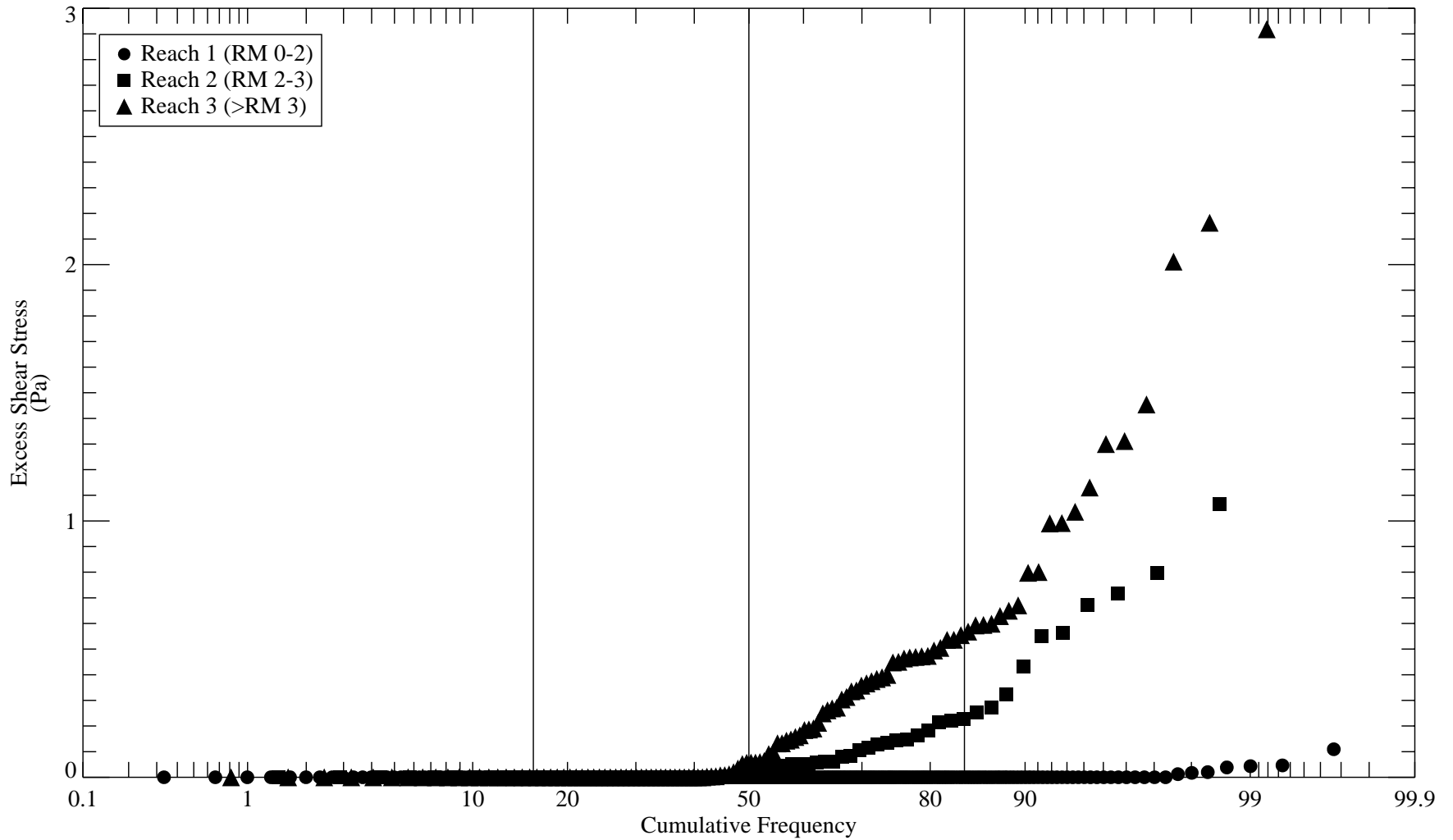


Figure 3-21. Cumulative frequency distributions of excess shear stress (based on maximum shear stress) in three reaches of the bench areas during flood tide period for 100-yr high-flow event, spring tide.

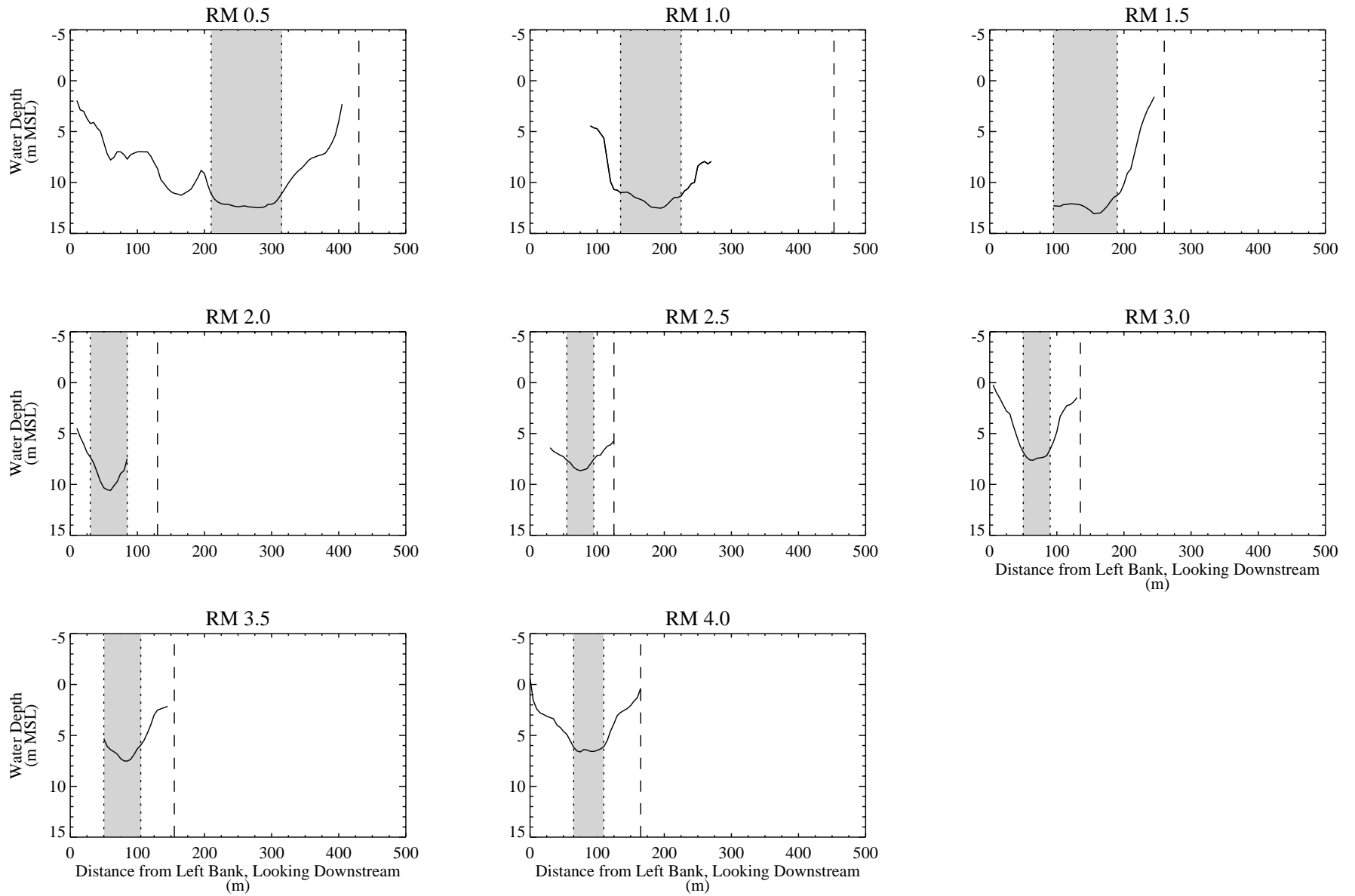


Figure 3-22. Cross-sectional profiles of LDW bathymetry at locations evaluated in ship-induced scour analysis. Navigation channel is denoted by shaded area.

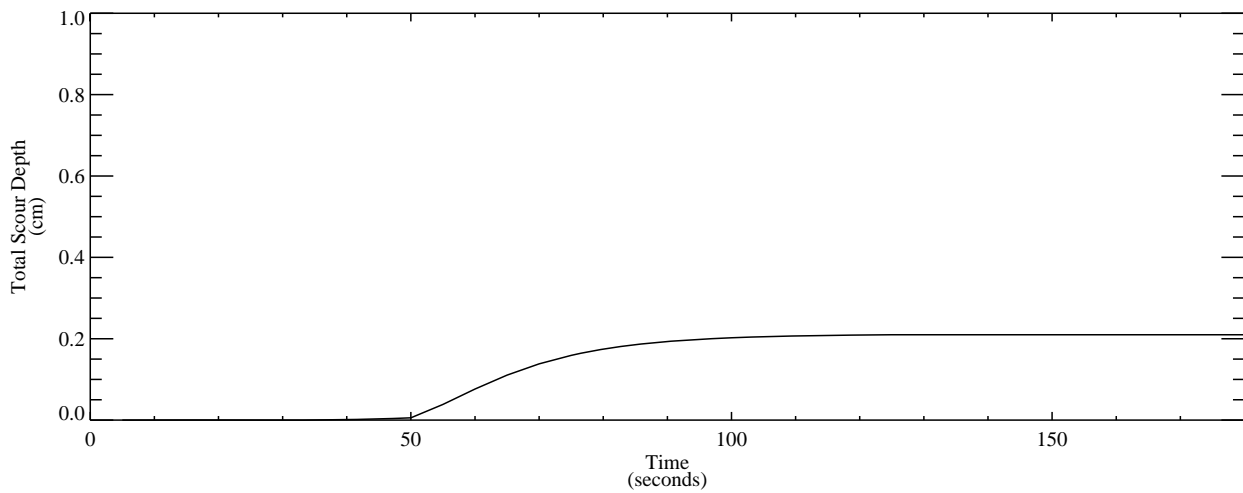
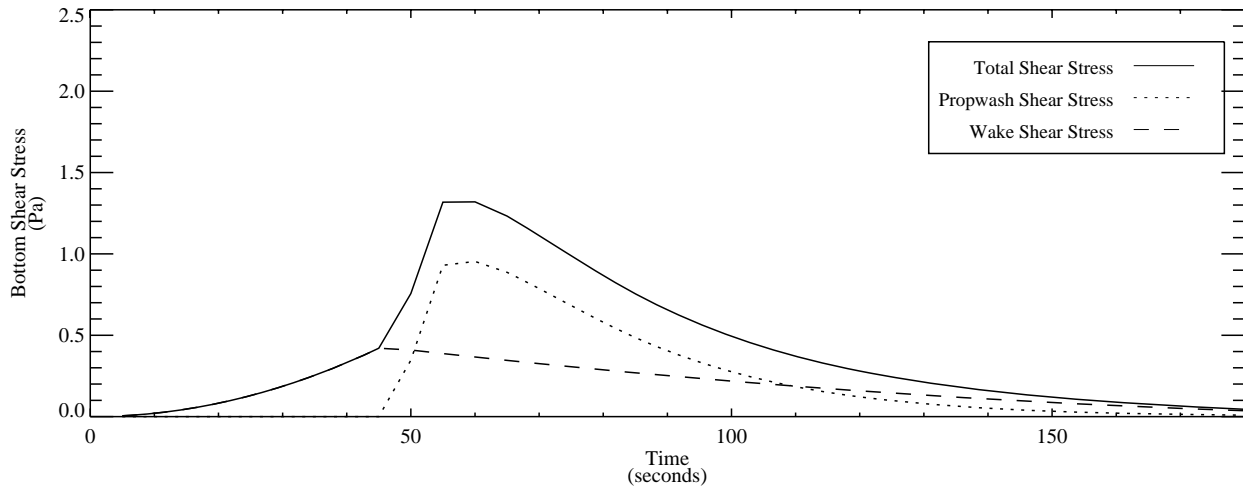
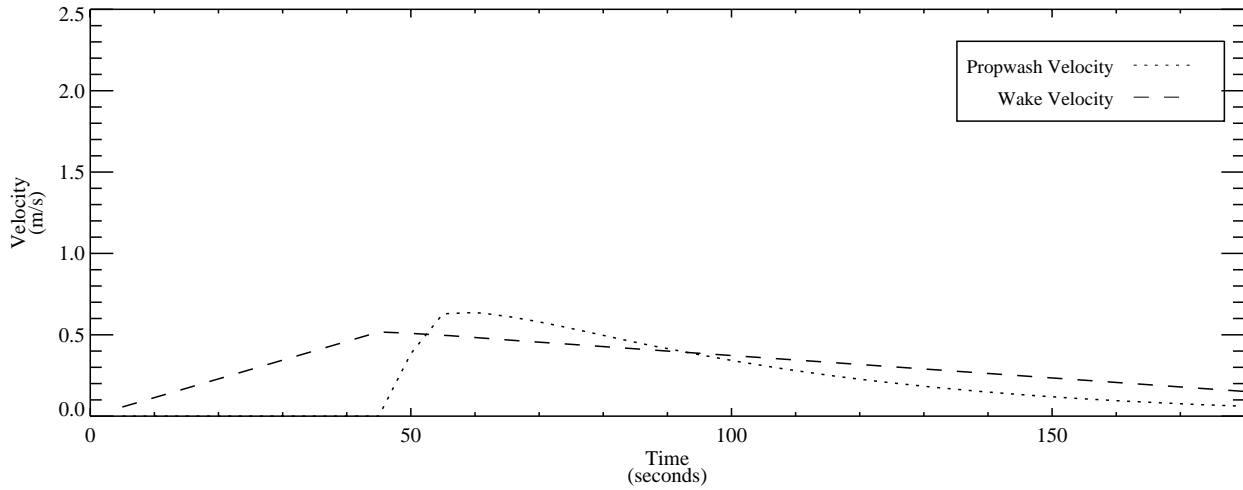


Figure 3-23. Temporal variation in bottom velocity, bottom shear stress and bed scour in the east bench area as a tugboat travels past an LDW transect at a speed of 5 knots.

Transect located at river mile 4.0.

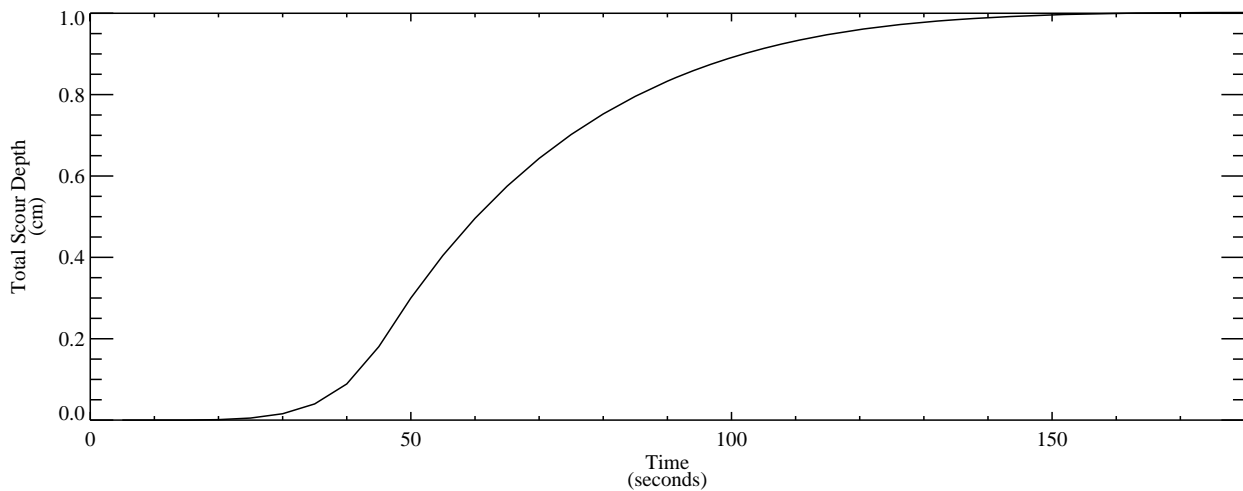
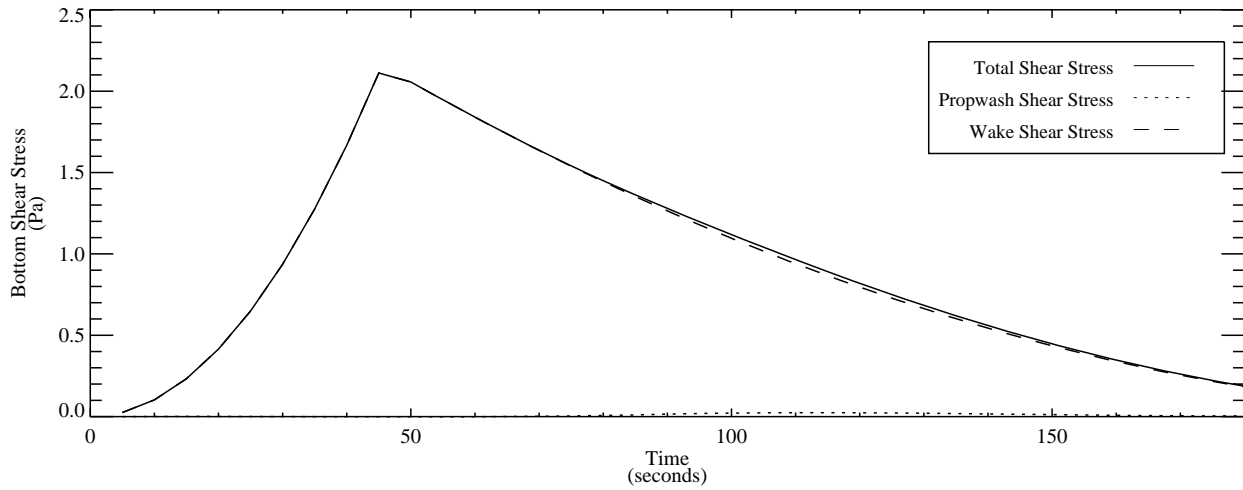
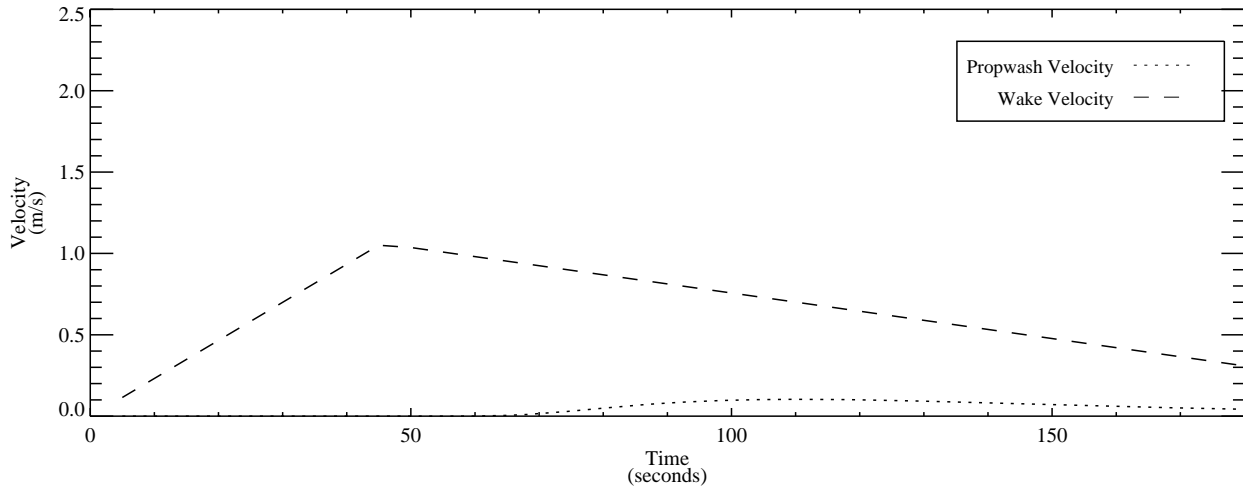


Figure 3-24. Temporal variation in bottom velocity, bottom shear stress and bed scour in the navigation channel as a tugboat travels past an LDW transect at a speed of 5 knots.

Transect located at river mile 4.0.

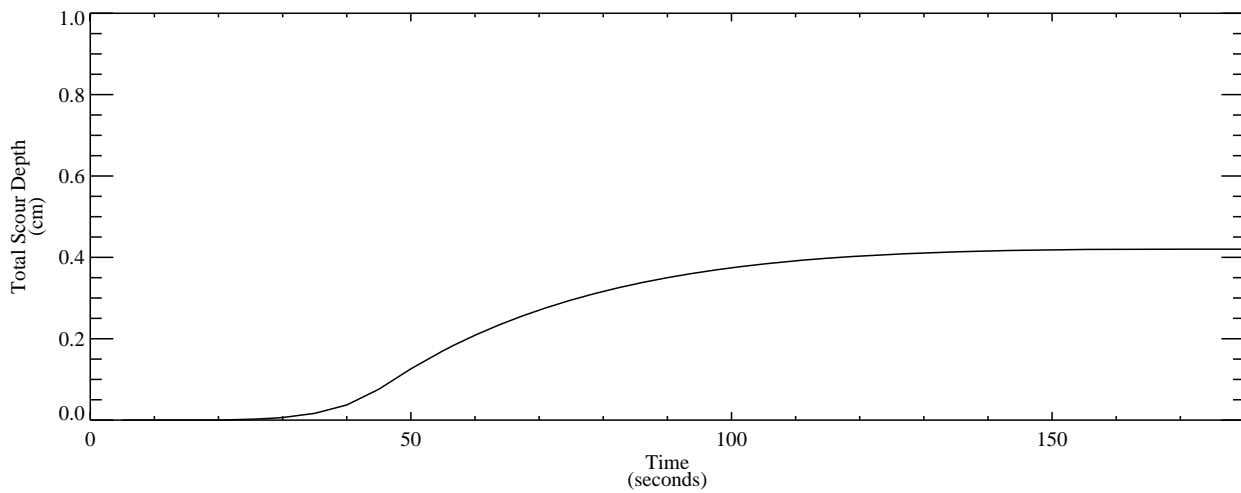
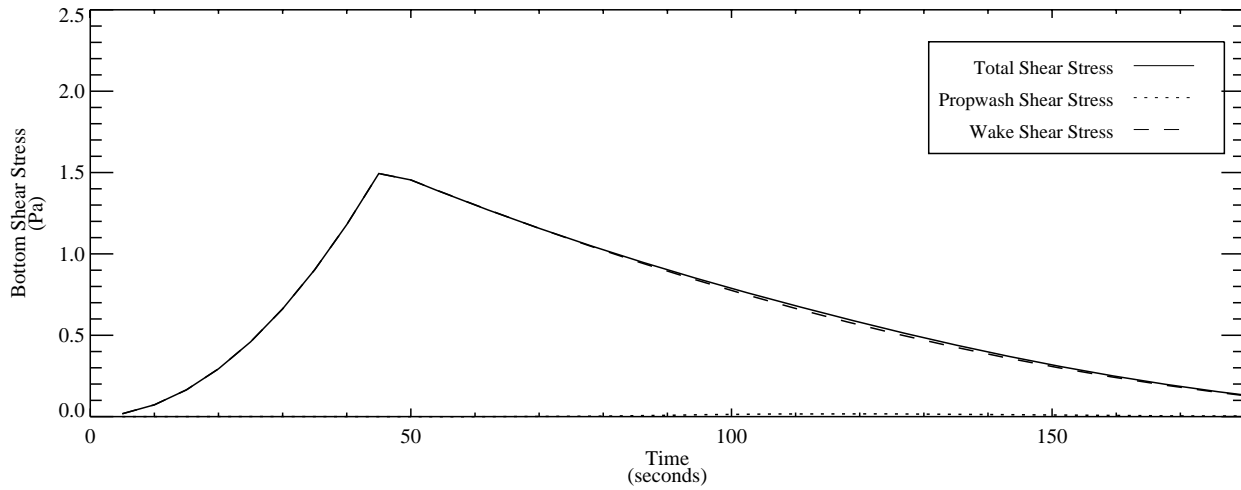
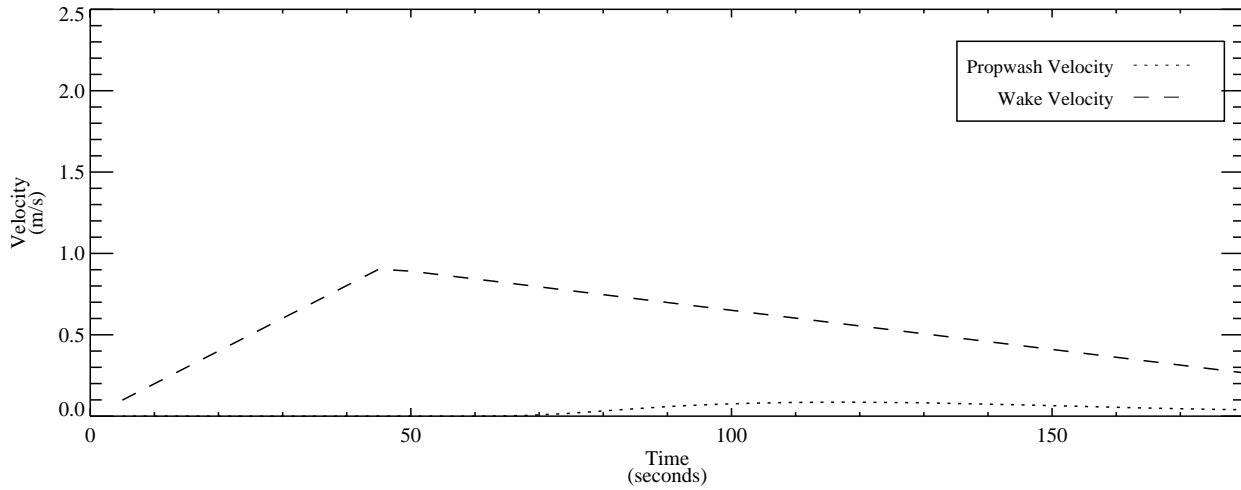


Figure 3-25. Temporal variation in bottom velocity, bottom shear stress and bed scour in the west bench area as a tugboat travels past an LDW transect at a speed of 5 knots.

Transect located at river mile 4.0.

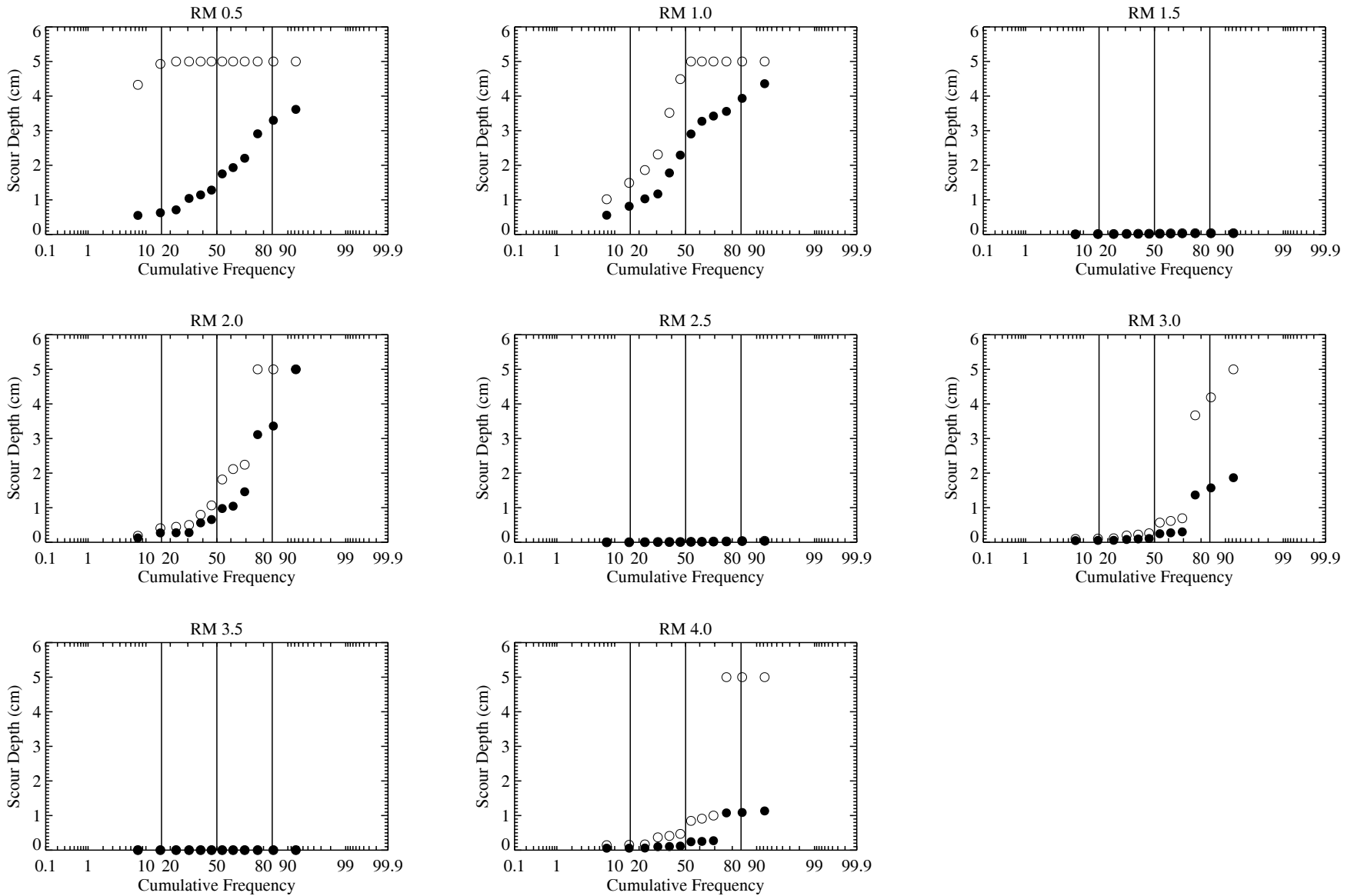


Figure 3-26. Cumulative frequency distributions of predicted average (solid circle) and maximum (open circle) scour depths associated with ship scour within the west bench area.

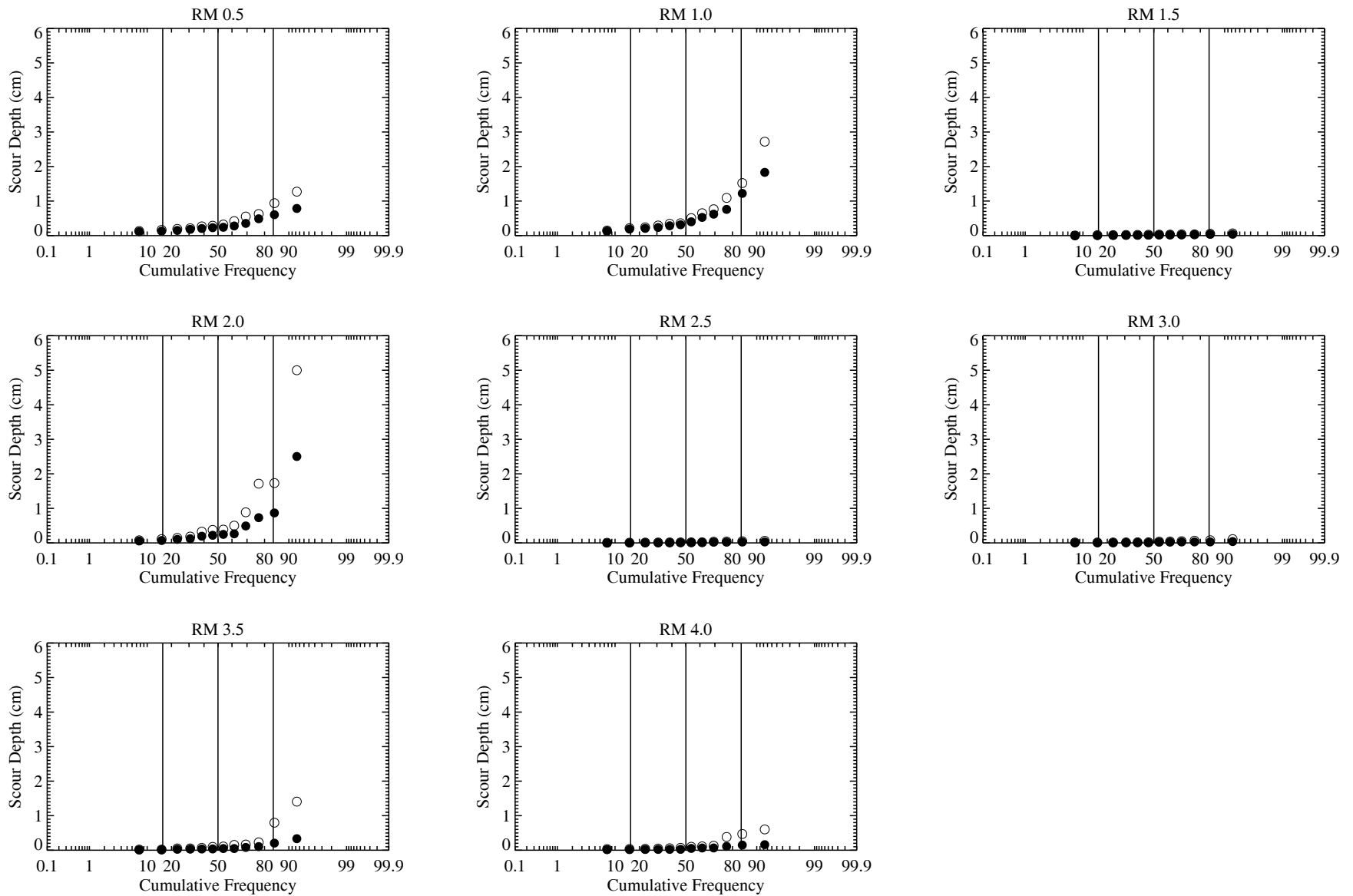


Figure 3-27. Cumulative frequency distributions of predicted average (solid circle) and maximum (open circle) scour depths associated with ship scour within the navigation channel.

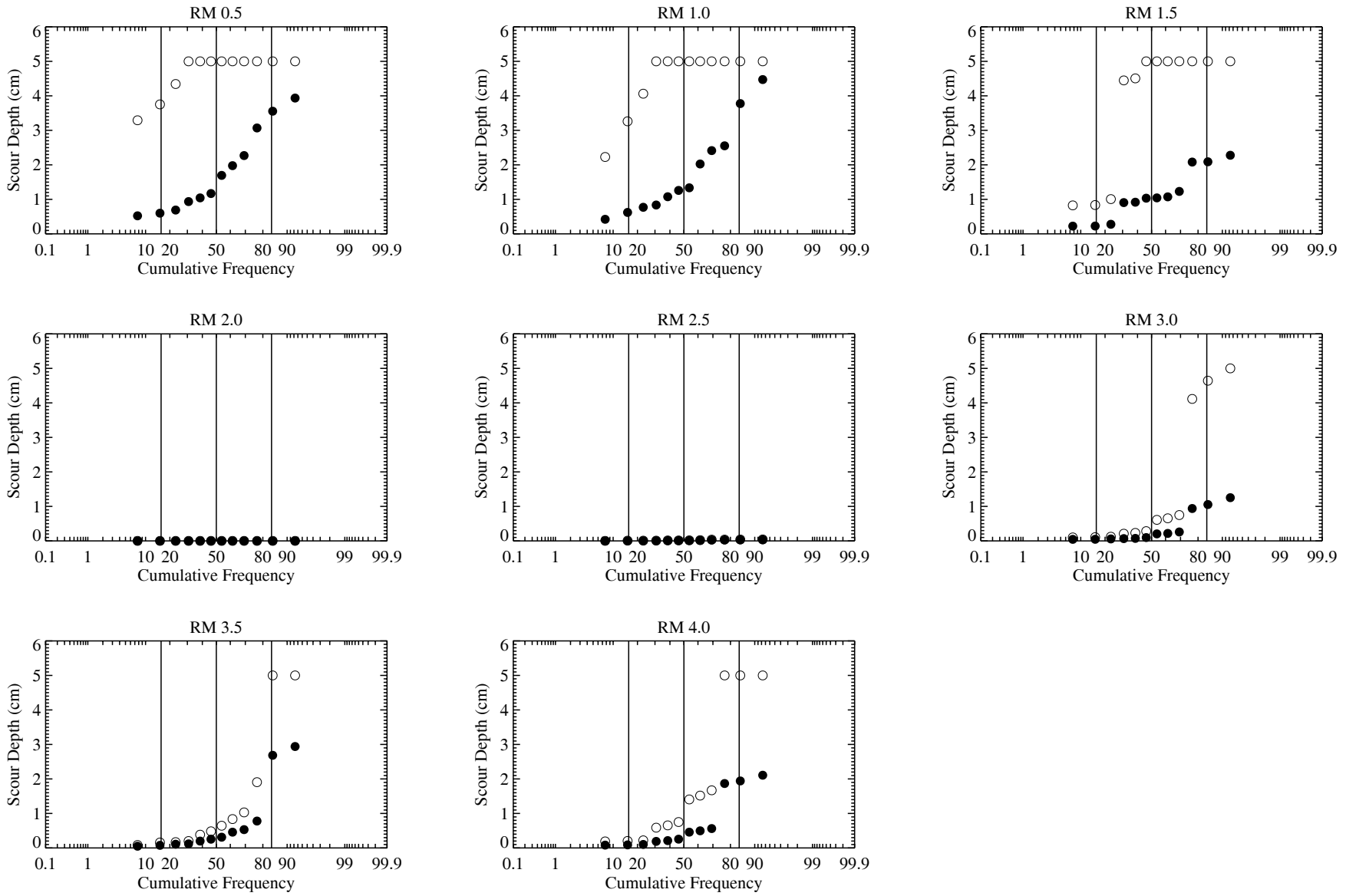


Figure 3-28. Cumulative frequency distributions of predicted average (solid circle) and maximum (open circle) scour depths associated with ship scour within the east bench area.

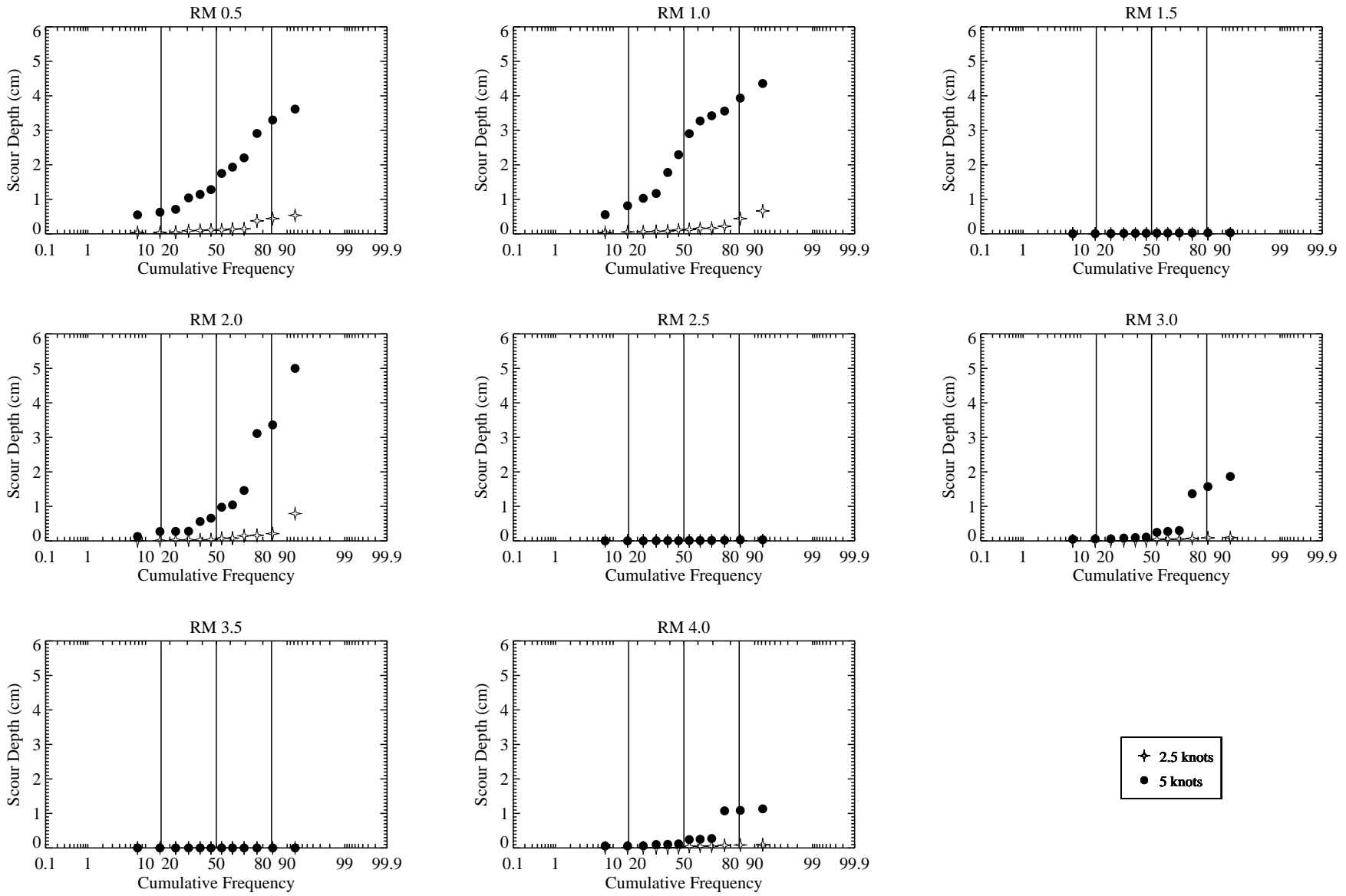


Figure 3-29. Cumulative frequency distributions of predicted average scour depths within the west bench area for ship speeds of 2.5 and 5 knots.

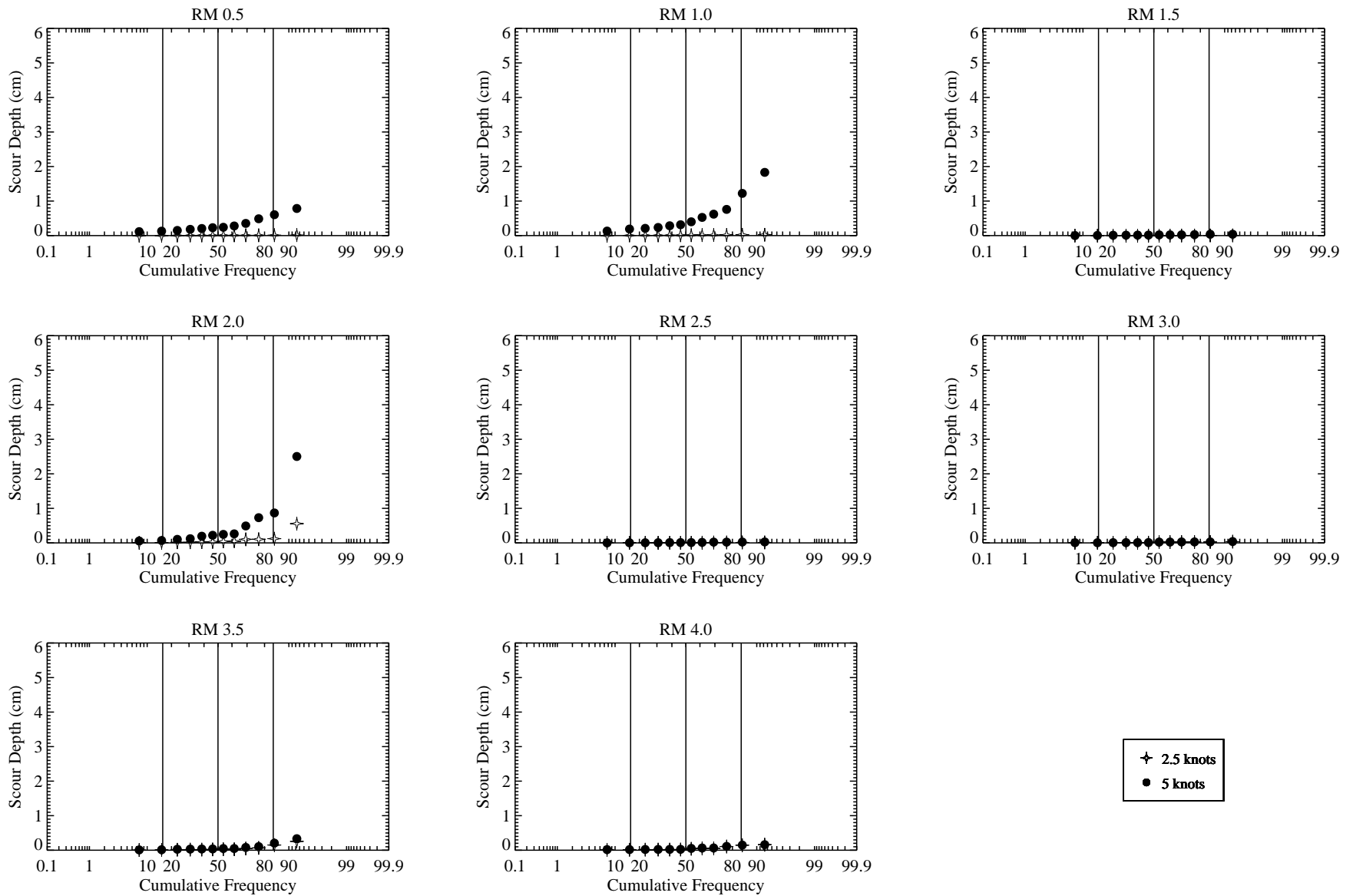


Figure 3-30. Cumulative frequency distributions of predicted average scour depths within the navigation channel for ship speeds of 2.5 and 5 knots.

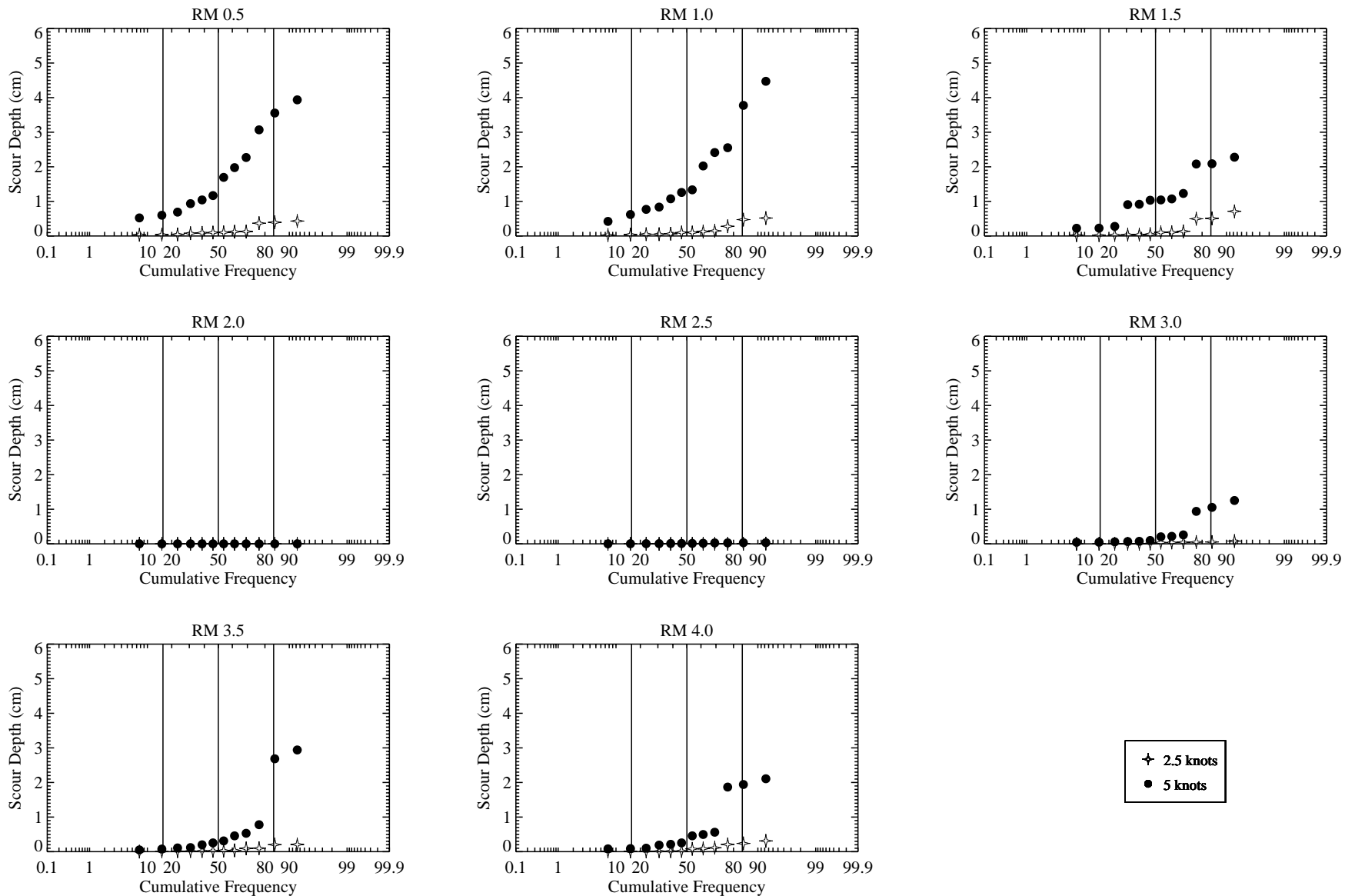


Figure 3-31. Cumulative frequency distributions of predicted average scour depths within the east bench area for ship speeds of 2.5 and 5 knots.

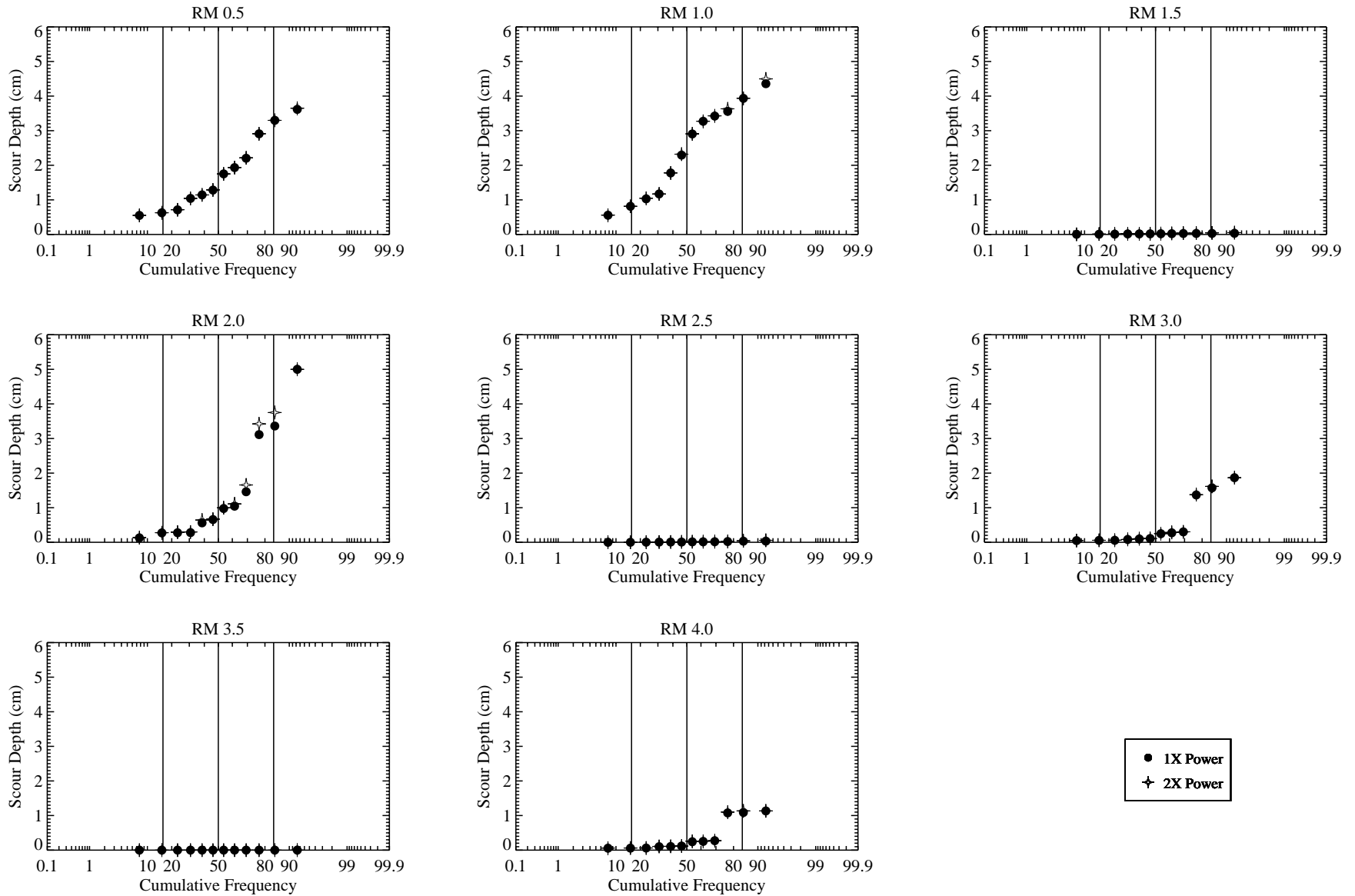


Figure 3-32. Cumulative frequency distributions of predicted average scour depths within the west bench area for the ship power sensitivity analysis.

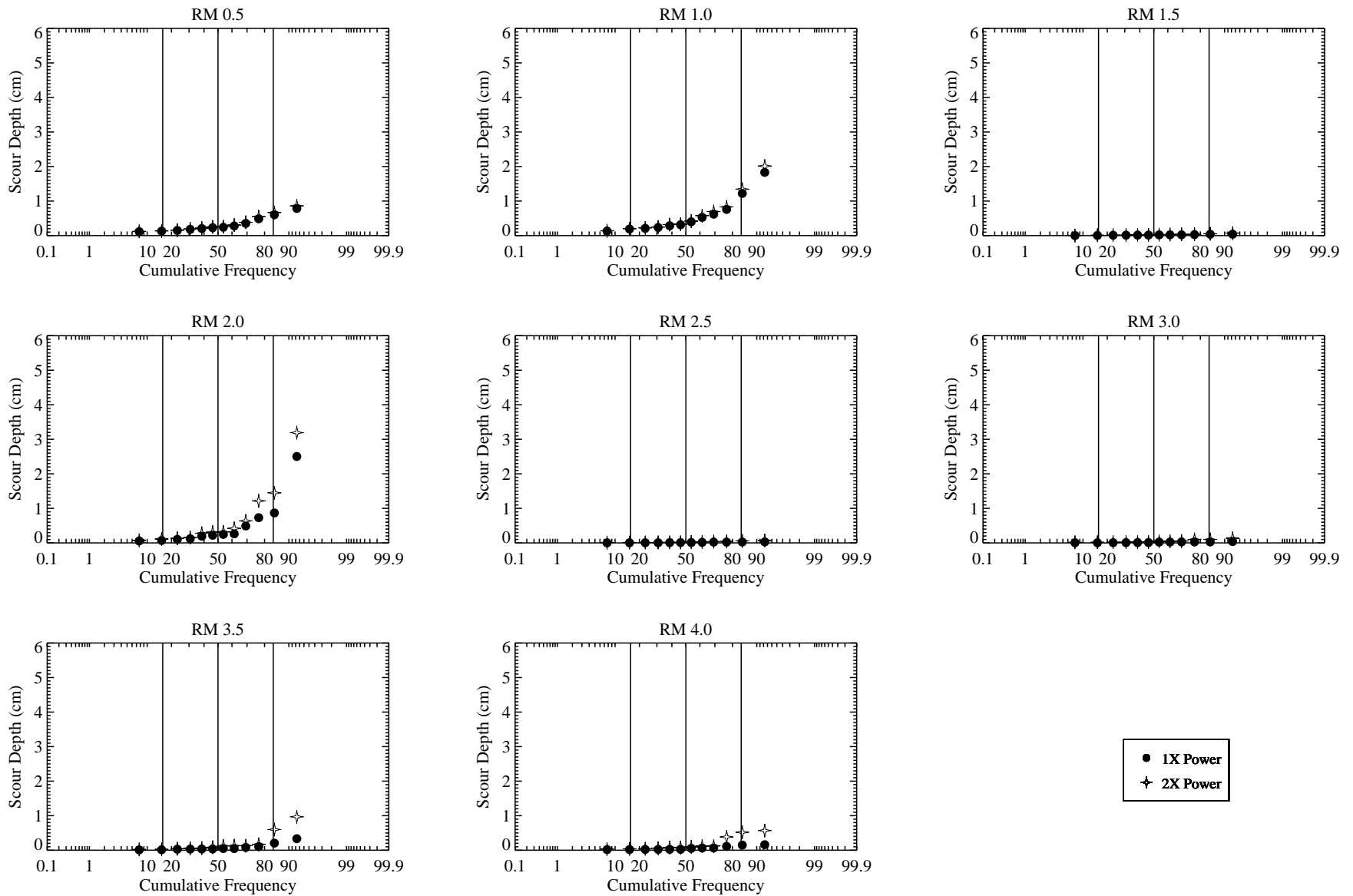


Figure 3-33. Cumulative frequency distributions of predicted average scour depths within the navigation channel for the ship power sensitivity analysis.

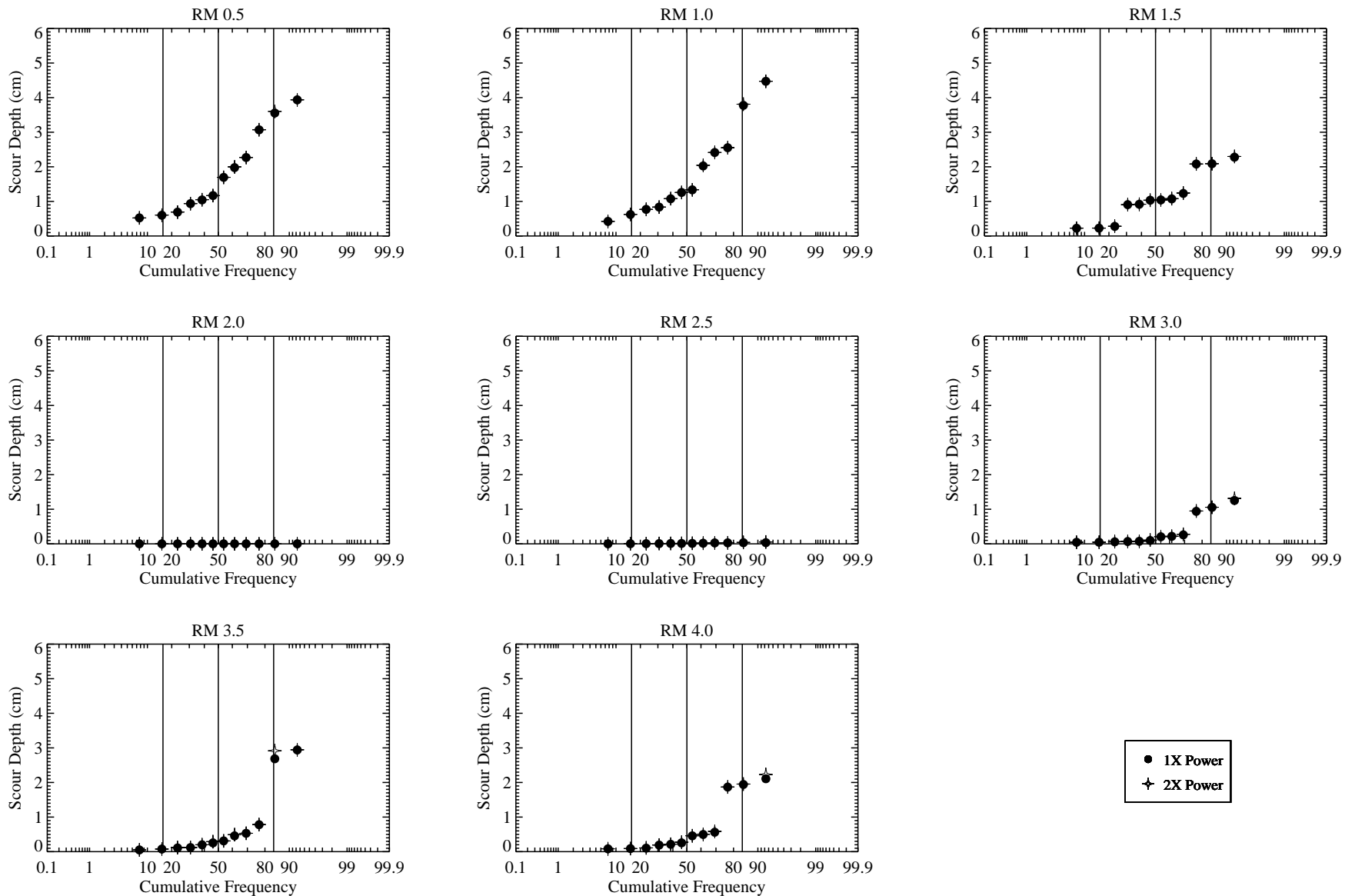


Figure 3-34. Cumulative frequency distributions of predicted average scour depths within the east bench area for the ship power sensitivity analysis.

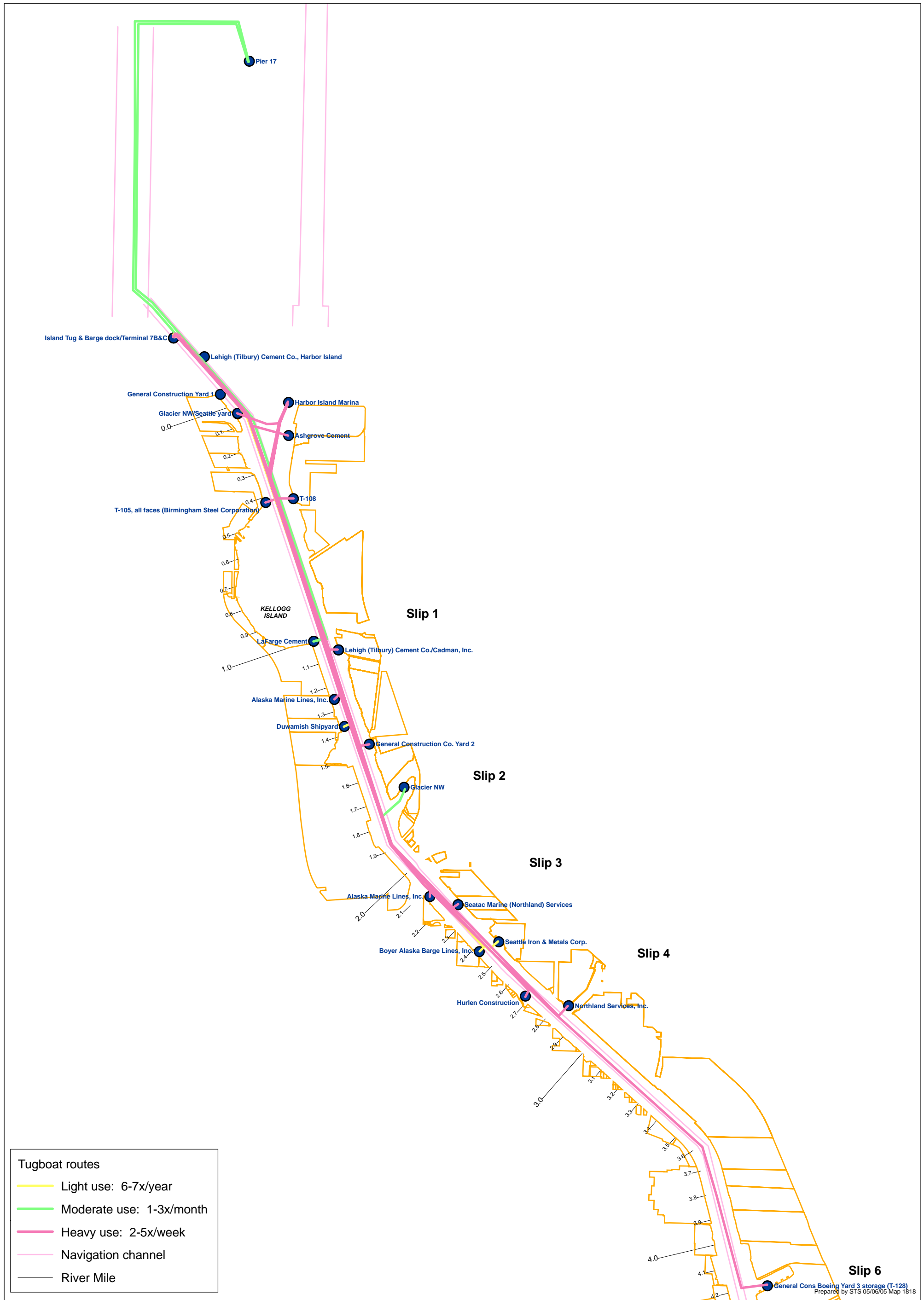
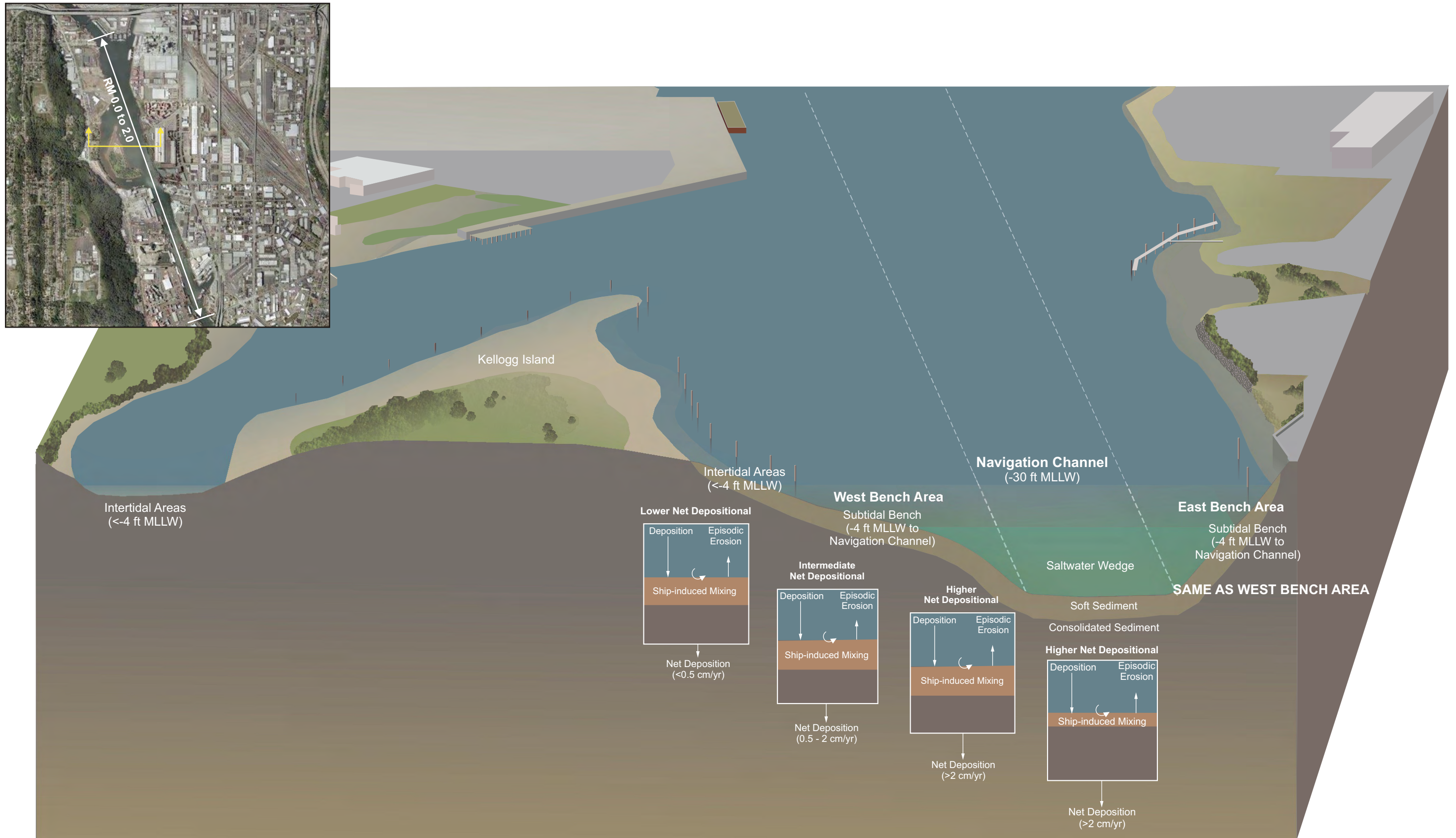
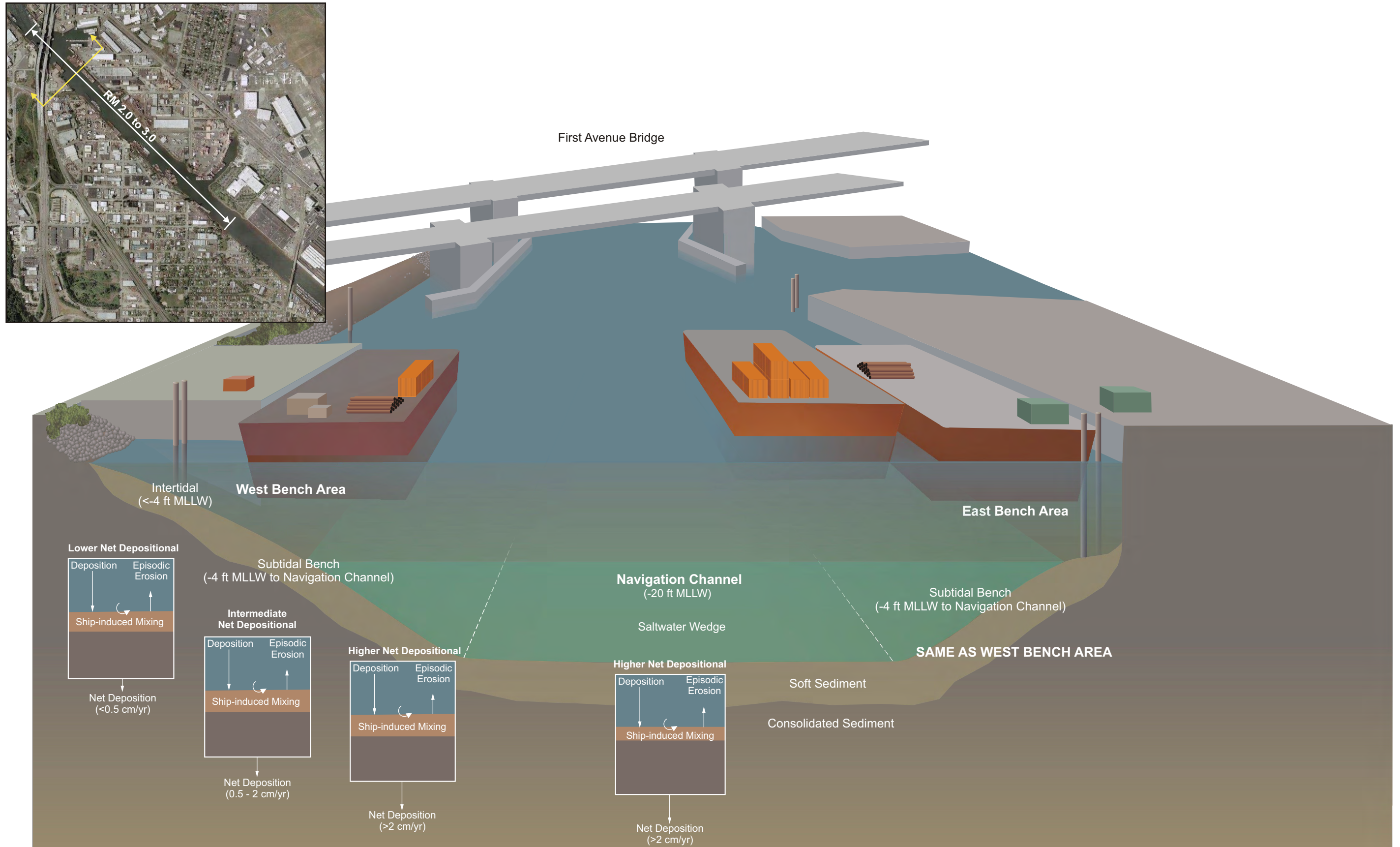


Figure 4-1. LDW Conceptual Site Model for Reach 1 (RM 0.0 - 2.0)



Notes: 1. Approximate net depositional rates from Sediment Transport Analysis Report, Windward and QEA 2006.
 2. Inserts are qualitative illustrations and are not to scale.

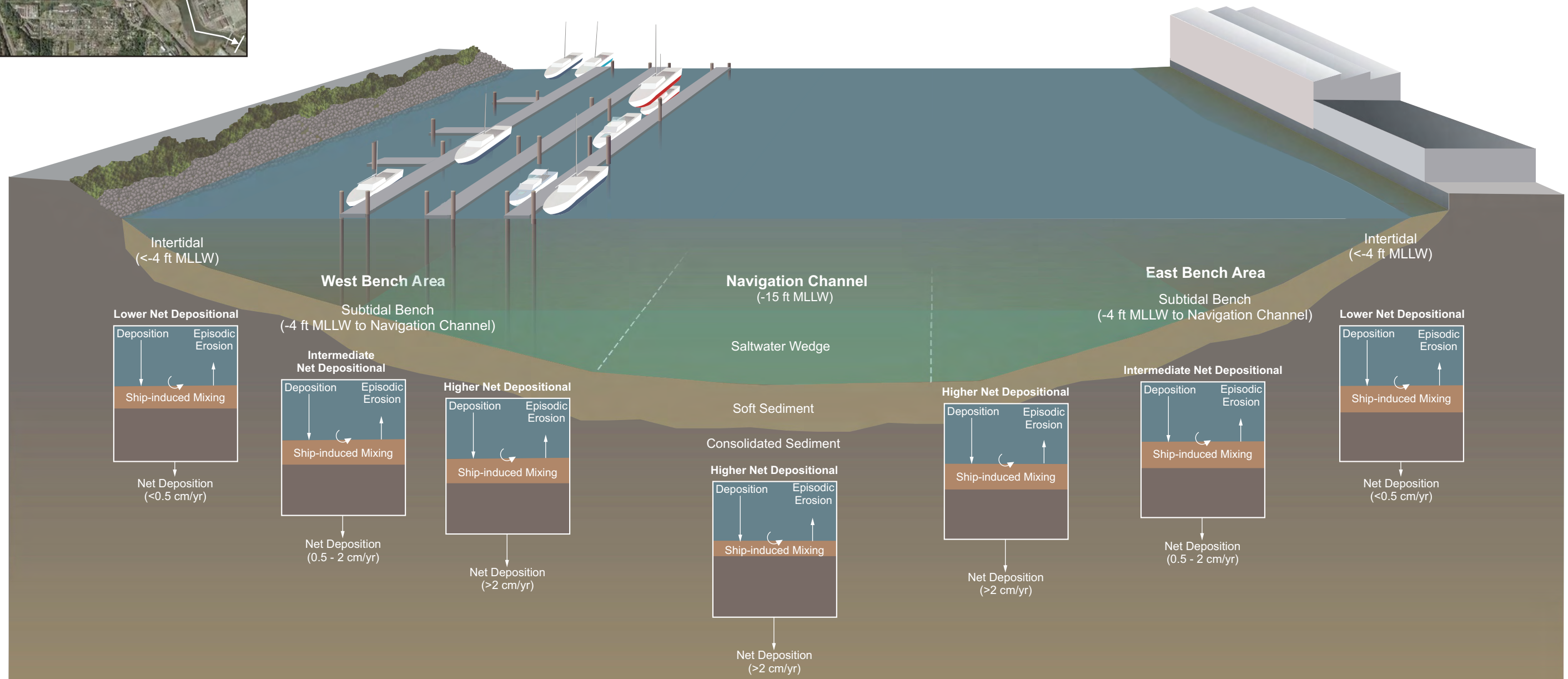
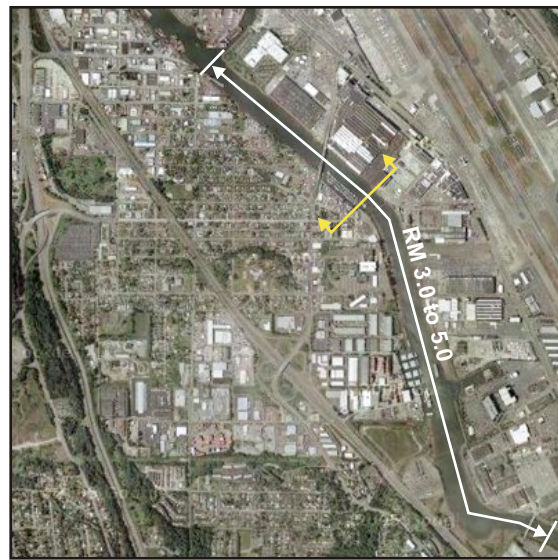
Figure 4-2. LDW Conceptual Site Model for Reach 2 (RM 2.0 - 3.0)



Notes: 1. Approximate net depositional rates from Sediment Transport Analysis Report, Windward and QEA 2006.
2. Inserts are qualitative illustrations and are not to scale.

Figure last updated on January 11, 2006

Figure 4-3. LDW Conceptual Site Model for Reach 3 (RM 3.0 - 5.0)



Notes: 1. Approximate net depositional rates from Sediment Transport Analysis Report, Windward and QEA 2006.
2. Inserts are qualitative illustrations and are not to scale.